The self-organized criticality as an explanation of fatigue failure for shape memory alloys

Clement Dunand-Chatellet

École Polytechnique
Department of Mechanical Engineering

Thesis

submitted to École Polytechnique in fulfilment of the thesis requirement for the degree of Doctor Of Philosophy

by

Clément Dunand-Châtellet

The self-organized criticality as an explanation of fatigue failure for shape memory alloys

Thesis defended the 05/16/2012 face to the jury composed of:

Reviewers:	Prof. André Chrysochoos	Université de Montpellier
	Prof. Eduard Vives	Universidad de Barcelona
Examinators:	Prof. Fernandino Aurrichio	University of Pavia
	Prof. Jean-Philippe Bouchaud	École Polytechnique
	Prof. Jérome Weiss	Université de Grenoble
Advisor:	Prof. Ziad Moumni	E.N.S.T.A. Paristech

I would like to dedicate this thesis to my family, my friends and my loved wife Léa.

Acknowledgements

This thesis arose in part out of two years of research that has been done since I came to the Materials and Structures group. During this period I have been supported by a great number of kind people who contributed to the achievement of the present work. It is a pleasure to convey my gratitude to them all in my humble acknowledgement.

In the first part I would like to record my gratitude to my supervisor *Ziad Moumni* who brought me to the extraordinary field of complexity. Above all the most needed, he provided me unflinching encouragement and support in various ways. His truly scientist intuition and enthusiasm has made him as a constant oasis of ideas and passions in physics research, which inspire and enrich my growth as a PhD student. I am indebted to him more than he knows.

Many thanks also to *Antoine Chaigne* who enrolled me as a PhD student in their laboratory. I am grateful to their contribution in the success of the present research and hope the self-organized criticality activity to be a major part of the laboratory research fields.

It is a pleasure to pay tribute to *Andreï Constantinescu*, *Stéphanie Deschanels*, *Lev Truskinovski* as well as *Jêrome Weiss* who are at the origin of the idea of using SOC in fatigue analysis. Thank you very much to the Agence Nationale pour la Recherche for funding the present work.

I am very grateful to Prof. *Eduardo Vives* and Prof.*André Chrysochoos* for their constructive comments. I am thankful that in the midst of their activity, they accepted to be members of the reading committee. A special thank to them also for their excellent contributions in the trends of criticality research. Their papers gave me the knowledges necessary to write this thesis. Thank you again.

Many thanks go to *Fernandino Aurrichio*, *Jean Philippe Bouchaud* and *Jêrome Weiss* who accepted to be member of the thesis examiners. Warm acknowledgments are given to *Jean Philippe Bouchaud* who is undoubtedly responsible for the success of this thesis, through the most exciting courses, I had the opportunity to listen, he gave about complex systems. He also contribute intensively to my growing interest in financial applications of physical models through the fruitful discussions we got.

To the role model for hard workers in the lab, *Lahcene Cherfa*, I would like to thank him for being highly involved in the laboratory. I am proud

to record that I had several opportunities to work with an exceptionally experienced technician like him.

I would like to thank *Corrine Rouby, Olivier Doaré, Anne-Lise Gloanec, Bertrand Reynier, Alain Van Herpen, Patrice Riberty and Régine Tanniere* for their enthusiasm and their help during the two past years.

Collective and individual acknowledgements are also owed to my colleagues whose present somehow perpetually refreshed, helpful, and memorable. Many thanks go in particular to *Abderrazak Traidia* and *Alexander Chidley* for creating such a great friendship at the office, for their perpetual humour and helpful ideas. It is a pleasure to thank *Mohammed and Xue* for their enthusiasm, friendship and the leaning they gave to me about their respective cultures.

I can not forget to thank *Emmanuel Bacry* who introduced to me Hawkes processes in the financial framework as well as *Haissam Ismael* who worked with me on this interesting topics. My acknowledgements are also addressed to people from the Statistical Arbitrage team of BNP Paribas, *Stephane Tyc*, *Boris Leblanc* and particularly *Julien Nguyen* who taught to me the necessary mathematics rigor required in coding activities of financial applications. Sharing discussions with him about sciences was a real pleasure.

Last but not least, I am pleased and full of emotion to thank my parents *Geneviève* and *Roger* as well as my brother *Julien* and all *my friends* for their great support throughout my life. Finally, my warmer acknowledgments are going to my wife *Léa* who was always here to support me during this adventure.

Levallois Perret, June 7, 2012.

Contents

List of Figures

Layout

The layout of the thesis can be sumed-up in six chapters in broad outline. The *first chapter* aims at presenting the collective EvoCrit projet and the associated subject to this thesis.

The *second chapter* will introduce the Ni-Ti shape memory alloys and their known properties in fatigue. Then, the concepts of complexity, as well as self-organized criticality, will be detailed since this constitutes the core of this thesis and a deep comprehension of these theories is required to understand the issues of this manuscript.

The *third chapter* deals with an experiment quantifying the changes that occur in the response of the material from its virgin state until its stable state through mechanical, thermal as well as acoustic measurements. Such an experimental device will reveal the emergence of complex and interlocked behaviors in the transient state. The aim is to demonstrate that a stable state is reached, whatever the quantity one is interested in, after a given number of cycles.

The *fourth chapter* is devoted to depict one fatigue experiment among others. Results are analyzed through the spectrum of SOC to extract from the shifts in distributions, induced by the changes in dissipative regimes, some precursory signals of initiation of fatigue. A comparison between the dynamics of earthquakes and the one encountered in fatigue is performed through a spatio-temporal analysis of the generated acoustic emissions. An attempt is made to demonstrate that the same critical dynamics can hold from the large scale of earthquakes down to the microscopic scale of the sample rheological structure.

The *fifth chapter* is a cultural chapter that invites the readers to travel across sciences through the concept of complexity. High-frequency financial data will be analyzed through mutually excited point processes models that were initially developed for earthquakes. Some troubling similarities in the dynamics of these, *a priori*, far away systems will be highlighted and subsequently applied to the temporal modeling of arrival times of waves in the transient state of shape memory alloys in fatigue. One objective is to adopt the global point of view suggested by self-organized criticality in sciences.

The *sixth* and conclusive chapter will summarize the scientific improvements brought by this thesis and introduce some outlooks for future studies. The goal is to have a reflexion about the reliability of the results that will lead us to discuss the added-value carried out by this first application of self-organized criticality in fatigue.

Several papers and conferences dealt with the works exposed in this thesis; all are reported in the appendix A. Readers will also found some mathematical reminders about specific points if needed.

Introduction

1

Contents

This chapter explains the common objectives of the EvoCrit project, like Evolution of Criticality, for the different partners that are involved in this adventure. The ideas at the basis of this study are presented and the different discoveries and problems leading to this PhD subject are exposed from its inception.

1.1 The ANR project EvoCrit

1.1.1 Scientific description of the project

Fatigue is among the less well understood mechanism of mechanical failure encountered in such a variety of structures ranging from nuclear reactors to micro-electronic connections in cell-phones. Failure in cyclic loading appears unexpectedly when the structure is operating in a safe and apparently steady state regime. The situation is particularly troublesome with early precursors of fatigue and monitoring microscopic evolution of damage is an urgent need.

In this project, we put forward a new set of ideas which open the way to experimentally distinguish various stages in the micro-development of fatigue. The approach is based on the study of the multi-scale statistical structure of the intermittent acoustic signal generated by cyclically loaded solids. In previous works, Weiss and Grasso (1997), Richeton et al. (2006) succeeded in identifying the peculiar power-law nature of similar acoustic signals in several classes of materials in monotonic loading. In the current project, the aim is to extend this approach to cyclic loading beyond the very first attempts of Vives et al. (2009) that are limited to few cycles.

In particular, we plan to develop an experimental method allowing one to discriminate between the power-law exponents and cutoffs generated by different deformation mechanisms. By tracing the proposed markers we shall be able to link the evolution in the structure of the acoustic signal to the changes in the collective behavior of defects. The originality of the project lies in the interpretation of the statistics of the microscopic events using the concept of self-organized criticality (S.O.C.).

SOC and the ubiquity of power-laws are the issues of great significance in contemporary science, giving a framework for understanding the emergence of complexity in a variety of natural systems, from earthquakes to turbulence. In this project we plan to extend this paradigm to fatigue and use the systematic changes in the structure of the critical (near critical) acoustic signals as a measure of closeness to ultimate failure.

The main theoretical idea is to identify fatigue failure with the crossover between two scale free regimes: dislocation based and microcracking based. Hence, decisive experiments on metals will be held and mathematical model will be developed in consequence to capture both the power-law signal and its transformation.

1.1.2 Role of partners

The ANR project is organized through a consortium of 4 partners:

1. Laboratoire de Mécanique des Solides of École Polytechnique ParisTech. LMS has a strong tradition in advanced mathematical modeling of complex mechanical phenomena. This partner provides a combined input for this project as, on the one hand, it has an experience in fatigue modeling and on the other hand it has an experience in modeling criticality.

2. Unité de Mécanique - Matériaux et Structures of École Nationale Supérieure de Techniques Avancées ParisTech. UME-MS has a broad experience in modeling multi-physics phenomena with strong thermo-mechanical coupling as in shape memory alloys.

3. Laboratoire de Glaciologie et Géophysique de l'Environnement of Université Joseph Fourier Grenoble - Centre National de la Recherche Scientifique. LGGE has a long experience on the analysis of plasticity, dislocations avalanches and criticality from acoustic emission measurements.

4. Matériaux Ingénierie et Sciences of Institut National des Sciences Aplliquées de Lyon. MATEIS has a broad expertise in acoustic emission: concerning acquisition, AE signals processing and source mechanisms recognition.

Consequently, the added value of the consortium is relatively crystal clear and the scientific complementarity of partners will be used to reach the common aim which is to find a statistical descriptor of fatigue in metallic material at the microscopic scale.

1.2 Originality of the PhD subject

1.2.1 Definition of the subject

Experimental studies have shown that in the life of a cyclically loaded structure one can identify several characteristic stages. This is the case for shape memory alloys (SMA). In the first, transient stage, the evolution of the microstructure is controlled by a hardening mechanism and after a finite number of cycles the system stabilizes in a shakedown state. The shakedown state marks the beginning of the second stage when the structure exhibits an almost fixed hysteresis loop due to the collective motion of microscopic mechanisms, namely phase change and dislocations motions. In the shakedown stage, the macroscopic evolution appears to be frozen, however, micro-activity continues to take place. Indeed, the macroscopic dissipated energy (which is the area of the hysteresis loop in shape memory alloys) remains unchanged in this second stage for cyclically loaded SMA until the failure. Meanwhile, the development of microdamage leads to the eventual change of the mechanism of the inelastic deformation. More specifically, primary defects eventually generate voids and micro-cracks which form microstructure of their own. The evolution of the patterns of micro-cracks leads ultimately to the nucleation of a macro-crack, whose rapid propagation brings the final failure of the material.

So far, early precursors of fatigue are practically unknown and we still do not have reliable prediction tools relating defects activity at the micro-scale with the failure at the engineering scale. Our goal is to furnish such quantitative descriptors and predictors. To achieve success in this direction, it is crucial to find a new way of performing macroscopic measurements which would reflect microscopic activity of different types

of defects. Consequently, acoustic emission seems to be a good candidate to recover the missing information about the current state of damage by using statistical analysis of the acoustic waves generated by the repeatedly loaded material. Instead of tracing individual inelastic effects, we will focus on the statistical signature of the microscopic evolution of a large number of deformation mechanisms which will enable us to perform probabilistic computations.

Acoustic emission (AE) is one of the most powerful non-destructive tool for the analysis of dynamical instabilities involving such topological defects as dislocations, twins, martensitic boundaries frictions and microcrack. By using AE sensors one can monitor the distribution of the internal instabilities in space, time and energy domains. Consequently, a complete analysis of the underlying activity can be provided to track in live how, when and where are occurring acoustic events. In this thesis, the evolution of damages is viewed through to the focus of collective phenomena by studying the scaling of acoustic signal instead of focusing on individual defects. So, the ultimate goal is to extract the statistical measure of closeness to ultimate failure.

1.2.2 Previous studies on the same subject

Recently, Perez-Reche et al. (2004; 2007) as well as Vives et al. (2009) demonstrated both experimentally and theoretically that the acoustic signal associated with the steady state inelastic deformation in SMA submitted to cyclic loading has a power-law or scale free nature. The novelty of this approach was in the interpretation of the acoustic signal in terms of frequency of the recorded microscopic events. To appreciate the unexpected outcome of the experiments, we recall that in classical theories of inelastic deformation it is assumed that the transition from discrete to continuum can be accomplished by simple homogenization procedure. A fundamentally different picture emerged from the above experiments: that of scale-free intermittent activity characterized by power-law distributions of avalanches sizes, time correlations and aftershock triggering as well as fractal patterns and complex space-time coupling. Most importantly, the expected "average" behavior of individual defects was not detected. The experiments showed that the intermittent character of the steady state inelastic deformation is due to the collective motion of millions of defects. The emergence of large fluctuations can be broadly assigned to the competition between the small-scale disorder (structural inhomogeneity, quenched defects, heterogeneities) and long-range interactions.

Meanwhile, these studies focused on the statistical properties of acoustic events until the steady state and didn't investigate the behavior of the material beyond. In this thesis, such an analysis will be performed until failure, to understand how fatigue born at microscopic scale through the evolution of the properties of the power-law distributions of acoustic signals.

1.2.3 Highlight of the originality and universality of this approach

We aim at the development of a thoroughly new method of a non-destructive testing, allowing the practitioners to monitor in real time the initiation of the fatigue crack formation of a cyclically loaded structure. The method includes a potential for the identification of the early precursors to ultimate fatigue failure which have never been attempted before. Behind this method is the idea of criticality which has not been used previously in fatigue studies. From a long term vision, a broad spectrum of industries, from aeronautical to bio-medical, will be interested in the development of such methods.

The proposed approach is based on a new way of monitoring the collective dynamics of defects during the fatigue life of structure. The novelty of our approach lies in the focus on the features in the acoustic signal that have not been studied previously. More specifically, we propose to use the scaling properties of the acoustic signals generated by the internal instabilities associated to collective depinning of a large number of defects as a measure of closeness to ultimate failure. The main theoretical idea is to identify precursory signals of fatigue from the crossover between different critical regimes.

The approach is truly multi-scale since criticality excludes in principle the possibility of conventional separation of scales. The originality stands in bringing together two seemingly unconnected concepts, fatigue and criticality, and in utilization of some of the most advanced concepts from theoretical physics to mathematics to achieve this goal. The fundamental interest is the new links that the proposed approach establishes between different research fields that require knowledges in many scientific disciplines such as applied mathematics, mechanical engineering, materials science or statistical physics. That is the reason why a miscellaneous bibliography will be developed in the next chapter.

Bibliography

2

Contents

This chapter is devoted to the introduction of the knowledges, concepts and tools required to read this thesis. It must be considered as an help for readers which are not familiar with these topics. A deeper analysis of the works covering the specific thematics of this thesis is done at the beginning of each chapter. Nevertheless, a peculiar attention is dedicated to introduce the concept of self-organized criticality which is unusual in the frame of fatigue.

2.1 Shape Memory Alloys and Fatigue

2.1.1 Shape Memory Alloys materials

Discovery and applications

The nickel-titanium alloys were first developed in 1963 by the US Naval Ordnance Laboratory and commercialized under the trade name Nitinol (an acronym for Nickel Titanium Naval Ordnance Laboratories). Their remarkable properties were discovered by accident. A sample that was bent out of shape many times was presented at a laboratory management meeting. One of the associate technical directors, Dr. David S. Muzzey, decided to see what would happen if the sample was subjected to heat and held his pipe lighter underneath it. To everyone's amazement the sample stretched back to its original shape.

Nowadays, the most popular alloys used in industrial applications are Cu-Al-Ni and Cu-Al-Zn for copper based alloys and near equiatomic TiNi, particularly in medicine and space applications. Among the several applications of SMA in different types of industries, one can cite:

- *Piping.* The first consumer commercial application for the material was as a shape memory coupling for piping, e.g. oil line pipes for industrial applications, water pipes and similar types of piping for consumer/commercial applications. The late 1980s saw the commercial introduction of Nitinol as an enabling technology in a number of minimally invasive endovascular medical applications. While more costly than stainless steel, the self expanding properties of Nitinol alloys manufactured to BTR (Body Temperature Response), have provided an attractive alternative to balloon expandable devices. On average, 50 percents of all peripheral vascular stents currently available on the worldwide market are manufactured with Nitinol.

- *Optometry.* Eyeglass frames made from titanium-containing SMAs are marketed under the trademarks Flexon and TITANflex. These frames are usually made out of shape memory alloys that have their transition temperature set below the expected room temperature. This allows the frames to undergo large deformation under stress, yet regain their intended shape once the metal is unloaded again. The very large apparently elastic strains are due to the stress-induced martensitic effect, where the crystal structure can transform under loading, allowing the shape to change temporarily under load. This means that eyeglasses made of shape memory alloys are more robust against being accidentally damaged.

Properties of shape memory alloys

What are shape memory alloys? SMA are fascinating materials which exhibit properties that usually do not characterize ordinary metals and alloys. Among these special properties, one can notice as examples, the shape memory effect (one way and two way shape memory), the superelasticity or the damping effect. These extraordinary properties lead to use

shape memory alloys as *smart materials* also know as new functional materials. Shape memory behavior refers to a peculiar thermo-mechanical behavior in which small changes of one or two of the three thermo-mechanical variables (temperature, strain and external stress) can induce extremely large modifications of the two other thermo-mechanical variables. This change of shape is based on a solid-solid phase transition between austenite and martensite which is induced by the change in thermo-mechanical variables mentioned before.

Martensitic transformation The martensitic transformation is a solid-solid phase change, from a solid phase called austenite into another solid phase with lower crystallographic symmetry called martensite. The lower symmetry of this phase enables the existence of several martensite variants defined by the orientation of their habit plane. The existence of a martensitic variant depends on the thermo-mechanical state. Two types of martensitic structures may exist within a SMA:

- self-accommodating martensite, when all variants are equiprobable. The martensite is said to be "twinned" in this case and no macroscopic strain is observed.
- detwinned martensite, when a stress state favors the growth of some particular variants of martensite; this leads to the apparition of a macroscopic strain.

In SMA, the martensitic transformation is a thermoelastic transformation, because the interfaces between phases are mobile enough to allow the shrinkage of the martensite plates through a backward movement Otsuka and Wayman (1998); it is crystallographically reversible. The crystallographical theory of the martensitic transformation has been studied by M. Wechsler and Read (1953), Bowles and Mackenzie (1954). The martensitic transformation is characterized by an inelastic transformation of the crystal lattice. It is a displacive transformation involving collective and cooperative motions of atoms, on a distance smaller than the lattice parameters, with no diffusion. The martensitic transformation is a first-order transition; during a martensitic transformation, martensite and austenite coexist, separated by an invariant plane. Volumetric and shear strains are created, with shear strain being far greater. During the transformation, a latent heat is absorbed or released, according to the direction of transformation. The amount of heat produced is proportional to the volume fraction of the transformed material.

Finally, the transformation can be either influenced by temperature or by stress. But beyond the words, let us introduced visually martensite and austenite through pictures captured from a movie realized during this thesis. The movie focused on several grains of a heated Cu-Al-Zn alloy that exhibits a phase transition. One can observe the progressive appearance of the martensite plates in figure 2.1.

Pseudo-elasticity Pseudo-elasticity is a dissipative phenomenon of the mechanically loaded SMA materials which occurs when the material are in the austenitic phase. The dissipative behavior is shown in the stress-strain

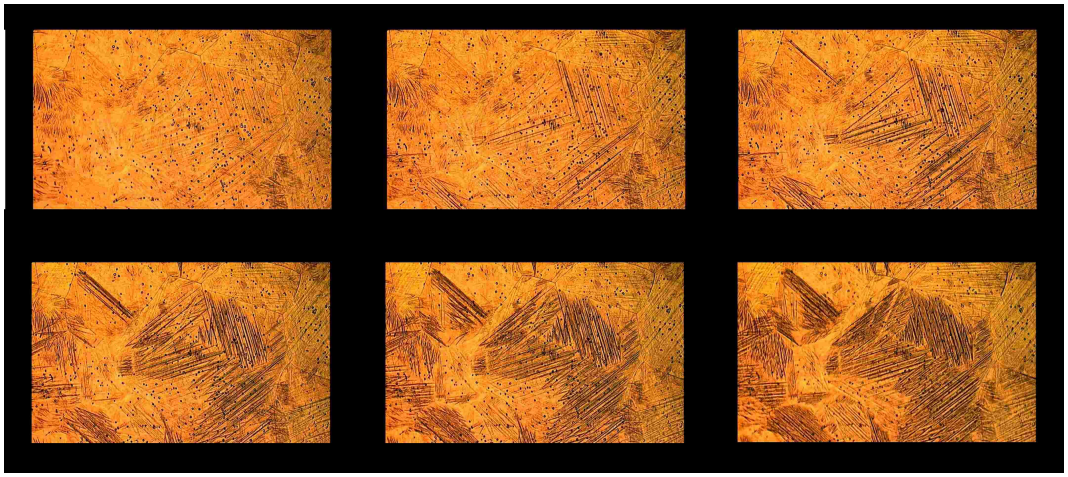

Figure 2.1 – *Appearance of the martensite plates under a thermally induced martensitic transition - ref: personal pictures*

space since the trajectory is not identical during loading and unloading which results in an hysteresis loop as shown in the figure 2.2.

The response of the material is elastic for an applied stress lower than σ^{Ms} which corresponds to the beginning of the phase transition plateau, the stress at the beginning of the phase transition denoted Ms for Martensitic Start. At the end of the plateau, which is determined by σ^{Mf}, the stress at the end of the martensitic transition denoted Mf for Martensitic Finish, the material is theoretically fully transformed and composed of oriented martensite. The response of the material for a stress greater than σ^{Mf} is elastic, it is the elastic domain of the martensite. The macroscopic deformation is important at this stage. During unloading, the reverse transition is observed, from martensite to austenite with values σ^{As} and σ^{Af} corresponding to the yield stresses of beginning and end of transformation of austenite. Coming back in austenitic state, deformation is recovered and the global deformation is null. This phenomenon is called pseudo-elasticity.

SMA display other unusual properties, like the super-thermic effect, magnetic shape effect, the one and two ways memory effect as well as the rubber-like effect that will not be detailed here. Meanwhile, the interested readers can refer to the very thorough book of Otsuka and Wayman (1998).

2.1.2 Fatigue of shape memory alloys

Experimental behaviors of SMA in cyclic loading

The theoretical pseudo-elastic behavior is only checked for the first cycles and the response is strongly modified upon cycling. Several experimental studies have been led on SMA in cyclic loading to analyze the modifications of the shape of the hysteresis loop with the number of cycles. The hysteresis loop is characterized by three main quantities, linked to the martensitic transition, that will be changed with cycles. These quantities are shown in figure 2.3 and detailed in the following items:

1. The stress of the beginning of the martensitic transformation σ_{Ms}

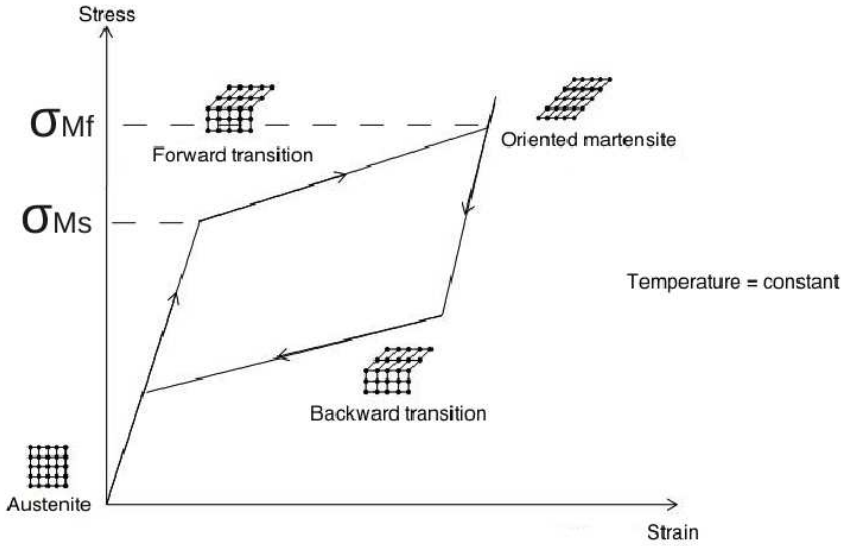

Figure 2.2 – *Schematic representation of a pseudo-elastic loading*

that decreases with the number of cycles. σ_{Ms} decreases with the increase of the number of cycles Melton and Mercier. (1979). Indeed, slip deformations induce internal stresses and permit the creation of oriented martensite in these areas and then it decreases the external stress needed to change the phase of the material.

2. The dissipated energy quantified by the hysteresis loop, which is the area of the loop, that decreases with the number of cycles. Moumni et al. (2005) explain that the area of the hysteresis loop is evolving during the first cycles and then it reaches the stable state and it stabilizes. This behavior implies a decrease of the dissipated energy per cycle with the number of cycles until reaching an asymptotic value for the stabilized cyclic behavior.

3. The residual strain ϵ_r increases with the number of cycles. The pseudo elastic behavior is not perfect, and it is well shown by the non-closed hysteresis loop. Since the first loading cycle, it remains a residual strain after unloading. Explanations of this phenomenon diverge. A first explanation Lexcellent et al. (2000) is that residual strain is a consequence of the existence of residual and oriented martensite which is not concerned by the phase transformation. A second explanation is that this residual strain is linked to microplasticity that occur during pseudo-elastic loading Bo and Lagoudas. (1999). This residual strain increases in a exponential form until reaching an asymptotic value, then, the material is in a stable state called shakedown state of the pseudo-elastic loading even if in reality it always remains an infinitesimal residual strain at the end of each cycle.

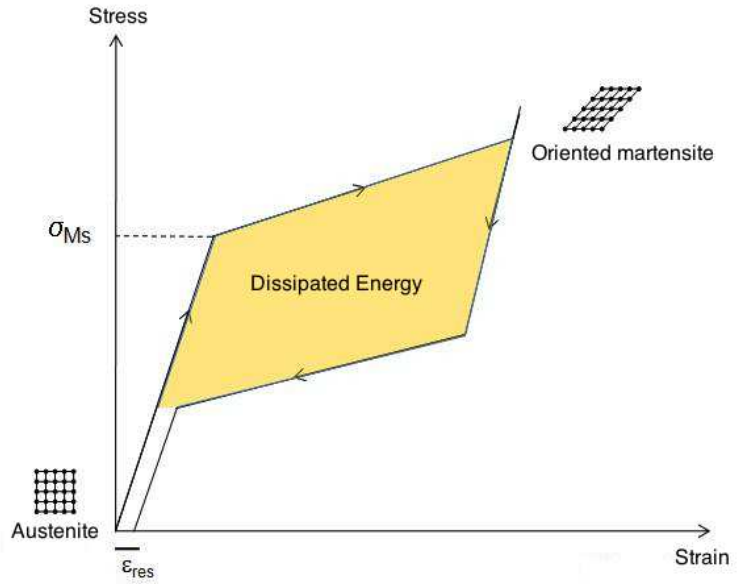

Figure 2.3 – *Three main variables of hysteresis loop*

The hysteresis loop

The hysteresis loop is of prior importance in fatigue comprehension of shape memory alloys because it is an indicator of the dissipated energy per cycle. Consequently, several authors studied the modification of the hysteresis loop. Meanwhile, it will not be presented in this manuscript since their approaches are totally different of the one taken in this thesis since these models used the thermodynamics formalism and a macroscopic point of view. These models are mainly theoretical and far away from the experimental considerations that will be at the basis of our understanding of mechanisms. Nevertheless, interested readers are invited to read the papers of Abeyaratne and Kim (1997), Tanaka et al. (1995), Lexcellent and Bourbon (1996), Bo and Lagoudas. (1999), Zaki and Moumni (2007) and Morin et al. (2010).

The highlight is only given on the model of Zaki and Moumni (2007) Moumni et al. (2005) that is partly at the inception of this PhD subject. Thanks to cyclic loading experiments on shape memory alloys, they noticed that the dissipated energy per cycle was diminished during the first cycles before stabilizing around a quasi constant value. Making the hypothesis that the major part of the lifetime of the material is in this stabilized phase, they tried to link the dissipated energy in the stable state and the number of cycles to failure. They brought to light an energy based law which validates experimental results in the tensile case.

The goal of this thesis lies in the continuity of this work to study thanks to acoustic emissions monitoring the micro-structural changes that occur when the dissipated energy seems quasi constant at the macro scale. The fact that it is not perfectly constant is a proof that some underlying microscopic mechanisms are still taking place although macroscopic shakedown seems to be reached. Those mechanisms can not be seen thanks to macroscopic variables, that is the reason why we hope to reveal this activity thanks to acoustic monitoring to quantify the evolution of internal

damages and find indicators of fatigue crack initiation at a microscopic scale.

Many experiments were performed during this thesis. These experiments involved several coupled devices. Among them are a servo-hydraulic loading machine, an acoustic emission monitoring system and an infrared camera. Consequently, readers that are not used to these experimental systems are invited to read the appendix A to understand how data are generated, recorded and filtered.

2.2 Complexity and self organized criticality

2.2.1 Introduction about complex systems

What is complexity? How to properly define complexity? Here are probably two very ambitious questions. This concept of complex systems is born with the interest of people about out-of-equilibrium dynamics (e.g. dynamical phase transition) and heterogeneous systems (e.g. spin-glasses). In each case systems are dealing a large number of elements with mutual interactions which are the base of an exchange of matter, of energy or of information with their environment. This constitutive parts of complex systems self-organize their internal structure and their dynamics to expose a novel and outstanding macroscopic behavior, also known as emergent property.

But let us define the common properties of complex systems Mitchell (2009):

- Complex collective behavior, all complex systems consist of large networks of individual components (ants, e.g. see figure 2.4, neurons, stock-buyers), each typically following relatively simple rules with no central control or leader. It's the collective actions of vast number of components that give rise to complex system. The occurrence of coherent large-scale collective behaviors with a very rich structure is a consequence of the repeated non-linear interactions among its constituents : the whole turns out to be much more than the sum of its parts.

- Signaling and information processing, all complex systems produce and use information and signals from both their internal and external environments.

- Adaptation, all complex systems adapt themselves, change their behavior to improve their chances of survival or success through learning or evolutionary processes.

Now, one can define more properly what is a complex system: it's a system in which large networks of components with no central control and simple rules of operation give rise to complex collective behavior, sophisticated information processing and adaptation via learning or evolution. Therefore, it can be defined as a system that exhibits nontrivial emergent and self-organizing behaviors.

Self-organized critical systems is representative of a sub-class of complex systems.

Figure 2.4 – *Bridge constituted by ants which is one of the most famous natural example of complexity*

2.2.2 Genesis of Self-Organized Criticality (SOC)

The Self-Organized Criticality (SOC) concept was introduced by Bak et al. (1988). In this famous paper, they made the hypothesis that systems consisting of many interacting constituents may exhibit some general characteristic behavior. One of their claims was that dynamical systems organize themselves into a state with a complex but rather general structure. The complexity of system stands in the fact that no single characteristic event sizes. One can not just consider one time and one length scale that controls the temporal evolution of these systems. Although the dynamical response of the systems is complex, the simplifying aspect is that the statistical properties are described by simple power laws. One other claim was that this typical behavior was developed without the "tuning" of any outside parameter, in this sense systems self-organizes. Moreover, the states into which systems organize themselves have comparable properties with the ones exhibited by equilibrium systems at the critical point. Therefore, these systems have been qualified as SOC.

The sandpile model In this pioneer article, Bak et al. (1988) introduced the sandpile model as a toy model to illustrate their concept. The functioning can be summarized as follows. When you first start building a sand pile on a tabletop, the system is weakly interactive. A sand grain drizzled from above onto a randomly chosen location on the tabletop has little effect on sand grains at other locations. However, as you keep dribbling sand grains from above onto randomly chosen tabletop locations, eventually the sandpile at one or more locations reaches a "critical state" where the pile cannot grow any higher without a breakdown of the pile occurring. These breakdowns can be of various sizes depending on the exact configuration of the sand pile at the time the breakdown occurs as shown in figure 2.5. Bak refers to these critical states as states of self-organized

criticality (SOC), i.e., states in which the system has self-organized to a point where it is just marginally stable. But, what does it mean to say that "breakdowns of all different sizes" can happen at SOC state? The dribbling of one more grain of sand onto a location in a SOC state can result in an "avalanche" or "sand slide", i.e., a cascade of sand down the edges of the sand pile and (possibly) off the edge of the table. The size of this avalanche can range from one grain to catastrophic collapses involving large portions of the sand pile. Bak conjectured that the size distribution of these avalanches obeys a "Power Law" over any specified period of time T. That is, he conjectured that the average frequency of a given size of avalanche is inversely proportional to some power of its size, implying that big avalanches are rare and small avalanches are frequent.

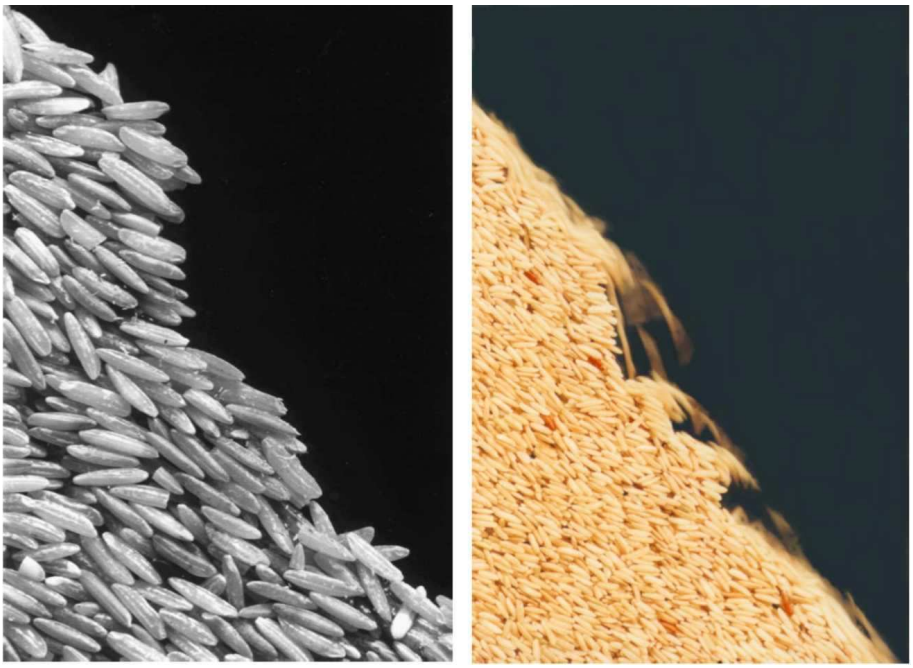

Figure 2.5 – *Pictures taken in experiments led on ricepile by Frette et al. (1996) to study experimentally the sandpile model*

Theoretically, a large number of discrete and sandpile models have been studied. This point is not the core of this thesis but interested readers can refer to the Abelian sandpile model Dhar (1990) which is the simplest and the most popular, and the models of Zhang (1989), Priezzhev et al. (1996), Takayasu (1989). In each case, these models do not aim at reproducing the exact dynamics of a sandpile, there are studies discussing this specific point Held et al. (1990), Jaeger et al. (1989; 1992), but rather at introducing a generic toy model able to capture the key mechanisms of a broad class of system. One can think to illustrate this point that a plane made with a sheet of paper reproduces several key phenomenon of the ability to fly of a real aircraft.

2.2.3 Characterization of the SOC state

Defining and characterizing SOC is not an easy task because we are dealing with a concept which needs to be well-specified. This definition must

be based on physical mechanisms rather than on observations. Among the literature, the definition which is the most rigorous in my point of view is the one given by Sornette (2003) which is quoted below :

> SOC refers to the spontaneous organization of a system driven from the outside into a globally stationary state, which is characterized by self-similar distributions of even sizes and fractal geometrical properties. This stationary state is dynamical in nature and is characterized by statistical fluctuations, which are referred generically to as "avalanches".

These avalanches, correspond to rare and sudden transitions that occur over time intervals that are short compared to the characteristic time scales of their posterior evolution. These crises, are the core of the main evolution inside the system and large event can be viewed, as defined by Sornette (2003) *as belonging to the natural non-linear organization of complex systems according to the SOC concept. They can result from the long-range power-law decay of spatial and temporal correlations and the heavy tail power-law distributions of even sizes*. It's essential now to distinguish how critical are these burst events. In a supercritical system, a single local event leads to an exponentially exploding process. In a sub-critical process, activity is exponentially decaying, always dying out. In the critical state, the activity is just able to continue indefinitely, with a power-law distribution of stopping times, reflecting the power-law correlations in the system. Thus, one has to be aware that SOC refers to complex system which are marginally stable, oscillating at the edge of order and disorder in a critical state.

These out-of-equilibrium systems are made of many interactive components and possess the following properties:

- a highly nonlinear behavior, which refers to the threshold response
- a very slow driving rate
- a globally stationary regime, characterized by stationary statistical properties
- power-law distributions of event sizes, and fractal geometrical properties which take into account the long range correlations.

Among SOC systems, another fundamental aspect is constituted by the threshold dynamics. The threshold must be highly considered since it acts as a local rigidity that allows the separation of time scales and produces a large number of metastable states. These conditions of time scale separation and metastability are essential for the existence of scale invariance in this class of systems. Scale invariance must be discussed here as it is an essential component of self-organized criticality. This property means that when an object is looked at different levels of magnification, its structures remains roughly the same. This was termed as fractals by Mandelbrot (1982) and mathematically, scale invariance can be captured by a power-law. For physical phenomena scale invariance is an indicator of the absence of any characteristic length or time scale in a spatially extended dynamical system with both temporal and spatial degree of freedom.

2.2.4 "Rain is earthquakes in the sky" - Christensen

Beyond, the theoretical example of the sandpile, several other systems from very various fields of sciences are exhibiting SOC behavior. Indeed, beyond being very beautiful, the citation of Christensen suggests an analogy between disconnected systems, a priori, that nevertheless share common properties in the frame of SOC. All these systems possess the following aspects:

- slowly driven non-equilibrium
- threshold dynamics
- Relaxation event dissipates energy
- Reaches statistically stationary state
  where $< influx >=< outflux >$
- Relaxation events of all sizes up to a system dependent cut-off

Based on these key properties, an attempt is realized to summarize examples of SOC in our day to day life in the following table:

System	Source	Storage	Threshold	Relaxation
Earth's crust [1]	convection	tension	friction	earthquakes
Landslide [2]	moisture	potential	friction	landslide
Atmosphere [3]	sun	vapor	saturation	rain event
Sandpile [4]	adding grains	potential	friction	avalanche
Snow avalanche [5]	snow	potential	friction	avalanche
forest fires [6]	sparking	heat	density	burn area

These examples are just a short list of all the phenomena that scientists have tempted to explain with SOC which provides a general mechanism for the emergence of complex behavior in nature. It has also been proposed that traffic Nagel and Paczuski (1995), magnetic fusion plasma Dendy and Helander (1997), river networks I. Rodriguez-Iturbe (2001), superconductors in a magnetic field Field et al. (1995), etc., all operate in a self-organized critical state.

Among these examples, one will be discussed intensively in the chapter 4, earthquakes. Attention will be given to detail each point of the former table and demonstrate how linked it is with the cyclic loading of SMA. Let us now turn to the suspected mechanisms that could lead to SOC.

[1] Bak et al. (2002)
[2] Malamud et al. (2004)
[3] Peters et al. (2001)
[4] Frette et al. (1996), Christensen et al. (1996)
[5] Bak et al. (2002)
[6] Malamud et al. (1998)

2.2.5 Scenarios leading to SOC

The mechanisms by which an open system self-organizes into a state with no characteristic scale is not unique. Several mechanisms have been studied in the literature and three different classes of systems are proposed to be at the origin of SOC.

- The first class of systems exhibits SOC as a result of its tendency to synchronize Corral et al. (1997). Meanwhile this tendency is frustrated by constraints such as open boundary conditions and quenched disorder which lead to a dynamical regime at the edge of synchronization, the SOC state.
- Extremal models are the second class to exhibit SOC due to the competition between local strengthening and weakening due to interactions Paczuski and Boettcher (1997).
- A third class of models is constituted by multiplicatively driven systems. Due to its multiplicative driving, criticality occurs even with periodic boundary conditions via a coarsening process. The observed behavior should be relevant to a class of systems approaching equilibrium via a punctuated threshold dynamics Sornette et al. (1995)

There are other suspected scenarios able to lead to SOC. Interested readers can refer to the thorough book of Sornette (2003) which gives the details of all of them.

2.2.6 SOC and material sciences

After the introduction of the concept of SOC Bak et al. (1988), different fields of sciences were reported as key examples of SOC. Among the first ones were the geophysics natural phenomena exampled with earthquakes Bak and Tang (1989), Sornette and Virieux (1992), snow piles Chen et al. (1991), or volcanic rocks Diodati et al. (1991).

Indeed, this pioneer work of Diodati et al. (1991) on the survey of the Strombolian activity through acoustic emissions was the first to verify that SOC provides a robust framework to understand the relaxing dynamics underlying AE phenomena. Scaling laws for time and amplitude distributions of the AE bursts were reported and the other key properties of SOC were checked one by one. This paper is the core of many other following studies in the domains of fracture and plasticity.

Fracture

The key property of the SOC systems is the scale invariance and consequently, considering the results of Sornette and Diodati at very large scales (earthquakes and volcano), it was natural to carry out studies about fracture at smaller scales. This was performed through the works of Petri et al. (1994) and Cannelli et al. (1993). These works were among the first to focus on the SOC formalism as an explanation of micro-fracturing processes. The applicability of SOC to micro-fracturing has been immediately

questioned, however, as power-laws alone are not unequivocal evidence for it Sornette (2003), Cannelli et al. (1993).

The year 1997 The year 1997 was prolific in interesting articles dealing with fracture. Subsequently to these empirical discoveries, Zapperi et al. (1997) introduced one of the first model that deal with plasticity and avalanche behavior in micro-fracturing process. This model, in the spirit of the random fuse model previously established by L. de Arcangelis and Herrmann (1985), takes a mesoscopic point of view and a very simple plastic relation between the effective Hooke tensor and damages that is sufficient to recover the empirical observations that is a plastic steady state with its associated power-law distributions for the size, energy of events and the time intervals between events.

Regarding the experimental advances, Garcimartín et al. (1997) presented experimental data underlying the strong analogy between the formation of a crack in composite materials and percolation in a fuse network. They brought empirical proofs that micro-cracks cluster along the final crack and that fracture can be thought of as a critical phenomenon.

At the same time, studies were also beginning to take interest in the comprehension of the scaling laws of the roughness of the fracture surface with the works of Bouchaud (1997). The morphology of fracture surfaces of various materials are reviewed. The observations are interpreted within the frameworkd of models of lines moving in a random environment. This suggests that fracture of heterogeneous materials could be seen as a dynamic phase transition.

Plasticity

The same year, one pioneer work stands the basis of the study of plasticity with the critical angle. This works is the one of Weiss and Grasso (1997) which revealed, in the monotonic loading of a single ice crystal, the strongly intermittent plastic flow characterized by jerks of dislocations with power-law distributions of energy. Few years later, Weiss et al. (2001), Weiss and Marsan (2003), Weiss and Miguel (2004) and Miguel et al. (2001) get through another step by realizing the following key discoveries:

- The viscoplastic deformation during the creep of ice occurs by a succession of avalanches which result from elastic interactions between dislocations
- Dislocation avalanches consist of a main shock correlated in time with a sequence of aftershocks
- The distribution of AE energies follow a power-law distribution scaling with an exponential cutoff which depends on the creep stage. They suggest the framework of non-equilibrium critical phenomena.
- Scale-invariant distribution of the locations of the avalanches of dislocations.

- Dislocations motions are coupled in space and time that organize themselves into avalanches that are themselves dynamically coupled into avalanche cluster, plasticity results from a collective phenomenon.

These findings are of prior importance to consider some results presented in this thesis.

Regarding the modeling aspect of these discoveries, Zaiser and Aifantis (2006) contributed intensively to the development of models that aim at capturing these lack of scales in plasticity. Then, other classes of materials extended the field of knowledges through the work of Richeton et al. (2006) who recovered results really similar to those found for ice in metallic single crystals. These works strengthened the idea of the universal character of plasticity which is sustained in Weiss et al. (2007).

Dimiduk et al. (2006) is another key contributor in the comprehension of the scale-free intermittent flow in crystal plasticity through the clever experiment he realized at the nanometer scale. Working at such small scales permitted to directly determine the sizes of discrete slip events which are distributed according a power-law ranging on three orders of magnitude. Moreover, the time structure exhibited by the material exhibited a shock-and-aftershock earthquake-like behavior. Miguel and Zapperi (2006) discussed this result drawing parallels with the previous works of Uchic et al. (2004) which dealt with the influence of the sample dimension on strength and the model of Zaiser and Moretti (2005) designed to account for fluctuation phenomena in crystal plasticity.

Finally, it is worthwhile to notice the article of Csikor et al. (2007) that demonstrated the universality of avalanche behavior in plasticity and elucidate the cross-over between intermittent and smooth plastic flow. It is explained that avalanche strains decrease in inverse proportion to sample size which results in difficulties to observe strain bursts in macroscopic sample. Meanwhile dislocation avalanches arise, on all scales, from the most basic feature of dislocation motions.

Martensitic phase transition

SOC has also received a particular interest from people who were working on materials displaying a first-order phase transition. These materials, slowly driven exhibit sudden and local changes in their strain field, for martensitic materials or in their local magnetization for magnetic materials. Indeed, the acoustic emission in ferroelastic systems is the analog of Barkhausen noise in magnetic materials Colaiori et al. (2004), Durin and Zapperi (2000). The avalanches generated during this phase transition reflect the fact that these systems dissipate energy, which causes the hysteresis loop, to go from one marginally metastable state to an other metastable state. The intrinsic distribution of disorder in the system determines the configuration of the metastable minima. Consequently, many studies were led in these two kinds of materials but the study of magnetic materials will not be treated and focus is made on the martensitic materials.

In this domain, Vives has undoubtedly contributed the most intensively to the discoveries of the SOC character of the phase transition of

SMA. The scale-free distributions of avalanche size and duration associated to the thermally induced martensitic transition were first reported in its precursory article Vives et al. (1994). Then, it was shown Vives et al. (1995) that the distributions are independent of the temperature indicating that the physical behavior is unchanged along the transformation. The first part to transform are statistically transformed as the last. This criticality can be understood in echo of the works of Sethna et al. (1993) on lattice models with quenched disorder following athermal dynamics that correspond to a local energy relaxation. This local character is responsible for the fact that systems evolve, when driven by an external field, through metastable states rather than an equilibrium path. Criticality emerges for a sufficient amount of disorder and it has been checked by the fact that dislocations are formed during the transformation process Pons et al. (1990) and consequently cycling through the transition enables to control the amount of disorder Perez-Reche et al. (2004).

Cyclic martensitic transition The question of the evolution of the power-law distributions upon cycling was first raised by Carrillo and Ortín (1997) found that cycling reduces the extent of power-law behavior. The energy barrier sizes encountered during the transition are scale-invariant, which sustained the complexity of the free energy landscape. Carrillo et al. (1998) also brought empirical evidences that this scale-free behavior hold for different alloys, that exhibit a phase transition, independently of their chemical composition, concentration, phase temperature, heat treatment, etc... The sufficient amount of disorder needed was quantified through the demonstration that, after few cycles, distributions became critically stable.

In the continuity of these works, it was shown that the distribution of the amplitudes of avalanches evolve, for an initially virgin sample, from supercritical to critical with the number of cycles by Perez-Reche et al. (2004). The first quantitative measure of the changes occurring from cycle to cycle was introduced through the statistical correlation between the AE patterns of the consecutive loops. The correlation is low in the first cycles and after roughly ten cycles the activity profile tends toward a stable pattern which exhibits a higher correlation. This result shows that the disorder evolves in such a way that the systems reaches a stationary metastable trajectory after the learning which then becomes reproducible. The dissipated energy is then a minimum according to Prigogine's theorem Prigogine I. (1977).

The driving mechanism of the transition has also been studied and recognized as strongly influent. All the studies previously exposed, focused on thermally induced transition. Heczko and Straka (2004) studied the strain driven martensitic transition of a Ni-Mn-Ga alloy. An asymmetrical response of the material between the behavior during loading and unloading is noticed.

Bonnot et al. (2008) adressed this question by submitting a Cu-Zn-Al single crystal to a stress and strain driven experiment. One conclusion was the inclusion of the strain hysteresis loop in the stress hysteresis loop showing a much large dissipation of energy in the second case. Moreover, the shape of the hysteresis loop is different since the stress-driven curve display a linear behavior during the transition, whereas the strain-

driven curve shows a yield point followed by strong instability of the force. Pérez-Reche et al. (2008) proposed a model to explain the influence of a soft driving (displacement is free to fluctuate and force is imposed) and hard driving (displacement is constrained and force can fluctuate). They found a crossover, determined by the driving mode, between two kinds of criticality. Soft driving corresponds to criticality whereas hard driving corresponds to self-organized criticality, the first one requiring the fine tuning of disorder whereas the second is disorder independent. They associated one different physical mechanism for each mode, the first one describes regime with nucleation whereas the second deal exclusively with propagation. Vives et al. (2009) recently led experiments for stress and strain driven Cu-Zn-Al SMA. The three important conclusions to keep in mind are that:

- The values of the energy distributions tend to stabilize with cycling as found for thermally induced experiments, meanwhile, exponents are first decreasing as a exponential for the stress driven transition whereas, it seems independent of cycles for the strain driven case.
- After stabilization, exponents does not depend on the driving rate.
- Exponents for the stress-driven case are larger than exponents for the strain-driven case which is in accordance with the model previously exposed.

These findings are of great importance since no study are specifically studying the behavior in fatigue of the SMA within the framework of criticality. As a consequence, these empirical evidences in cycling will be our unique points of comparison.

A large range of study in martensitic transition are also devoted to the modeling of the hysteresis, the evolution of the micro-structure and the correlations as well as the jerky nature of the transformation. It will not be developed here but interested readers can refer to the works of Sreekala et al. (2004), Ahluwalia et al. (2004), Cerruti and Vives (2008), Perez-Reche et al. (2007) or Salman and Truskinovsky (2011).

A major part of this thesis focused on the concept of self-organized criticality which embedded the power-law distributions of times and energies of the analyzed system. As a consequence, it comes naturally that a precise mathematical definition of what is a power-law is necessary. The fascinating world of the power-law distributions and their associated scale-free property and mathematical definitions can be found in appendix A for readers who are not used to this kind of distributions.

2.3 Conclusion

This bibliographical chapter enabled to introduce the knowledges regarding the triptych of this thesis SMA, fatigue and SOC.

It has been explained what are shape memory alloys and how their properties are transformed with cycling, noticeably, the evolution of the

hysteresis loop in the stress strain diagram during the transient phase until its stabilization in the stable state.

On another hand, the SOC concept was introduced with its constitutive properties, non-linear and threshold response, stationary conditions and power-law distributions of the size and duration of events. Consequently, scientists made used of this concept in a wide range of areas, from geophysics natural phenomena to fracture and for the martensitic transition. Studies of the martensitic transition in the SOC framework, revealed an evolution of the exponents of the power-law distribution in the first cycles.

3 Multi-scale characterization of the shakedown state

Contents

This chapter provides an original experimental characterization of the shakedown state of a shape memory alloy structure under cyclic loading. Three synchronous measurements, mechanical, thermal and acoustic enable to define properly the different stages encountered in the transformation of the material response from virgin to stable state. A complex behavior in the interlocked thermo-mechanical responses of the material is revealed through the complete experimental device.

The aim of this chapter is to analyze the different dissipations of energy due to the repeated loading of SMA. It will be done through mechanical, thermal and acoustic measurements. A unified approach of the martensitic transition and its evolution with cycling is proposed through this experiment.

The challenge is to know if the cyclic loading of NiTi SMA displays a critical behavior, what are the corresponding exponents of the power-law distributions and how they evolve from the initial to the shakedown stage. The results found for copper-based alloys allowed being optimistic about the expected conclusions.

3.1 The shakedown state

We are introducing here the term shakedown state in fatigue analysis in comparison with plasticity studies. Indeed, it was initially used to describe a macroscopic stabilization of the plastic response of a material. In this thesis, we are dealing with pseudo-elasticity rather than plasticity but we will use the term pseudo-elastic shakedown state which refers to the stabilization of the responses (acoustic, thermal, mechanical) of a repeatedly loaded SMA in a strain stress diagram. Consequently, a bibliography is devoted to underline the key properties that were previously studied to quantify the evolution of the key properties of an SMA through cycling due to the martensitic transition, plastic effects and micro-damages.

Solid-solid phase transition between different crystal structure of shape memory alloys (S.M.A.) was widely studied over the past few years Delaey et al. (1974). There are numerous methods used to understand how the martensitic transition (MT) takes place:

- **Microscopic observations** Among the studies that focused on the structural changes that are operated at the microscopic scale to understand the modification of crystallography one can report the following results needed for the comprehension of our experiment. The typical change observed is a structural change from a cubic (austenite) to a less symmetric phase (variant of martensite). Among the selected variant types of martensite that are symmetrically equivalent the system chooses the ones that are optimally oriented with the applied stress, which also results in large inhomogeneities in the strain field Shaw (2000). This transformation is not reversible due to the hysteresis phenomena but the sample can recover its initial shape when the stress is released. This is due to the existence of free energy barriers much larger than thermal fluctuations, which originated from the interplay of the elastic interactions and disorder Salje et al. (2011). Moreover, the transformation is never realized at 100%, but rather 70% and the transformation begins after a given non-zero strain (approximatively 0.7% strain) observed by optical microscopy Brinson et al. (2004). The observed plastic deformation accompanying the stress-induced phase transition has been attributed to the motion of the dislocations lying in the matrix at the interface with martensite Miyazaki et al. (1986), Jiang et al. (1997). These different dislocation activities and arrangements, detailed in Norfleet et al.

(2009), are associated to hysteresis loss, decrease in transformation stress and remanant strain Gall et al. (1998), Melton and Mercier. (1979). The cycling effect was also reported by the observations of Brinson et al. (2004) who showed that there is an accumulation of localized plastic deformation within the grains upon load cycling. This localized deformation rises in magnitude with each cycle, producing a significant residual martensite, macroscopically visible.

- **Calorimetric monitoring** Perez-Reche et al. (2004), Bonnot et al. (2008), Gallardo et al. (2010) studied the MT thanks to calorimetric devices. Perez-Reche et al. (2004) demonstrated that the effect of thermal cycling on a copper alloy was essentially a diminution of the entropy change, of the area of the hysteresis loop and a decrease of the starting temperature of the transition. These three quantities decline during the first cycles before stabilizing after approximatively 10 cycles. Gallardo et al. (2010) realized a deep advance by showing that calorimetric and acoustic spikes have the same physical origin and showing that the energies recorded by the two methods are distributed as power-laws with the same exponent during a thermally induced phase transition of a copper based alloy.

- **Acoustic emission monitoring** This question was detailed in the bibliographical part regarding the martensitic phase transition in the section about criticality in material sciences. For memory, the main results are the ones of Vives et al. (1994; 1995), Perez-Reche et al. (2004; 2007), Pérez-Reche et al. (2008), Vives et al. (2009) and a new result which is the contribution of Vives et al. (2011). The main conclusions are that the MT displays a scale-free character for the size and duration of the avalanches Vives et al. (1994; 1995). Cycling results in the evolution of the exponents during the first cycles and then it stabilizes for thermally induce MT on copper based alloy Perez-Reche et al. (2004). The distributions are evolving from power-law with exponential cut-off to pure power-law distributions after roughly 15 cycles. Perez-Reche et al. (2007) introduced the knowledge that cycling can be viewed as a training process. This means that during such a loading and reloading process, SMA self-organize towards criticality. the material tends to avoid the high energy barriers which separate local metastable states to find an optimal energy path . An evidence of this is the reduction of the dissipated energy. Finally, one has to notice the key role played by the dislocations that are responsible for the scale-free character of the phase transition since it is the ability of the material to develop an optimal amount of disorder that makes possible the attainment of criticality Pérez-Reche et al. (2008).

  Recently, Vives et al. (2009) reported the differences that exist when the MT is stress or strain induced (previous studies where thermally induced), notably, it was noticed that cycling is needed to reach a critical state for stress-driven experiments whereas strain driven experiments are initially in a SOC state. Consequently, the exponents of each type of transition were different and only those for stress induced transition are evolving in such a manner reported previously,

other are constant. In the prolongation of this study, Vives et al. (2011) recently studied the difference of the front propagation of the MT for stress and strain induced transitions. The main conclusions are that AE enable to observe the propagation of fronts and subfronts and results found are in coherence with optical images Bonnot et al. (2008). Concerning the dependence of cycling for the stress induced MT which is our point of interest, there is a clear change between the first loop and the successive in the way the front is propagated. There is an increase of the AE activity and a decrease of the velocity of the front upon cycling.

- **Infrared thermography measurements** The thermo-mechanical coupling in SMA is generally explained by the martensitic phase change being a first-order transformation that absorbs/releases latent heat. During a pseudo-elastic cycle, the direct phase change is exothermic: the latent heat is released to the surroundings. If the heat exchange with the surroundings is not sufficient, the released heat causes an upturn of the material temperature. During unloading, the reverse phase change is endothermic resulting in an absorption of latent heat and causing a temperature contraction if heat exchange with the surroundings is not sufficient Van Humbeeck (1991), Shaw (2000). Recently Pieczyska et al. (2006), Daly et al. (2007) revealed experimentally through infrared thermography measurements that the stress induced martensitic transformation is accompanied by an exchange of heat. Beyond this fact, a strain rate dependence was observed and the higher the strain rate, the higher the temperature change Zhang (1989). New experimental attempts are realized to make the link between infrared measurements and image correlation measurements in the framework of the martensitic transition Delpueyo and Grediac (2011).

  The martensitic phase transformation is accompanied by the formation and disappearance of thermal strips which are visible with infrared thermography measurements. The pattern formation of strips is the core of several papers Pieczyska et al. (2006), Daly et al. (2007), Gadaj et al. (2002). Indeed, it was recently shown Kim and Daly (2010) that stress-induced phase transformation can propagate either by a single, clearly delineated front, or alternatively by the offshoot of small branches from the primary class front. A single martensitic front can change to a branched front in the middle of phase transformation. The nucleation/coalescence of these small branches directly corresponds to a load drop/rise in the macroscopic stress-strain curve.

  Nevertheless, among the few studied that address the evolution of heat generated through cycling He and Sun (2010), Kim and Daly (2010), one can understand that the number of nucleation sites is enhanced and the delineation of the stress-induced martensitic phase fronts drops down as cycle number is increased. However, although the transformation becomes more homogeneous during cycling, there is a remarkable amount of strain pattern memory in the martensite from cycle to cycle. Consequentlyhe initial manner in

which the martensite accomodates strain in the first cycle strongly dictates how the martensite will accomodate strain in future cycles. Thus, one can argue that the local elastic stress fields in the martensite are driven by a dislocation structure and martensite nuclei that largely stabilize during the first loading cycle.

- **Macroscopic observations of the consequences** The macroscopic effect of the stress induced MT was denoted by Moumni et al. (2005) who noticed that the area of the hysteresis loop collapses with the number of cycles and then was almost fixed in the shakedown stage for a NiTi sample. It was also demonstrated that cycling induces an accumulation of residual strain which can be explained by the accumulation of slip deformation. These slip deformations induce internal stresses that can assist the formation of stress induced martensite Bo and Lagoudas. (1999). Other phenomena were detailed in the bibliographical part about the fatigue of the SMA.

Consequently, one can notice the huge number of results regarding the MT which are meanwhile difficult to compare. Indeed, materials, methods and experimental conditions are always different. Moreover, only few studies addressed the cycling effect, Perez-Reche et al. (2004), Carrillo and Ortín (1997), Vives et al. (2009; 2011) which strongly affect the response of the sample and no study focus on this effect for a large number of cycles. Subsequently, we propose to lead an experiment with coupled recording devices as done by Perez-Reche et al. (2004), Gallardo et al. (2010) for a large number of cycles to study the inter-locked thermo-mechanical properties of SMA.

3.2 Experimental devices

SMA sample

Experiments were performed with a quasi-equiatomic polycrystal NiTi (50.3% at. Ni) SMA specimen. The geometry of the specimen is a simple wire of 3 mm diameter and 150 mm long. The transformation temperatures are Ms=261K for the martensitic starting temperature and As=303K for the austenite start temperature, it was determined by DSC measurements. Prior to the cyclic loading sequence, the sample received an 30 minutes annealing at 773K to make sure that it is internal-stress free and that the vacancy concentration is minimum. The grain size of the sample is 0.04 mm and the orientation was not determined. The sample come from the french company NiTi France.

Uni-axial Machine

The sample is fixed in the grips of an uni-axial MTS loading machine inside a thermal chamber at 324K to ensure that the material is in the austenitic state. The applied loading sequence is a repetition of triangles from 0.1 MPa to 700 MPa (force controlled with a imposed frequency of 0.05Hz) , thus, the response of the material is pseudo-elastic.

Acoustic emission device

Regarding acoustic emission measurement (PCI-2 acquisition system from European Physical Acoustics), a 22 dB recording threshold was determined before experiments associated to pre-amplifiers of 60dB and analogical filters with the following bandwidth [400kHz, 1MHz]. The values of PDT, HDT, HLT are respectively 200, 800 and 1000 μs. Acoustic sensors (Nano30) were clamped on the wire to ensure acoustic coupling that was checked thanks to pencil lead break procedure before and after the experiment. This enables to check the quality of the recorded waves. A second experimental procedure was performed before and after the experiment. Pulses are sent by sensor 1 inside the material, the time to be recorded by sensor 2 is verified in accordance to the wave propagation speed. The amplitude of the wave recorded must reach a minimum level. The same procedure is applied to sensor 2. The sensors are placed at a distance of 100 mm and only the waves that are recorded by the two sensors are considered. The pair of hits recorded must be separated in time by less than 0.08ms to be considered since it is the time required for a pulse to travel from one sensor to the other and the minimum amplitude is fixed to 80dB. This technique enables the rejection of environmental noises (grips, electrical noises, extensometer, etc...).

Infrared thermography device

Regarding infrared thermography measurement, an infrared camera (FLIR S60 IR) was used with a 50 micron macro lens at a 50 Hz image frequency. A calibration procedure was realized to set the emissivity. To record the temperature field, the specimen surface was coated using black candle powder and the thermal chamber was covered with black tissues. The data acquisition and the post-processing were realized thanks to ThermaCam Researcher software.

3.3 Acoustic, thermal and mechanical synchronized responses

Our aim is to characterize the shakedown state through different signatures; i.e. mechanic, thermal and acoustic signatures. The transition from the initial transient state to a stable state can be divided in two distinct periods, denoted by P1 and P2, that respectively extend from cycles 1 to 15 and 15 to 100. The study is limited to the cycle 100 since the aim of the next chapters is to quantify what happen when the material is cyclically loaded in the stable state. The following subsections will only expose the facts. The discussion about the interpretations of the interconnected results and how it is related to other works will be done in the section named *"Cross analysis"*.

Stabilization of the mechanical response

The strain-stress response of the material to the imposed cyclic loading exhibits a pseudo-elastic behavior. One can see in figure 3.1 the cyclic

pseudo-elastic curve as a function of the number of cycles, for all the cycles (left) and for specific cycles (right). The two important features to notice are:

1. the modification of the shape of the loop that displays some phase transition plateau in the initial cycles which disappeared after 15 cycles. The area of the loop is significantly reduced during P1 and also during P2 but in a less significant way.

2. the increase of the residual strain is visible during the first cycles and becomes more difficult to distinguish after, even if it continues to exist.

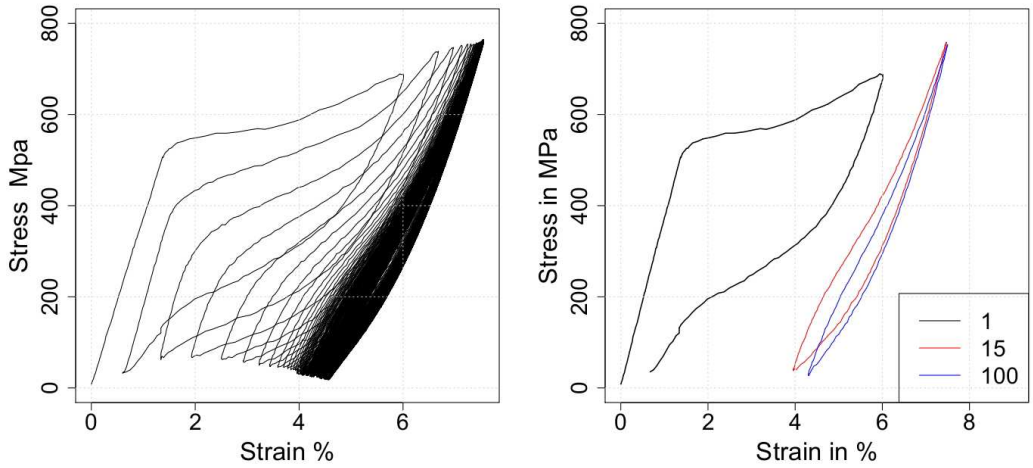

Figure 3.1 – *Cyclic stress strain curves*

The two points previously discussed are easily quantifiable, as shown in figure 3.2, where the dissipated energy per cycle (left) and the cumulated residual strain (right) are plotted. It is worthwhile to notice that the large downturn of the dissipated energy as well as the large upturn of the cumulated residual strain mainly take place from cycle 1 to 15. The variations that occur during the second period P2 are to low to be considered as transient anymore. Then, after the cycle 15, the material can be considered in the stable state looking at the dissipated energy and the cumulated residual strain.

Stabilization of the thermal response

The thermal response is made of three important properties that are detailed below:

1. The first one is the exothermic character of the direct phase transition and the endothermic of the backward phase transition. This property is illustrated in figure 3.3 (left) looking at the evolution of the temperature upon cycling, in one location of the sample. The oscillating character of the temperature, in a twenty second period,

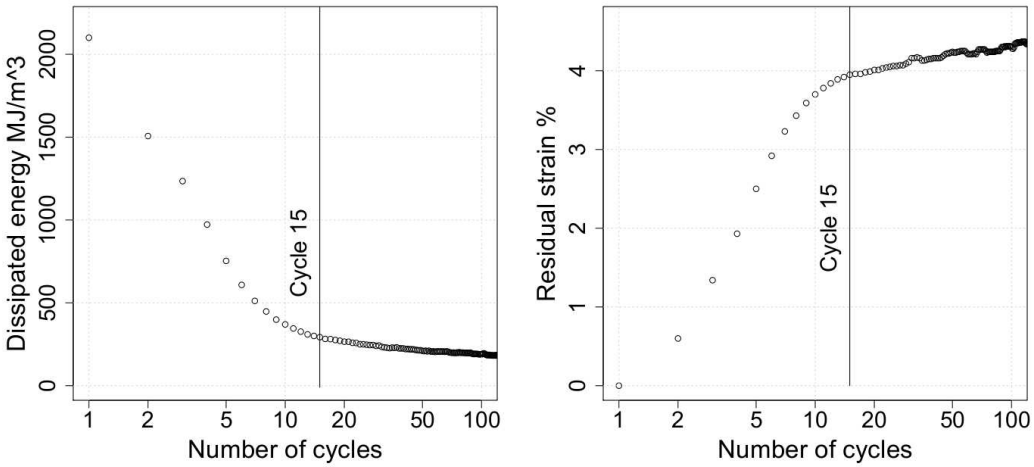

Figure 3.2 – *Dissipated energy (right) and cumulative residual strain (left) as a function of the number of cycles*

reveal the thermal modifications implied by the martensitic transition.

2. The second noticeable property is the decrease of dT, the variation of the temperature, with the number of cycles which corresponds to thermally dissipated energy as shown in figure 3.3 (right). There are two remarkable facts in the evolution of the recorded temperatures. The first one is the large decline of temperature that exists during P1, that is in coherence with the mechanical behavior previously exposed. The other one is the second frequency that seems to be hidden in the signal since the amplitude of the variation of the temperature is modulated by 1.5 degrees with a frequency of 10 cycles as shown in the inset of the figure 3.3 (left) which is the same graph but plotted for 100 cycles.

3. The third property investigated is the formation of bands during the forward and backward transition which are visible in the different photos taken by the infrared camera along the forward transition as shown in picture 3.4. The different transformed and untransformed areas exhibit strong temperature differences and geometric patterns revealing a complex structure in the way transition occurs. These bands tend to disappear with the number of cycles as shown in the figures 3.5 and 3.6. Consequently, at the end of P1, no more bands are visible. These measurements of temperature are realized along a line in the tensile axis direction and the oscillations are the results of the martensitic transition captured at a given time in figure 3.5 and for all the time in the map of figure 3.6. The fact that the temperature displays a slope for cycle 15 results is the fact that it is captured at a given time and consequently a thermal gradient exists in the sample due to the diffusion of the transformation front.

After 15 cycles, the evolution of the variation of temperature is quiet constant and the transformation bands have disappeared. Consequently,

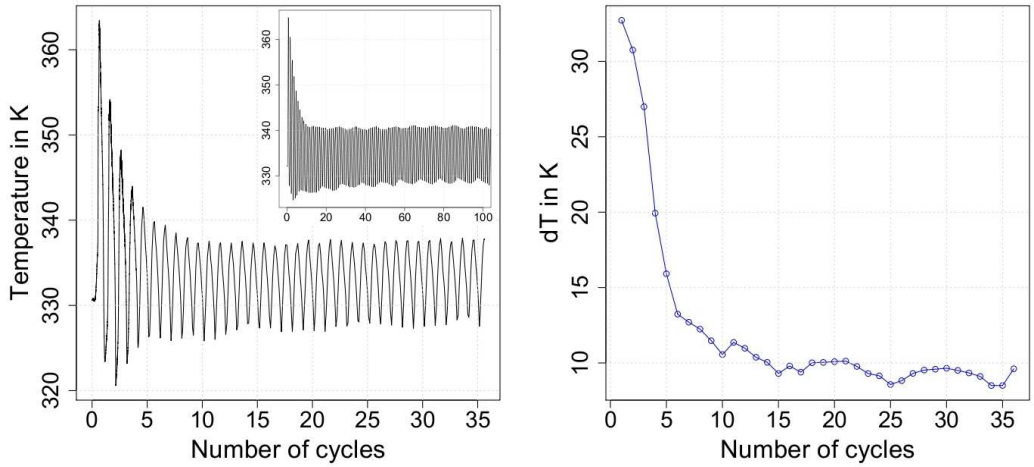

Figure 3.3 – *Evolution of the variation of temperature for a given location in the sample (left) and amplitude of the variations of temperature per cycle (right)*

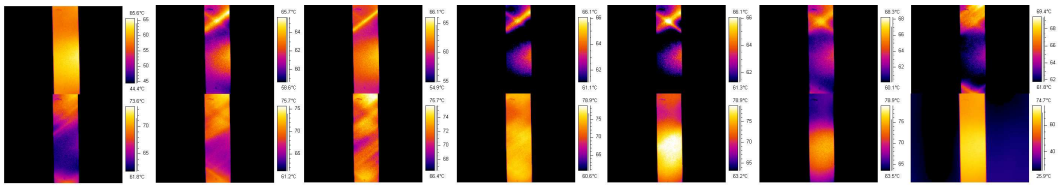

Figure 3.4 – *Visualization of the transformation bands*

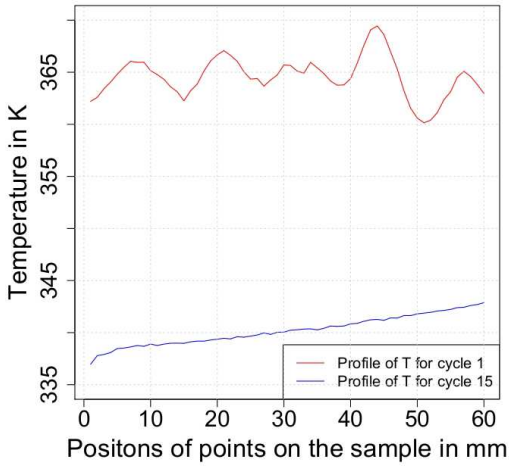

Figure 3.5 – *Visualization of the disappearance of the transformation bands*

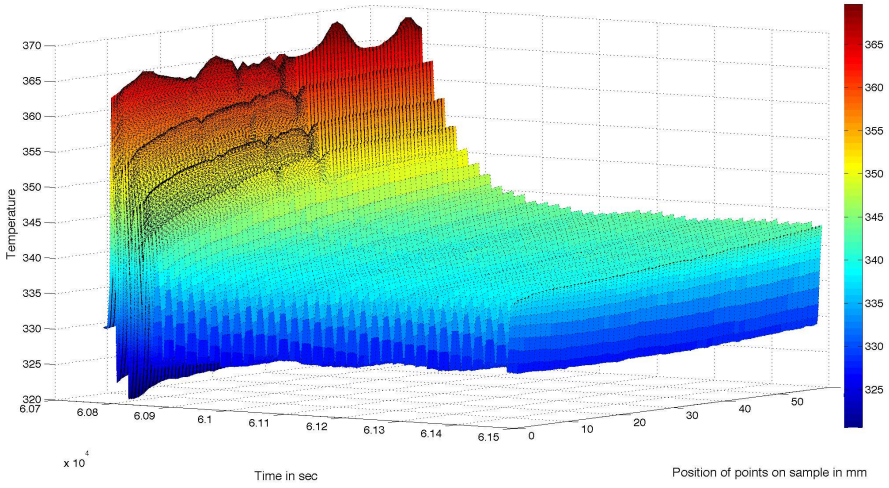

Figure 3.6 – *Space Time Temperature map*

the material can be considered as in the stable state from the macroscopic thermal point of view.

Acoustic response

The analysis of the acoustic response will be led following the two topics that are, the evolution of the cumulative energy first, and then, the evolution of the distributions.

Evolution of the cumulative energy and the number of hits The cumulative energy of the generated acoustic waves also carries out information about the non-linear behavior of the response with cycles as shown in figure 3.7 where the cumulative energy is plotted (left) and the number of waves generated per cycle, in a semi-log graph (right).

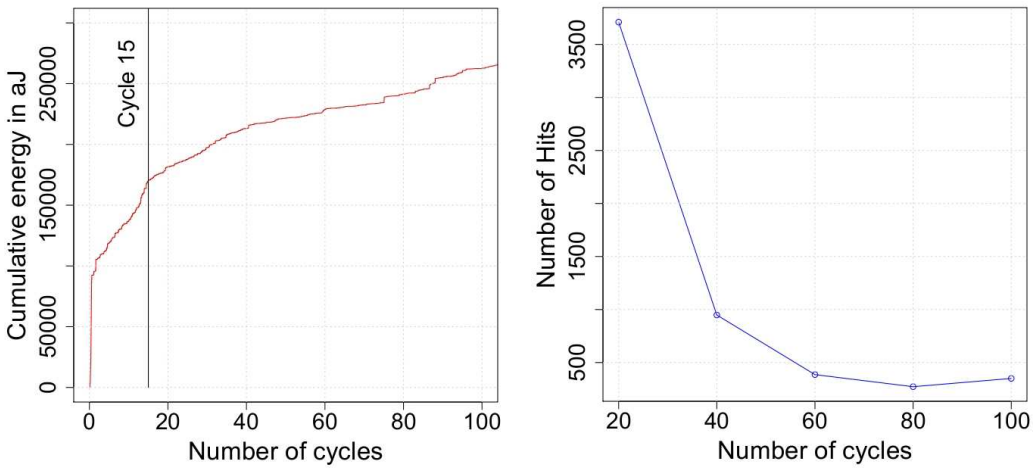

Figure 3.7 – *Acoustic cumulative energy as a function of time and number of acoustic waves*

It is noteworthy that regarding the previously denoted periods, the synchronization in time in the response is remarkable. During P1, there is a huge increase of the cumulative energy of acoustic waves generated inside the material before it reaches a constant dissipative rate regime in P2. The dissipation in P2 is in coherence with those already found, the material continues to dissipate energy but in a slower and constant way. For future studies, it could be interesting to separate hits recorder during the forward and the backward phase transition to reveal the asymmetric character of the release of acoustic energy.

Another quantity that helps to understand this strong change of response is the number of events as a function of the number of cycles that is illustrated in the right panel of figure 3.7. It is plotted for 20 cycles periods since the number of generated waves is low in the beginning of experiments in comparison with what it will become when damage takes place as it will be shown in the next chapter. This choice aims at reducing the errors of the computed exponents from the distributions. Given this discretization, the number of waves sharply drops between cycle 20 and 40 and then continues to be reduced slowly until cycle 60. Then the number of waves is stabilized. This behavior is consistent with the ones exposed previously, the activity is intense during the first cycles and then tends to slow down.

Evolution of the distributions The rate of acoustic waves generated and the rate of dissipation of energy are strongly modified, consequently, one can expect the distributions to be also altered with cycling.

The distributions of energies and time intervals are power-laws with exponential cut-off, as shown in figure 3.8, of the following form $p(X) \approx X^{-\alpha} exp(-\beta X)$ where X denotes the observed quantity of the wave, α the parameter governing the power behavior and β the one attached to the exponential behavior. α corresponds to ϵ for the energy and to τ for the time intervals. β corresponds to λ for energy and to ω for times intervals. The values of ϵ and λ are reported in figure 4.13 and the values of τ and ω in figure 4.14.

From a qualitative point of view, the left panel of figure 3.8 reveals that energies are distributed according to a power-law distribution that holds over one decade and half. Nevertheless, cycling induces criticality as denoted previously by Perez-Reche et al. (2004) and Vives et al. (2009) since the minimum value for which holds the power-law regime drops with the number of cycles as shown in the left panel of figure 3.9. Moreover, a quantitative analysis, reveals the decrease of ϵ with the number of cycles whereas the variations noticed on λ are insignificant and does not highlight any relevant change in the quiet inexistent cut-off.

The distributions of time intervals are reported in the right panel of figure 3.8. It is worth stating that cycling causes a contraction of the range on which the distributions are applied as illustrated on the right panel of figure 3.9. Indeed, it is crystal clear that the first distribution embeds a first power-law regime attached to the very short time intervals that are unequivocally absent in the subsequent distributions. This is mainly explained by the declining number of events generated per cycle that stems in longer time intervals. Thus, the systems seems to evolve from a tem-

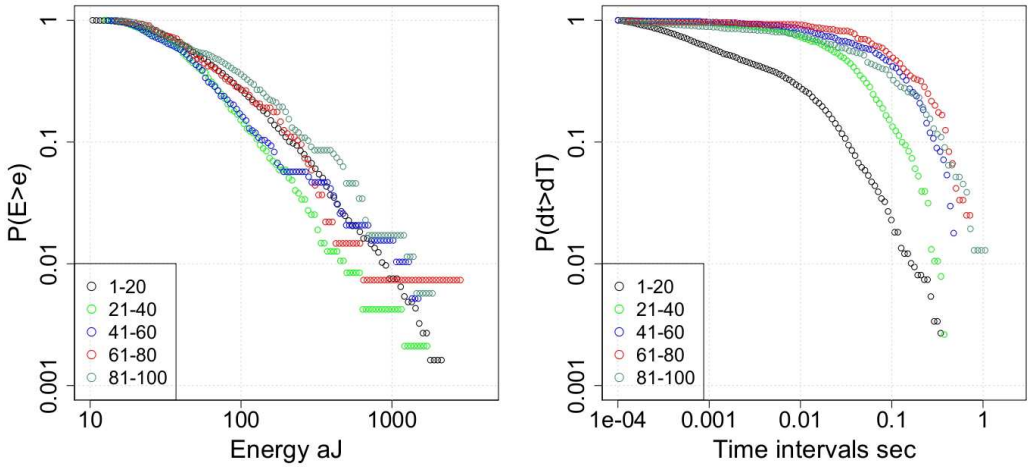

Figure 3.8 – *Counter-cumulative distributions of energy and time intervals*

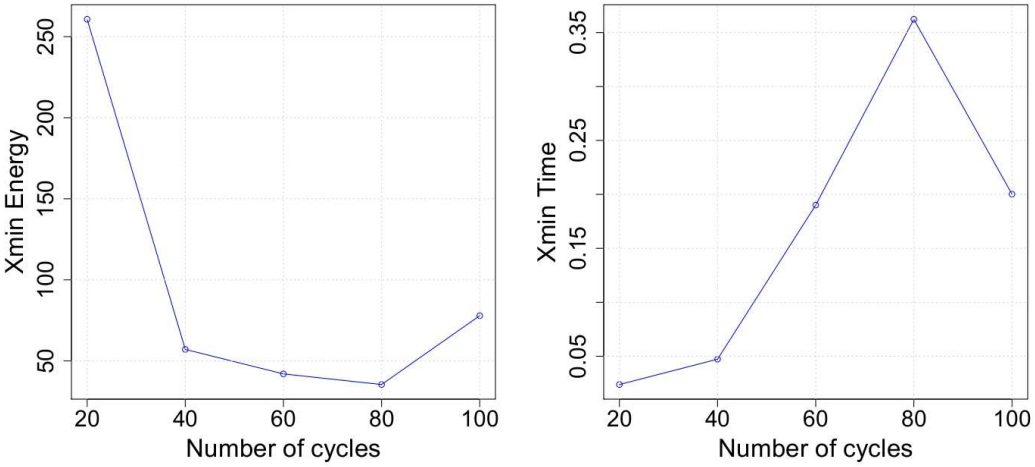

Figure 3.9 – *Values of X^{E}_{min} and X^{dT}_{min} as a function of the number of cycles*

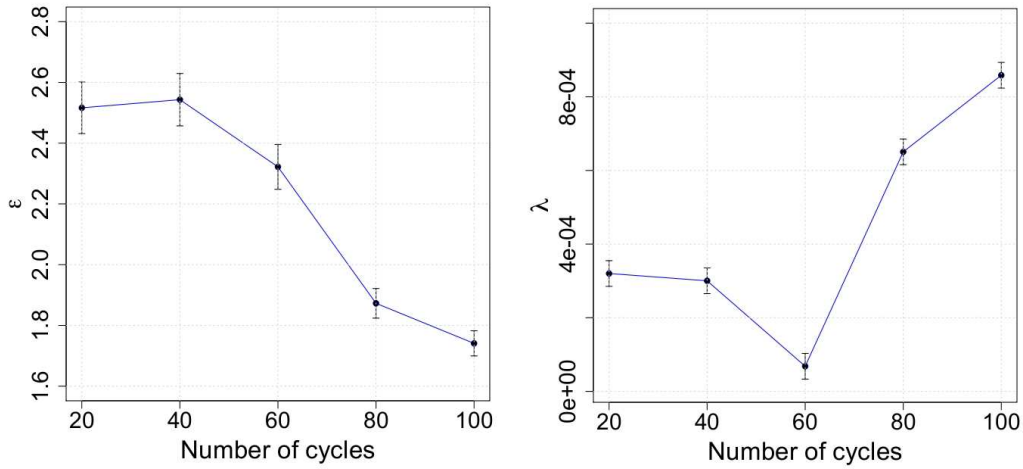

Figure 3.10 – *Values of ϵ and λ as a function of the number of cycles*

poral structure governed by two power-laws in the early beginning of the experiment to an exponential time structure supporting the random character of time arrivals of waves. This is quantitatively checked from the low values of τ and the high values of ω, exposed in figure 4.14, that strengthen the visual observations of a disorganization.

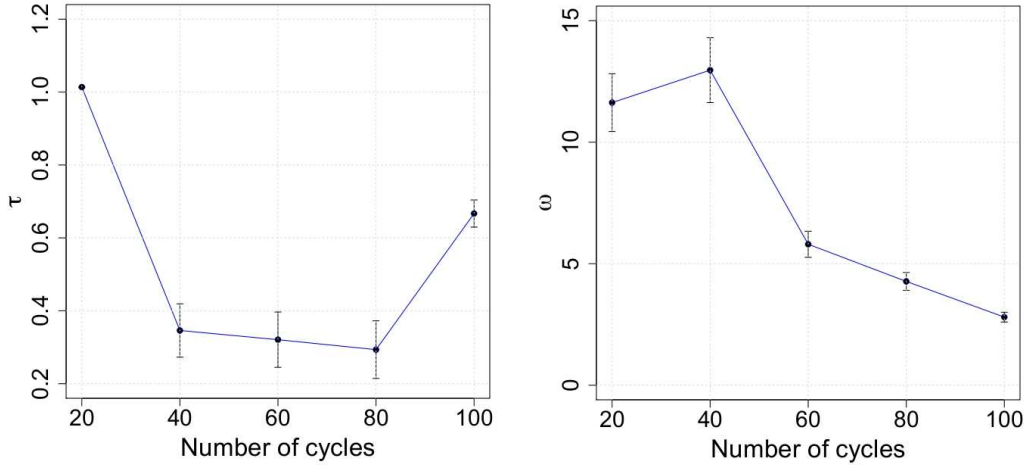

Figure 3.11 – *Values of τ and ω as a function of the number of cycles*

To sum up, the important rise of the dissipated acoustic energy, as well as the strong decrease of the number of hits in P1 coupled to the stabilization of the dissipative rate and the quiet constant number of generated hits tend to support the previous findings arguing that the material is in the stable state after 15 cycles. These results are also reinforced by the evolution of the time intervals distributions during the first cycles that supports a changing temporal structure and the more critically induced character of energy.

Results regarding each experimental method have been presented and

attention is now devoted to the interpretation of these conclusions and their discussion regarding works of other authors.

3.4 Cross analysis

It appears crystal clear that the material reached the shakedown state after 15 cycles. The main clues of this statement are summarized in the following points:

- The decrease of the dissipated energy computed from hysteresis loop
- The rise of the accumulated strain
- The diminution of the variation of temperature during the transition
- The disappearance of the transformation bands
- The increase of the acoustic cumulative energy released from the material
- The reduction of the number of acoustic waves
- The evolutions of the distributions for the energy and the time intervals

All these changes are synchronized in time, roughly speaking around the 15^{th} cycle.

Discussion on the mechanical response

The first point to discuss is the modification of the shape of the hysteresis loop that was already reported by Moumni et al. (2005). This can be explained by the accumulation and saturation of residual strain. Indeed, with increasing the number of cycles, the slip deformations increase the density of dislocations, Miyazaki et al. (1986), Jiang et al. (1997), Pons et al. (1990) which obstructs the formation of martensite in a similar way to the stain hardening in plasticity. Indeed, the inter-facial friction between adjacent martensite variants during their reorientation process favors the creation of dislocations Otsuka and Wayman (1998), Morgan and Friend (2001). The growth of certain martensite variants due to applied stress and their reorientation lead to gradual dislocation accumulations at the interface between martensite colonies Liu et al. (1999a). The hardening effect observed is mainly due to this effect Xie et al. (1998). However, since the value of the maximum constraint applied is fixed (stress-controlled loading) and since upon unloading the stress and strain states return almost to the same point, the size of the hysteresis loop necessarily decreases. When the residual strain stops its evolution (saturation) the hysteresis loop stabilizes in a way comparable to plastic shakedown.

Discussion on the thermal response

The second point to discuss is the dwindling of the amplitude of the variation of temperature that occurs during the forward and backward transitions. This is intimately correlated with the finding of Perez-Reche et al. (2004) in thermally induced martensitic transition for copper based alloys stating that the entropy and thermal dissipated energy decrease during the 10 first cycles before being stable. This property results from the fact that the number of nucleation sites is raised with the number of cycles due to the multiplication of the nucleation sites which is caused by the rupture of large variants into smaller ones Kim and Daly (2010). Thus, with cycling, the transition tends to be increasingly homogeneous. One other striking evidence of the diminution of the temperature amplitude during the first cycles is the falling-off of the transformation stress Melton and Mercier. (1979). It is know that stress inducing martensite under mechanical cycling results in a decrease of the forward transformation stress, while the reverse transformation stress stays nearly constant. This is attributed to the local elastic stress-fields developed during cycling that are attributed to changes in dislocation structure, governed by the way martensite accommodate strain and the retention of martensitic nuclei McCormick and Liu (1994), Miyazaki et al. (1986) that largely stabilize during the first cycle.

The transition takes place through the growth and the shrinkage of martensitic plates as shown in the photos previously exposed 3.4. The angle formed between these plates and the tensile axis is consistent with the results found by Vives et al. (2011) and the predictions of the phenomenological theory of martensite Otsuka and Wayman (1998). But, one can observe that the transition propagates by a single, clearly delineated front that changes to a branched front.

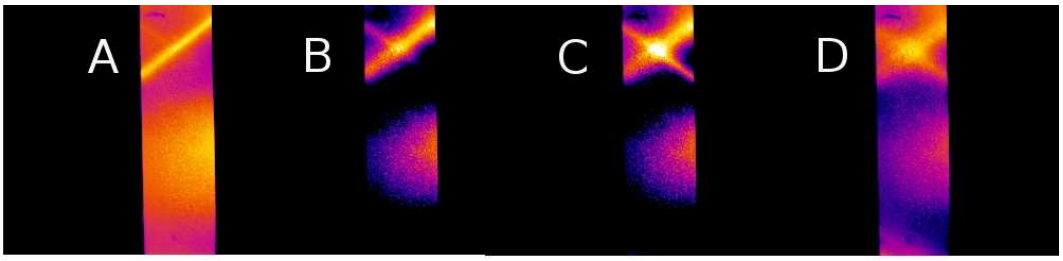

Figure 3.12 – *Nucleation of a branch*

The nucleation/coalescence of each branch corresponds directly to a small drop/rise in the macroscopic stress-strain curve as shown in figure 3.12 and as explained in Kim and Daly (2010). This phenomenon can also be seen also in the stress strain curve of the first cycle with the associated acoustic emission recorded (filtered) as presented in figure 3.13. One can appreciate the coupling existing between the acoustic, mechanical and thermal recordings. The acoustic waves are in front of the heterogeneity on the stress-strain curve and associated in time with the thermal visualization of the nucleation of a branch. The inhomogeneity in the phase transition process can be seen through three signals that displays a specific

character; large energetic AE emission, drop/rise in the strain stress curve and the appearance and crossing of thermal straight lines.

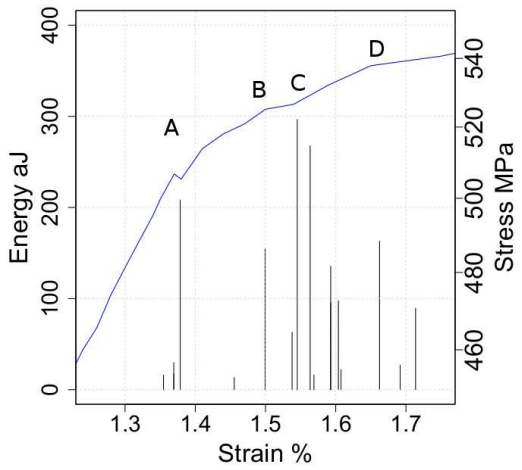

Figure 3.13 – *Stress-strain curve of the first cycle zoom at the bend and AE*

The multiplication of nucleation sites with cycling make the bands invisible as soon as the material is in the shakedown stage. Nevertheless, there is a strong pattern memory and even if the bands are no more visible with an infrared camera, the transformation occurs throughout the material at all strain levels and considering the areas outside the large localized bands as martensite free nor the areas inside the bands as completely martensite is a mistake as demonstrated by Brinson et al. (2004). They explained that the formation of bands is linked to the volume fraction of martensite inside the material. From cycle 1 to 15, one can see a clear phase transition plateau in Fig. 3.1 and bands can emerge since a large ratio of the material shifts from one phase to another. Meanwhile, when the volume fraction of residual martensite is enhanced, the volume of material able to transform is lower and consequently, complex patterns of bands are more difficult to create. Then, the volume fraction of residual martensite stabilizes and the temperature range also as shown in 3.3.

Brinson et al. (2004) also stated through their photos that that the stress-induced martensitic transition begins at a strain of 0.7% which corresponds to the appearance of the first plates of martensite. For this same strain, the acoustic device begins to record some acoustic waves and consequently we decided to repeat the experiment and to stop it at a strain of 0.7%. Optical micrography shown in 3.14 confirms their statement since one can see the first plates of martensite.

Discussion on the acoustic response

The last points to discuss are the conclusions drawn from the acoustic measurements. The first one concerns the rise of the cumulative energy which is significantly linked to the dwindling of the number of generated waves. In the first cycle, the density of moving dislocations is extremely high compared to the density of static dislocations and consequently a

Figure 3.14 – *Micrography of a NiTi sample at a strain of 0.7%*

large amount of dislocations are moving cooperatively that results in a large number of waves. The amount of disorder will be tuned upon cycling by the development of dislocations that will act as nucleation sites that will fix the transition path followed by the system on subsequent cycles Pons et al. (1990). The cumulative energy rises extremely rapidly due to the very large number of moving dislocations that need to be fixed on grain boundaries, inclusions and other defects with cycling.

In this sense Perez-Reche et al. (2007), Pérez-Reche et al. (2008), explained that training induced criticality. In particular, the critical character of the avalanches and the smoothing of the hysteresis profile only emerge after multiple thermal cycling through the transition in Perez-Reche et al. (2004) or mechanical cycling in Vives et al. (2009). In this context the power-law distributions over a few decades of avalanche sizes is viewed as a sign of proximity of the system to a critical point. Criticality then emerges only as a result of tuning the disorder. This tuning of disorder is realized through the development of a dislocational activity during training Cuniberti and Romero (2004), more precisely, the degree of defectiveness first increases and then saturates Pons et al. (1990). The attainment of criticality is due to the ability of the crystal to develop an optimal amount of disorder. This modification in the amount of disorder has been reported as changing the characteristics of the AE generated during the transition and consequently as modifying the exponents governing the distributions of the size of events. Perez-Reche et al. (2004), Carrillo et al. (1998) reported the dwindling of ϵ and λ, arguing for a shift from a power-law distribution with exponential cut-off to a pure power-law, after approximatively 12 cycles for thermally induced transition of a copper based alloy. More recently, Vives et al. (2009) showed for a stress induced martensitic transition of a copper based alloy that the distributions of energies also evolve upon cycling but in the opposite sense. In our case, the decrease of ϵ from 2.5 to 1.8 is similar to the one found by Perez-Reche et al. (2004) and reflects that the relative number of small avalanches decreases with respect to the number of larger avalanches. Nevertheless, the final value reached, 1.8, is identical to the one found by Vives et al. (2009). The coincidences of these experimental facts, that are synchronized in time, in variation and in value, for different materials with different shapes and different loadings reinforce the critical character of the martensitic transi-

tion. The evolution regarding the value of τ is coherent with the one of the number of cycles since the decrease of τ tends to rise the probability of the large time-intervals which is consistent with a lower number of acoustic waves per cycle. Unfortunately, there is no result in the literature that permits a comparison.

3.5 Scientific improvements

From an experimental point of view, this is the first experiment led on a Ni-Ti SMA that involves simultaneously force, thermal and acoustic recording devices. The characterization of the shakedown state from a mechanical, thermal point as well as acoustic were already realized but independently and mainly for copper based alloys. A unified approach of the shakedown state was proposed in this chapter. The novelty stands in the demonstration realized that training is also necessary to reach the critical state in a stress-induced martensitic transition as it is for thermally induced for copper-based alloy Perez-Reche et al. (2004) and for stress-induced for copper-based alloy Vives et al. (2009). Meanwhile, all these studies are stopped in the early beginning of the shakedown state and attention is not devoted to understand how the evolution of the disorder induced by the development of fatigue damages will affect the response of the material and particularly the distributions of energy and time. The next chapter aims at extend the acoustic study led in this chapter until the failure of the specimen.

Fatigue failure & SOC

4

Contents

Fatigue failure is investigated, in this chapter, through the framework of SOC. Acoustic recordings betray the transitions operated by the materials between dissipative regimes upon cycling. Different distributions of the main properties of acoustic events (energy, time, space) are found accordingly to the considered domains. Two scale-free regimes are identified, the first one being attached to the dislocation activity and phase tranisitons, the second one to the formation of cracks. Such a long-term organized process lets the comparison with the fracture in earthquake dynamic affordable.

4.1 SOC, seismology and materials

4.1.1 Long term organization of earthquakes and fatigue

Earthquakes are natural mechanisms which are often viewed as a paradigm of self-organized criticality (SOC) Bak et al. (1988). The SOC concept aims at explaining how large scale properties can emerge from the repeating interactions occurring at smaller scales. The key discovery of SOC was that a complex system, slowly driven by an external field, may naturally evolve toward a critical state represented by the ensemble of metastable states through which the system passes via an avalanche-like dynamics whose amplitudes and durations follow power-laws. The macroscopic behavior then exhibits the spatial and temporal scale invariance typical of the critical point of a phase transition, but most importantly without externally tuning any parameters.

The SOC is now conjectured as the underlying mechanism of scale invariance in a wide variety of dynamical systems related to damages within material sciences. Criticality has been recognized as a key factor in different physical systems at the two opposite ends of the observable scale range; from crystal plasticity Dimiduk et al. (2006), Uchic et al. (2004), Miguel et al. (2001) to earthquakes dynamics Bak and Tang (1989), Chen et al. (1991), Bak et al. (2002). The common properties of these systems are the following: they are spatially extended, constituted by many non-linear interacting elements and they include a threshold dissipation dynamics.

Crystal plasticity and dislocations dynamics have received a particular attention Weiss and Marsan (2003), Miguel and Zapperi (2006), Richeton et al. (2006), Zapperi et al. (1997), Weiss et al. (2007) to demonstrate that these physical mechanisms display the properties of SOC systems. These results support an emerging view that a statistical framework creating a coarse-graining description of dislocation response is needed to bridge the gap between the behavior of individual behavior of dislocations (widely studied by TEM post-mortem analysis and in situ experiments) and the collective behavior of dislocations (widely studied by the experiments exploring the mechanical response over a large macroscopic volume). To link the micro to the macro scale is a long-standing problem of material sciences. Rather than concluding about the macroscopic behavior from the observation of the microscopic or from homogenization and averaging procedure; one can try to find a scale-free set of variables that describe the deformation along time suggesting that such coarse-graining set exist Sethna et al. (1993). Then, the conclusion is that dislocation motions belong to the same universal class of earthquakes, sand piles or magnetic domain dynamics. Following the same methodology, it has been demonstrated that some hysteresis phenomena belongs to SOC, as the martensitic phase transition Vives et al. (1994), Perez-Reche et al. (2007), Carrillo et al. (1998) or the Barkhausen noise Cizeau et al. (1997), Durin and Zapperi (2000), Cote and Meisel (1991), O'Brien and Weissman (1994).

The emergence of SOC in plasticity has been established for fracture Richeton et al. (2006) or creep experiments Weiss and Grasso (1997). As the paradigm of SOC is constituted by earthquakes dynamics which also deals with fracturing phenomena, it sounds natural that some studies aim

to do the links between these a priori similar systems. This was performed by Weiss and Marsan (2003), Weiss and Louchet (2006) that underline the generic nature of the complexity of plastic deformation in creep deformation and its analogy in the space-time coupling of the avalanches. Recently, Marsan and Weiss (2010) studied the space/time coupling in brittle deformation at geophysical scales of the Artic sea-ice cover supporting once again these analogies. Creep of ice, like fracture of Earth crust or Artic ice-cover share the common property of long-term organization of the ultimate event. In that sense, fatigue also seems to be the right candidate since failure arises as the result of large number of repeated loads. A clear parallel can be drawn in perspective of the key ingredients that make earthquakes dynamics as a SOC system and the fatigue process. The words in normal fonts refer to earthquakes whereas words italicized refer to fatigue failure.

1. The first shared property is the threshold response. The threshold response can be associated with the stick-slip instability of solid friction or to a rupture threshold thought to characterize the behavior of a fault upon increasing applied stress. *In the same time, the threshold response is typically given by the intermittent motion of dislocations inside the material and the Peirl's barrier. These motions are controlled by the local stress which is a function of the impurities in the lattice, the geometry of grains and the applied load. These threshold will be modified by the nucleation of cracks and the accumulation of plastic deformation.*

2. The slow driving rate is associated to the slow tectonic deformations induced by the motion of one tectonic plate over its neighbors. At its base, the lower crust and the mantle also play a role in this slow driving rate. But, something important to notice is the separation of time scales between the driving tectonic velocity, cm/yr, compared to the velocity of slip, m/s. *The slow driving rate is associated to the stress applied by the tensile machine over the sample. We are working with very low strain speed, 0.1 µm/s. This distinction of time scales also exists when one considers the velocity of dissipative phenomena (avalanche of dislocation, micro-crack formation, failure of the sample).*

3. Power-laws of size, time as well as fractal properties reflect the scale invariances that exist in the system . These properties are the signature that we are dealing with a "multi-scale" system, as it probably takes place in the crust by the repetitive action of rupture cascades. Within the SOC hypothesis, the different portions of the crust are correlated over long distances by the action of earthquakes which permits to release energy and transport the stress field fluctuations in the different parts of the crust many times back and forth to finally organize the system. *This topics will be detailed in the results of experiment but we will demonstrate that time intervals as well as energy are self-similar during specific period of the life of the sample. Moreover, a spatial analysis will allow to claim that the distribution of the locations of events is fractal. This would enable to consider the important rule played by the long-range correlations between avalanches of dislocations and micro-cracks in the landscape of internal stresses.*

Despite these similarities, a multi-scale analysis of the fatigue process is still lacking whereas it displays, a priori, all the required conditions to be integrated in the SOC framework. So, a natural approach is now to study the space time coupling that takes place during the development of damages induced by cyclic loading. This analysis will be done in perspective of the results found in the earthquakes dynamics and consequently three main objectives are pooled in this chapter.

The first one is to demonstrate that the shakedown state is left during the fatigue experiment in favor of other dissipative regimes. Each period of dissipation must consequently be linked with physical dissipative phenomena like dislocations or micro-cracks. In the same time, the study of the distributions with the progressive accumulation of damages is also a key quantity to investigate the path to failure from the nucleation of micro-cracks and their subsequent merging to contribute to the failure of the specimen.

The second ambition is to investigate several loads and frequencies in the cyclic loading of the sample to evaluate the robustness of the SOC interpretation given in the previous chapter to experimental changes. One can expect, in the SOC framework, that the response of the material should be unchanged (in the statistical sense) from its virgin state to failure, whatever the loading modes. The universality idea is that SOC emerges without any fine-tuning and keeping the assumption of a slow driving rate, consequently, this must be investigated.

The third and last goal is to demonstrate that both systems, earthquakes and fatigue failure, can be thought as SOC systems sharing three well established laws which are the Gutenberg-Richter law Gutenberg and Richter (1949), the Omori's law Omori (1894) and the fractal space distribution of hypercenters Kagan (1991).

4.1.2 Experimental procedure

In this chapter, nine experiments will be presented, the choice is made to first focus on one of them. This will enable to deeply study for one experiment how energy, time and space variables are impacted by repeated loading and then the 8 remaining experiments will enable to study the driving rate sensibility.

So, for the first experiment studied, an identical quasi-equiatomic polycrystal NiTi SMA (50.3 % at. Ni) was used. The sample is a 150 mm long and 3 mm diameter wire. The transformation temperatures are determined by DSC measurements and their values are M_s=261 K and A_s=303 K. All these experimental values are the same for the 9 samples used. Consequently these experiment were realized at 324 K to ensure a pseudo-elastic loading.

Regarding the acoustic device, two Nano 30 sensors were place at a distance of 95 mm and the values set for the nine experiments are summed-up in the following table.

The mechanical loading was realized using a uni-axial loading servo-hydraulic machine and a thermal chamber. For this first experiment the pseudo-elastic loading sequence was force controlled with a sinus loading between σ=0.1 MPa and σ=650 MPa with a frequency of 0.05 Hz, 20 sec-

Threshold dB	Amplifiers dB	Filter kHz	PDT μs	HDT μs	HLT μs
25	60	400-1000	200	800	1000

Figure 4.1 – *Acoustic parameters used for the nine experiments*

onds a cycle. Fatigue failure occurred after 3154 cycles but now, let's deep inside the study of the acoustic parameters that are time, space and energy which will reveal how the system is evolving with repeated loading.

4.2 From space to time through energy

The macroscopic dissipation of energy computed from the area of the hysteresis loop was unable to furnish some indications of change in the dissipation of energy from the shakedown state to the failure. Acoustic emissions are used to have a comprehension of phenomena at lower scale and the first natural corresponding quantity to look at is the cumulative release of energy computed from each relaxed acoustic wave. This quantity is plotted in figure 4.2 and hopefully, it displays some variations upon cycling. Indeed, the response exhibits three distinct dissipative regimes with different increasing rates, each one of these periods and will be referred as P1, P2 and P3 in the following analysis. Nevertheless, a careful observation of P1 highlight that the first dissipative regime does not start from the first cycle and the change from the shakedown state to the first dissipative regime is the topic of the following subsection.

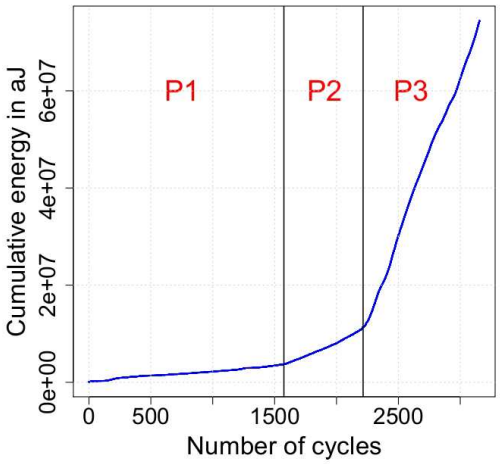

Figure 4.2 – *Cumulative energy as a function of the number of cycles*

4.2.1 Modification of the shakedown stage

In the previous chapter, the focus was realized on the 100 first cycles to demonstrate that the shakedown state is reached after roughly 15 cycles for all the observable variables. Meanwhile, this constant behavior does not remain unchanged until the failure since it was noticed in figure 4.2

that the materials passes through different dissipative regimes. Consequently, the well-established period leading the material from the shakedown state to a first dissipative regime is studied.

The right panel of figure 4.3 is representative of the intermittent and jerky release of energy in the material whereas the left panel illustrates the associated cumulative energy. An identical behavior to the one of the former chapter is observed with a large amount of relaxed energy and then the stabilization of the dissipation rate. Nonetheless, after 150 cycles, the response turns to a higher rate of dissipation and then recovers a stabilized behavior after 300 of cycles with a new relaxation rate. One can expect that the change noticed in the energy response is also accompanied by a change in the distributions which are plotted for the considered period for time intervals and energy in figure 4.4.

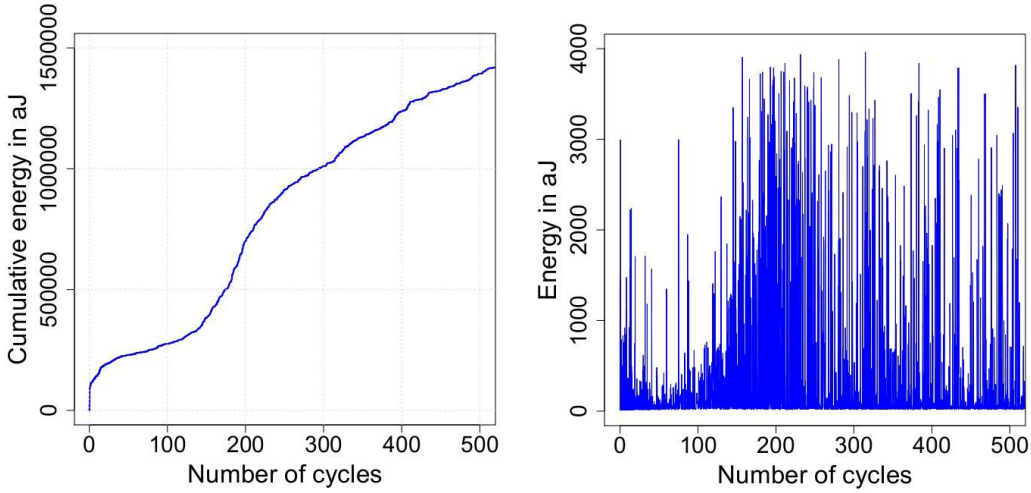

Figure 4.3 – *Cumulative energy (left) and instantaneous release of energy (right) between cycles 1 and 500*

The distributions of time intervals is unchanged after the shakedown state which betrays a random structure of time arrivals. Even so, the distributions of energies are strongly modified since the distributions of the 2 first 50-cycles periods are distributed according to a given type of power-law whereas the 3 subsequent display a shallower slope favoring the large events and finally the system turns back to stable power-law distributions with different shapes.

To conclude about the degradation of the shakedown state, one can argue that after reaching the stable state the system rapidly turns to another dissipative regime through a transient state that is visible through the cumulative released of energy. Moreover, the arrival times are statistically unchanged and remain random whereas the distributions of energy are modified by this change in the relaxation process of energy and afterwards stabilized in a new scale-free regime with an exponent roughly equal to 1.5. But now let us turn to the analysis of the three periods P1, P2 and P3 early observed in figure 4.2.

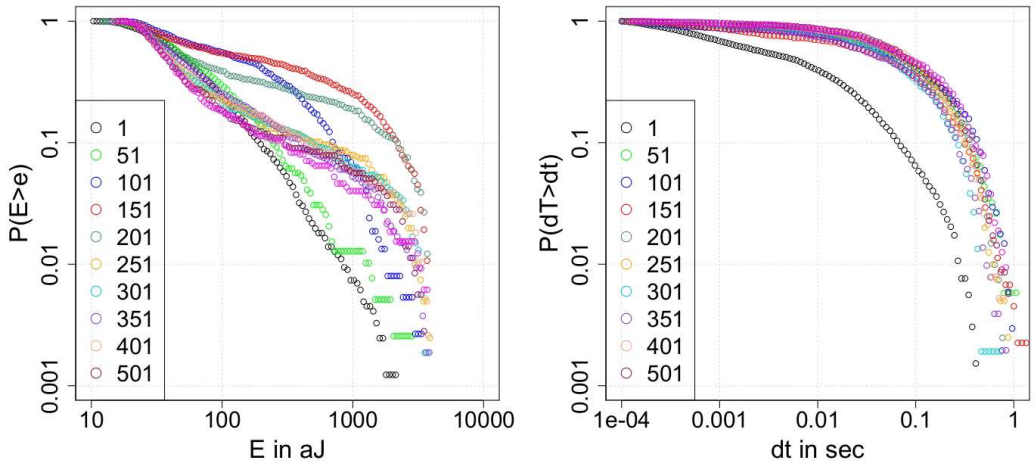

Figure 4.4 – *Distributions of energies (left) and time intervals (right) for 50 cycles periods from cycle 1 to 501*

4.2.2 Three dissipative regimes

A first quick analysis of the three dissipate regimes can be led by simply looking at the visual texture of the instantaneous acoustic response in each period with different zoom levels as shown in figure 4.5. The left panel underlines the increase in density of events as well as the rise of occurrences of large events periods after periods. This enables to rapidly understand the different rates associated to each period and also to build some first intuitive conjectures of the underlying dynamics. Notably, one can pay attention, on the right panel, to the first cyclic structure that emerges in the response of energy in P2 and to the indubitable periodic structure that exists in P3. The time-energy structure that arises each 20 seconds is made of two patterns spaced by 10 seconds. The periodicity is totally correlated to the applied load since the loading period is 20 seconds long and consequently the maximum and minimum stresses are 10 seconds spaced. Intuitively, one feels like relating these two patterns to the opening and closing of an existing cracks and particularly because of the asymmetry of the generated signals. This point will be discussed further in the chapter, and the second focus is made on the transition periods between P1/P2 and P2/P3 that are illustrated in figure 4.6.

Special attention is given to the transitions periods since the shifts from one dissipative regime to another one correspond to the modification of the underlying mechanisms (intensification, modification of creation of physical mechanism). Once again the periods of transitions respectively plotted for P1/P2 and P2/P3 bring to light major changes in the responses that will be further analyzed in correspondence to the modification of power-laws in these specific time domains.

Finally, one can take interest in identifying the number of waves released during the experiment to understand the dynamics of the process, figure 4.7. This quantity is intrinsically linked to the cumulative energy but enables to forecast if the variations are due to an intensification process in time or in energy or both. The important differences between each

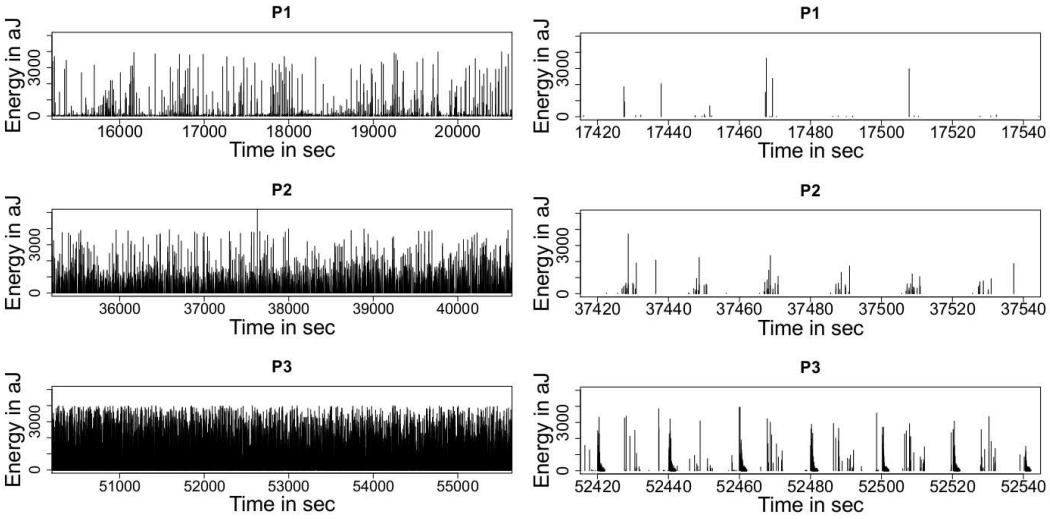

Figure 4.5 – *Zoomed shots of the instantaneous release of energy for P1, P2, and P3*

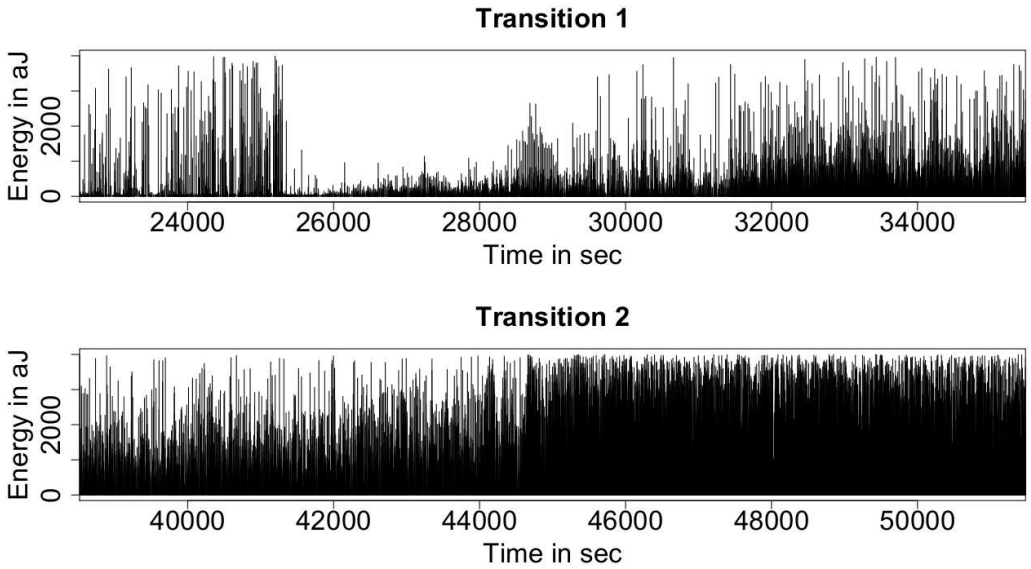

Figure 4.6 – *Instantaneous release of energy during the transitions between P1/P2 and P2/P3*

period is emphasized, P1 being less active than P2 which is in turn less active than P3. The transitions between dissipative regimes are characterized by the rocket of the number of waves. The first large slump is associated to the transition from the virgin to the shakedown stage, P1 unveils a quiet stable number of events as well as P2 whereas P3 is marked by a large peak and a final oscillating slope.

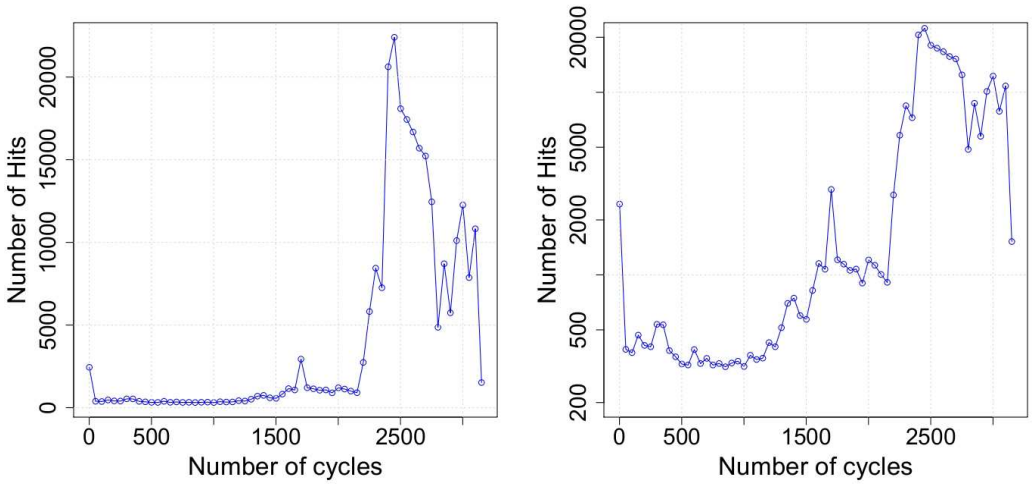

Figure 4.7 – *Number of generated waves for 50 cycles periods plotted in regular and semi-logarithmic axis*

The natural questioning concerns the locations of where and when the events arose. This is apprehended with a complete overview of the fatigue process in the following subsection.

4.2.3 Mapping of failure

The space-time map is represented in figure 4.8. The sample used for this experiment was a 3mm diameter wire and the spatial resolution of the sensor is 0.5mm, consequently, only one direction will be investigated. The bulk of the bursts emanates from two areas and one coincides with the failure occurrence place, at 70mm. The two white lines separate the dissipative regimes and one can notice that the area P2 corresponds to the highest number of generated events. Nevertheless, it was shown in figure 4.7 that P3 is the most active period, consequently, if the number of events seen is lower than in P2, it is the indication that a visual threshold effect hides the large number of low energy waves present in the system. Subsequently, a new plot with a lower threshold is plotted in figure 4.9 and one can appreciate, the tendency of waves to widespread over all the spatial range of the specimen with cycling. This property of events arising from everywhere in space allows to conjecture about a potential scale-free spatial distribution of events. This specific point will be discussed further in the chapter.

The tendency of the system to develop some kind of structure statistically organized upon cycling seems to be a reasonable frame of mind given the qualitative observations of time, energy and location realized

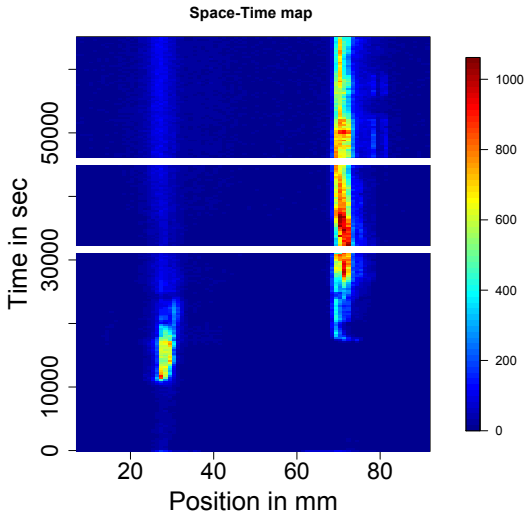

Figure 4.8 – *Space-Time map of events*

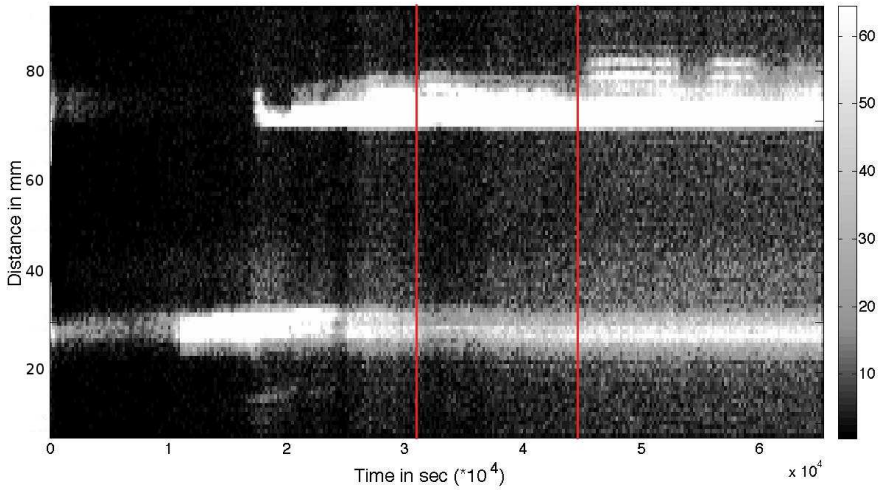

Figure 4.9 – *Space-Time map of events with low threshold*

through this second section. To go further in the analysis, an investigation of the distributions of these quantities sounds as necessary.

4.3 Scale-free behaviors

4.3.1 Distributions of energy, time and space-intervals

Among the requirements to qualify a system as SOC stands the scale-free notion attached to the size and duration of events. Another condition refers to the fractal geometrical properties necessary to account for the long-range correlations. So, these three quantities, energy, time intervals as well as space intervals will be investigated through their empirical cumulative distribution functions. The study of space may seem surprising but the qualitative evolution of the spatial intervals between successive events will give the knowledge of the clustering evolution of events with cycles.

Empirical cumulative distribution functions

To simplify the discussion, it is recalled the cycles referring to the transitions P1/P2 and P2/P3 ar respectively 1575 and 2215. The distributions of energy, time intervals and space intervals are respectively plotted in figures 4.10, 4.11 and 4.12.

The first panel of figure 4.10 and 4.11 will not be commented since it refers to the degradation of the shakedown state which has already been discussed. Then, the goal is to appreciate the variations of distributions in the matter of the dissipative regimes P1, P2, P3.

Regarding the empirical distribution, 4 periods are worth being noticed, a first from cycle 300 to 1350 which roughly corresponds to P1, a second from 1350 to 2400 which encompasses P2 and the transitions P1/P2 and P2/P3, a third from 2400 to 2800 and a last from 2800 to failure. These 4 periods are mainly governed by the losses recoveries of the scale-free behavior of energy.

- The hallmark of the first period is the constant scale free pattern of energy and the unchanged random time-structure of time intervals. The only quantity subjected to changes is the spatial distribution of events that is radically changed (be careful that the scale of the two first panel is one decade large than the others). The modulation of the slope is easily interpreted by looking at the figure 4.9 where a clear correlation exists between the increase of the slope from cycle 500 to 1000 and the spatial organization of the events around the 30mm coordinate line which reflects an enhanced probability to be clustered in space. This behavior is radically changed for cycle 1000, since the slope collapses indicating a larger tendency of events to be widespread in the sample. This behavior is explained by the nucleation of another cluster of events along the 70mm coordinates.

- The two key characteristics of the second period are the loss of the critical behavior for energy just before the transition P1/P2 and its

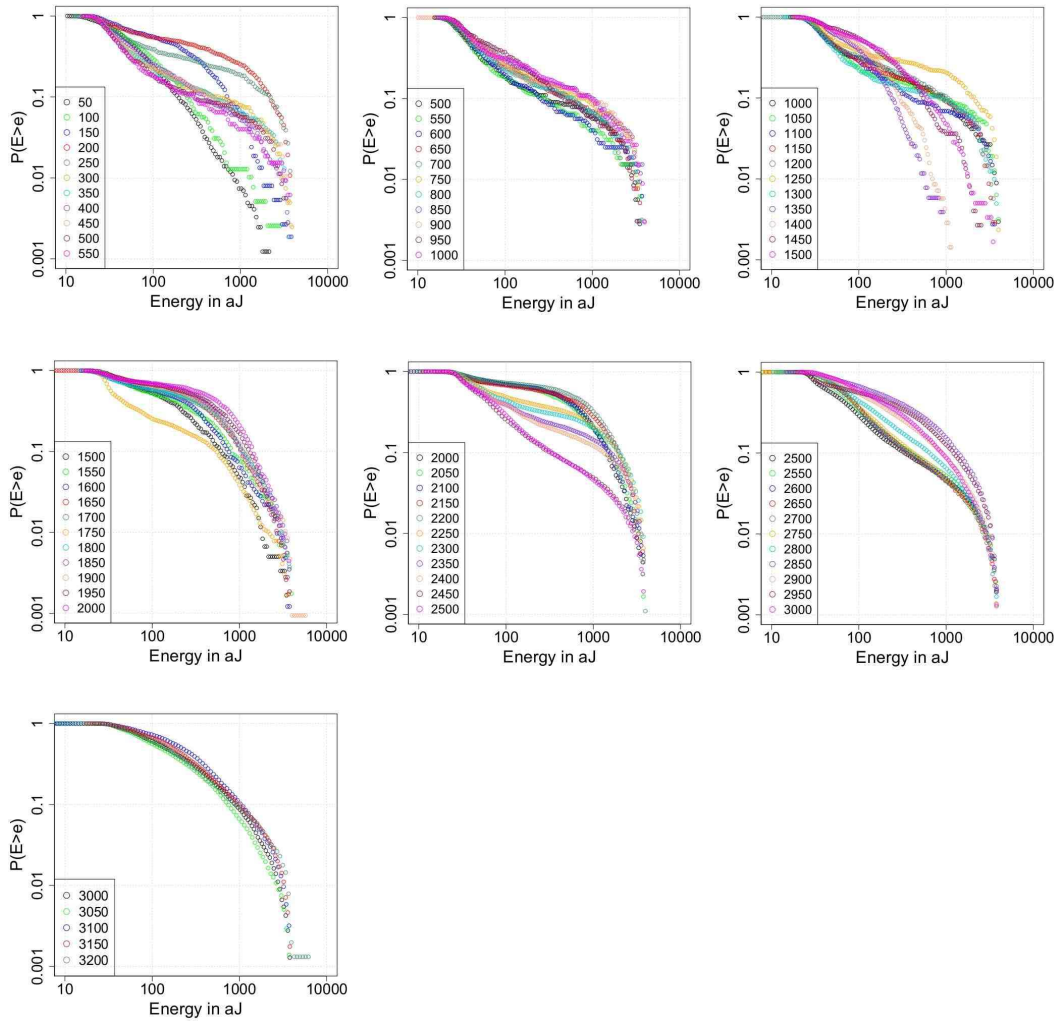

Figure 4.10 – *Distributions of energies for 50 cycles periods for the whole experiment*

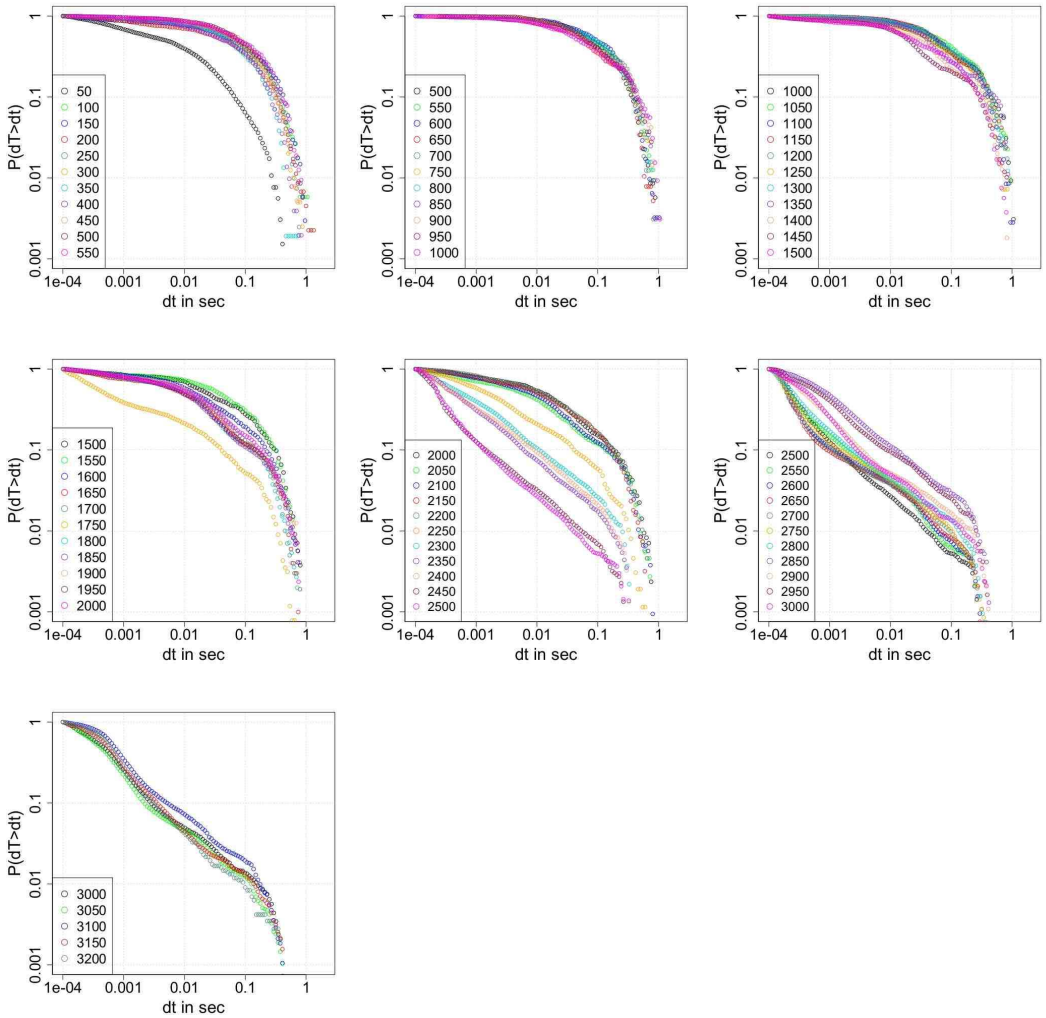

Figure 4.11 – *Distributions of time intervals for 50 cycles periods for the whole experiment*

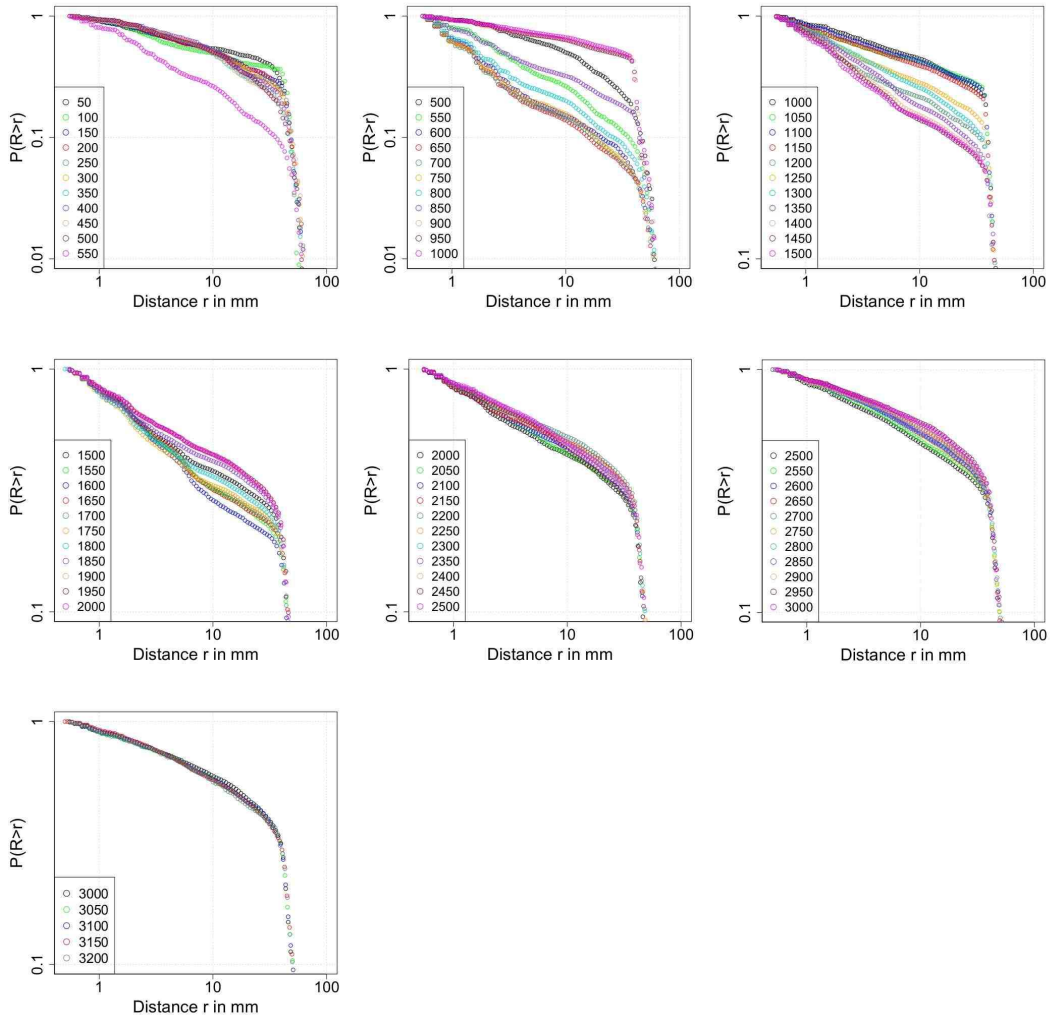

Figure 4.12 – *Distributions of space intervals for 50 cycles periods for the whole experiment*

recovery just after the transition P2/P3 for the first part and the progressive appearance of a scale-free time structure after P1/P2 that is undoubtedly established after P2/P3. In the same time, it is worthwhile to highlight the rise of the number of events as shown in figure 4.7.

- The third period is typified by the scale-free distributions of energies, time and space intervals synchronously. This critical behavior only occurs one time during the experiment meanwhile a large decline of the number of events befalls. The system self-organizes into a critical state upon cycling. The distribution of energy and time intervals are quiet constant whereas the variations in space intervals let appear a slow decrease of the slope revealing a large tendency of the system to relax events from everywhere.
- The last sequence is characterized by the loss of the power-law feature for energy and the tendency of time intervals distribution to display some super-critical queue. The slope of the distance distributions continues to be shallower cycle after cycle.

Analysis of the power-law distributions

The quantification of the previously noticed behaviors is realized thanks to the fit of a 2 parameters power-law distribution of the following type:

$$p(x) \approx x^{-\alpha} e^{-\beta x} \tag{4.1}$$

Like exposed in the previous chapter, such kind of distribution aspires to capture the hybrid character of the distribution empirically found that are sometimes, exponential, or power or mixed. In practice, the distributions are fitted as explained in the paper of Newman (2004), Mitzenmacher (2004) and the two papers considered to be essential reading Clauset et al. (2009), Vuong (1989). One can refer to the following correspondence table to identify the exponents presented in the figures 4.13, 4.14 and 4.15.

Theory	Energy	Time intervals	Space intervals
α	ϵ	τ	ρ
β	λ	ω	ψ

These curves will not be detailed since it is just a way to transcribe again what was directly observed on the empirical curves. One can for example effortlessly distinguish the periods of scale-free distributions of energy (high value of ϵ and low value of λ) from the exponential distributions of energy (low value of ϵ and high value of λ). Nevertheless, it is worthwhile to remark that the values of the power-law distributions after their recovery are different from those that hold in P1 but similar to the one the first cycle. Two last comments concerning the general evolutions of τ and ρ, the first one rises indicating a larger clustering in time whereas the second one declines denoting a more extensive spatial distribution of events that support a self-organization toward criticality.

Some clues about this propensity of the system to exhibit such temporal structure were hidden in the figure 4.5 that was illustrating the emergence of compact temporal patterns that will be examined in the following section.

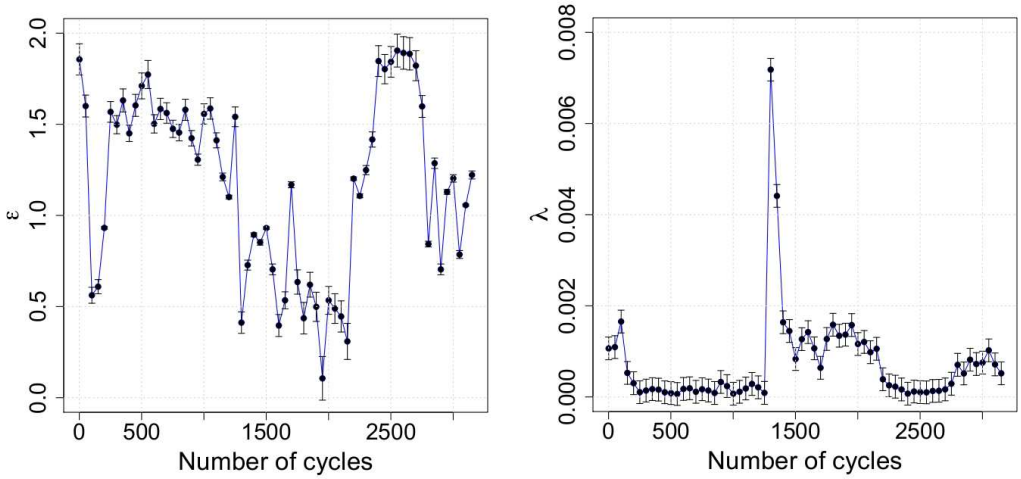

Figure 4.13 – *Values of the exponents of the 2 parameters distribution function for energy*

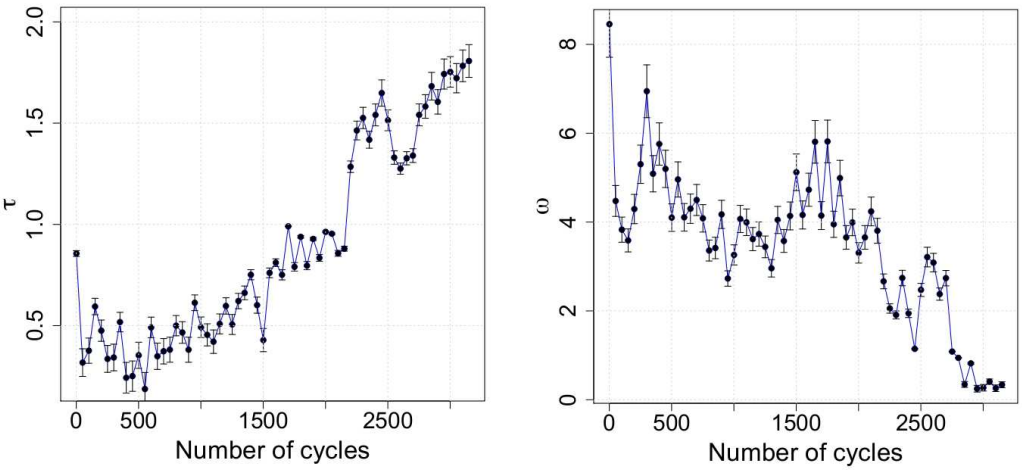

Figure 4.14 – *Values of the exponents of the 2 parameters distribution function for time intervals*

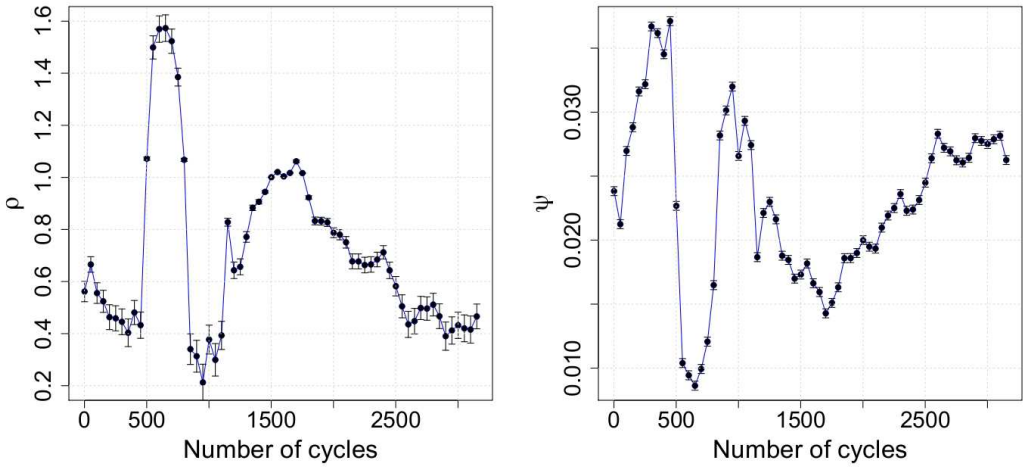

Figure 4.15 – *Values of the exponents of the 2 parameters distribution function for space intervals*

4.3.2 Emerging patterns

The third period is worth being studied with caution since it displays some intriguing phenomena regarding fatigue failure. Indeed, the synchronous scale free behavior in the beginning of P3 for time, space and energy (recovery) is accompanied by the explosion of the underlying activity coupled to the emergence of some cyclic patterns. One example of the typical response encountered is illustrated in figure 4.16 in the beginning of P3. The release of energy in each cycle in P3 is realized through these two patterns-like behavior. The patterns are spaced in time by half a loading period (10 seconds) and the one represented in the left panel of figure 4.17 corresponds to the minimum loading period of the sample whereas the right one is associated to the highest stress. These two specific patterns are earthquake-like exhibiting a similar foreshock, mainshock and aftershock structure.

It is worthwhile to notice that the emergence of these patterns is synchronized with the explosion of the number of generated waves as well as the recovery of the scale free behavior of energy. This specific period is also typified by a scale-free distribution of time and space intervals. Moreover, the periodic character of the response, synchronized with loading, associated to the asymmetry in the signal strongly suggest that this critical period is associated to the creation of micro-cracks in the sample. As a consequence, the left pattern of figure 4.17 is assimilated to the closing of the micro-cracks and the right pattern to the opening of micro-cracks.

Regarding the evolutions of the distributions, it was noticed that the power-law behavior of energy was lost during P3 and consequently, it should be visible in the specific patterns exhibited by the acoustic response. This is shown in figure 4.18 where one can see 3 distinct two-cycles periods that are occurring in P3. The first one (top panel) is captured just after the transition P2/P3 and during the recovery of the scale free behavior of energy. The second one corresponds to the critical state where all

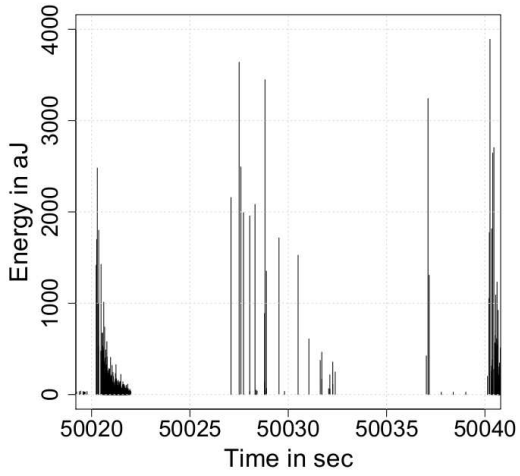

Figure 4.16 – *Visualization of response of the* 2501^{th} *in the third dissipative regime*

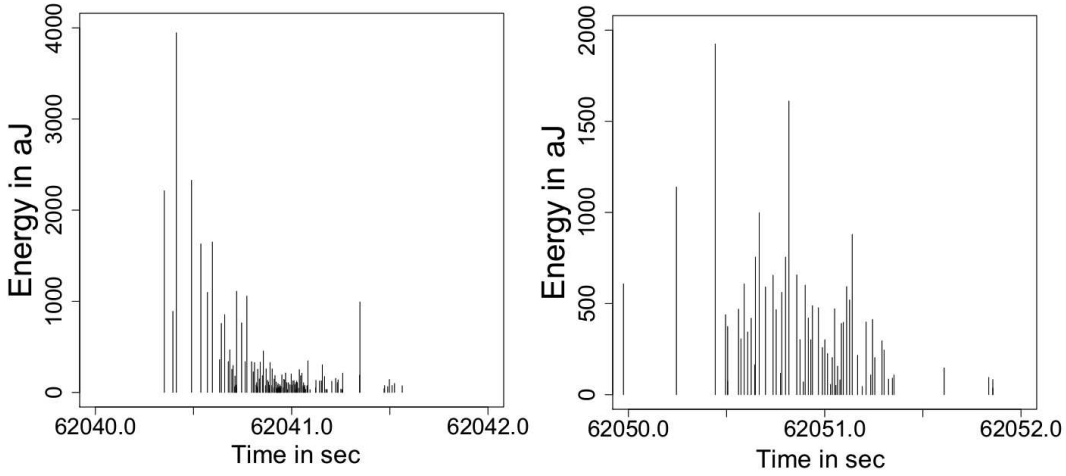

Figure 4.17 – *Visualization of the two earthquake-like patterns*

the variables are distributed as power-law and the last one focuses on the end of the experiment when the critical state is lost.

These graphs aim at underlying that the changes detected in the distribution functions which may sound as fuzzy are physically strong. Indeed, from the evolution between the first and the second panel, the shifts in the organization of the signal and the growth of the patterns exposed earlier are noticeable. The same evolution is blatant between the second and the third panel, where the pattern associated to the traction of the sample is considerably modified by the add of a large amount of low energetic events. The clustering in time is also remarkable if one remembers the response of the material in P1 shown in figure 4.5 since the turns to two clusters of events and silence in between whereas waves arrived in a random way in P1, a temporal structure emerged.

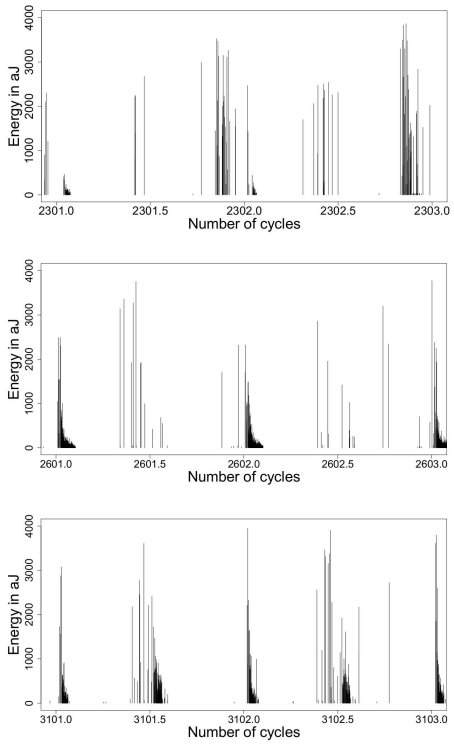

Figure 4.18 – *Evolution of the response during P3*

Thus, the last dissipative regime is associated to fracturing damaging modes with the nucleation, merging and growth of cracks. This sounds as really interesting but let us observe how robust are these results to loading modes with the analysis of other experiments.

4.3.3 Driving rate dependence

One important question scientists have commonly to face to is the influence of the experimental parameters. This topic is surely among the most studied in fatigue, one can for instance think to $S-N$ curves.The approach adopted here is rather different since the SOC framework suggests a universal type of response, statistically at least, for the system whatever the tuning of external parameters.

Consequently, 9 fatigue experiments were conducted, each one with different loading parameters that are sum-up in the table 4.19. The acoustic parameters used for these experiments were introduced at the beginning of this chapter.

Number	Stress MPa	Frequency Hz	Failure
1	600	0.033	5496
2	650	0.033	3781
3	700	0.033	2089
4	600	0.05	3128
5	650	0.05	3154
6	700	0.05	2706
7	600	0.1	2757
8	650	0.1	1685
9	700	0.1	2269

Figure 4.19 – *Parameters of the 9 fatigue experiments and associated number of cycles until failure*

The number of cycles to failure is logical and relatively well ordered regarding the experimental conditions. The experiments chosen as example during all this chapter is the experiment 5 since it corresponds to medium parameters. But, for the sake of comparison, the 9 cumulative energy curves are presented in figure 4.20. This picture has to be read in row and column since along one row, the frequency is unchanged and the stress is modified and the contrary applied for column.

An empirical observation that was obvious during the experiments is well exemplified on these curves. The faster is the driving, the smaller is the number of recorded waves and the lower is the cumulative energy and the same conclusion applies for the stress. This is evident if one pays attention to the respective values of energy for the nine experiments.

In order to make this reading pleasant, a detailed analysis of each of the nine experiments as the one performed previously will not be realized. Nevertheless, the key points to bear in mind will be pointed out.

The attention is first drawn to the similar shape in the cumulative release of energy. All are constituted of the same regimes, a first linear one, a bended transition period and a last linear regime of dissipation with a high rate. This is a blatant mimetic behavior to the one noticed in experiment 5, which has more abrupt transitions due to the statistical filtering that was performed to clean the dataset for a belt-and-braces study, but it was initially the same smooth curve. Thus, this behavior is extremely important since it implies that whatever the loading conditions, the dissipative pattern of energy for each sample is unchanged, only the transition times are modified.

As a consequence, one can hope that the behavior of the distributions and more generally, all the conclusions drawn above about the fatigue process, remain true for all the experiments since it was mainly dictated by the cumulative energy curve. If this is verified, it could constitute a first milestone in a global approach of fatigue for SMA, based on two dissipative regimes, one which is dislocation based and one which is crack based, these being separated by a transition periods

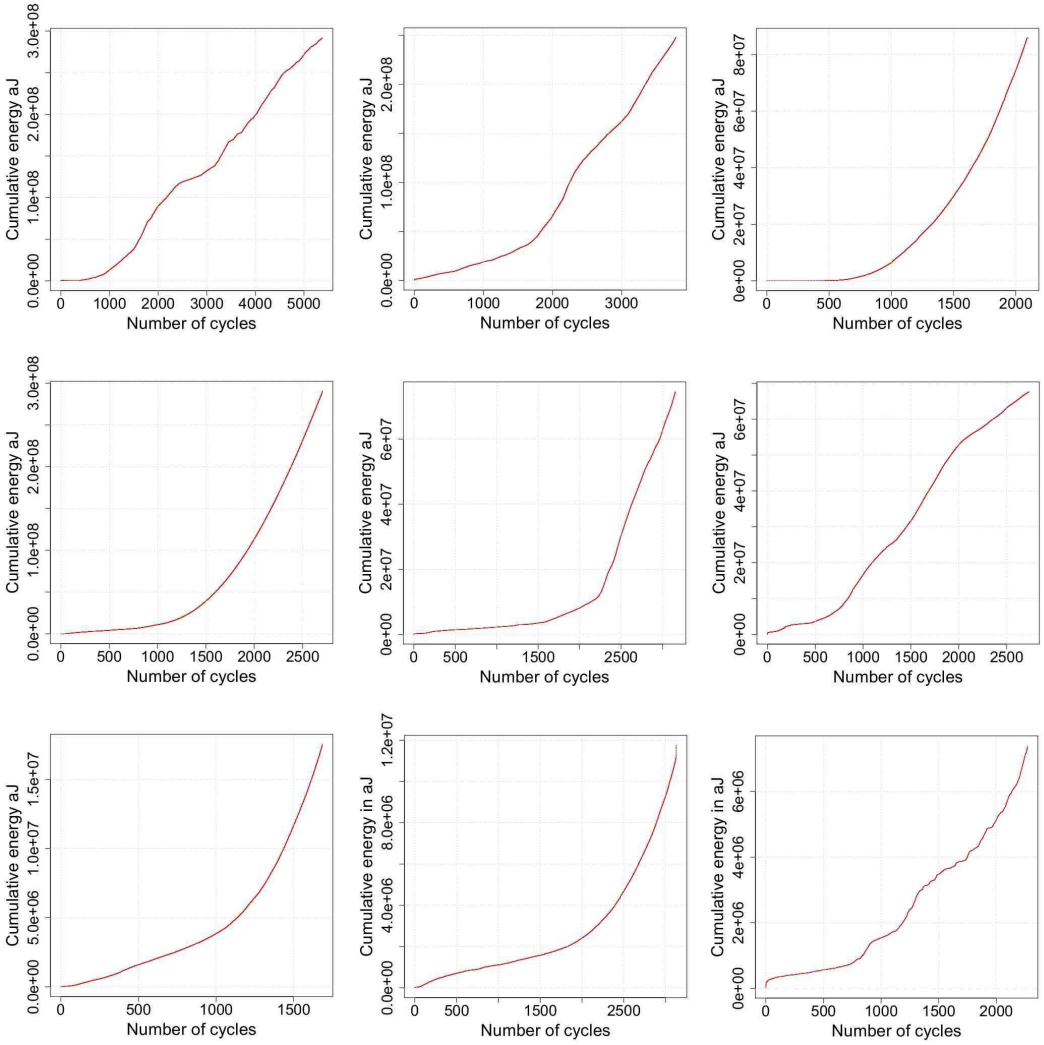

Figure 4.20 – *Cumulative released energy for the nine experiments. Each row is equi-frequency, each column is equi-stress.*

This checking analysis has been performed for all the experiments and the same conclusions as the ones exposed previously hold. Some examples of results are introduced to testify the identical conclusions. One can take a look to the values of ϵ and λ for the experiment 4 or to the values of τ and ω for experiment 3 and the space-time maps of experiments 2 and 7 that are simply revealing common dynamics as those noticed in figures 4.13, 4.14 or 4.9 for experiment 5.

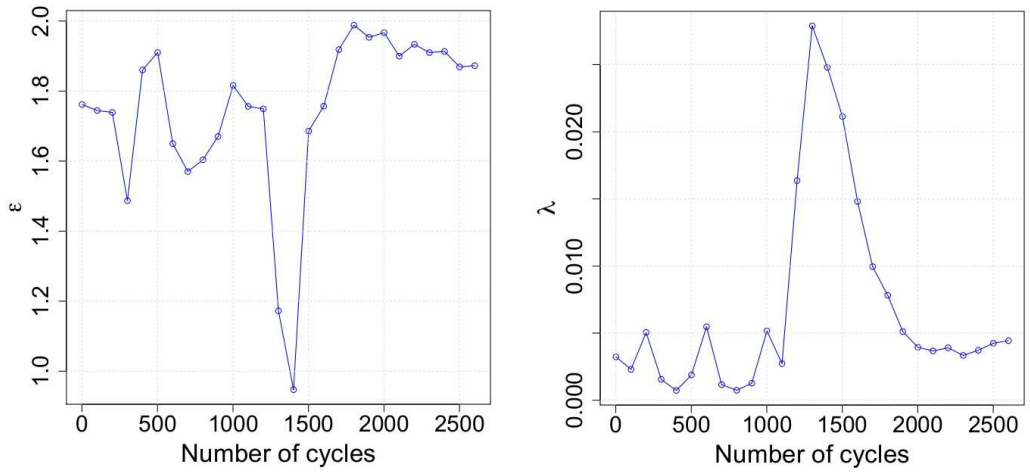

Figure 4.21 – *Values of ϵ and λ for the 4^{th} experiment*

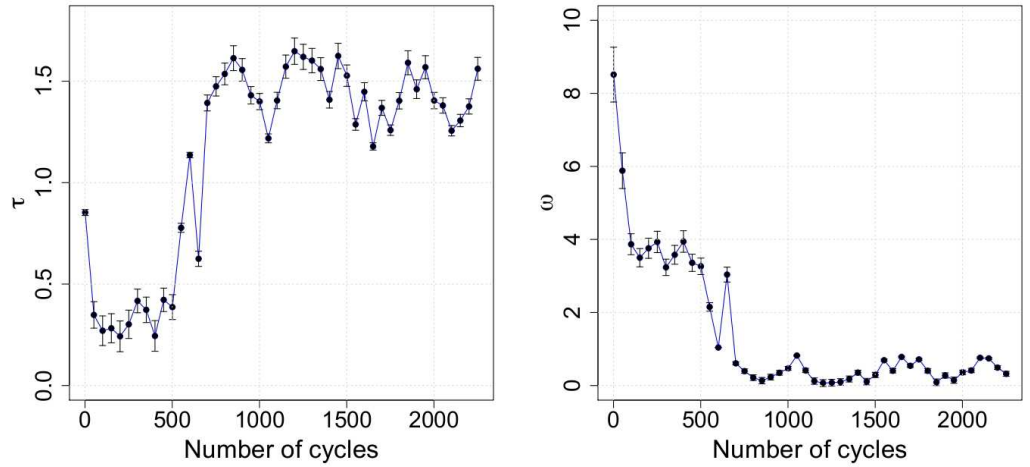

Figure 4.22 – *Values of τ and ω for the 3^{rd} experiment*

The same change in the power-law behavior is exhibited by the variations of ϵ before and after the transition from the first to the third dissipative regime as shown in figure 4.21 for experiment 4. In the second dissipative regime, an identical loss of the power-law behavior is perceptible, symbolized by the jump of λ that is recovered afterwards. The scheme followed by τ and ω is also the same since, for experiment 3, the time structure is immediately lost in favor of an exponential distribution of ar-

rival times during the first dissipative regime (low τ, high ω), as exposed in figure 4.22. Then, a slow self-organized time structure takes place in the material during the second dissipative regime and a pure power-law regime holds in the last period (high τ, low ω). Moreover, the space-time maps, illustrated in figure 4.23, also underline the presence of long range correlations in the third dissipative regimes of experiments 2 and 7 with a widespread activity that is relevant of the fractal character of the distributions of the locations of waves. To conclude about the properties shared by all the experiments, it is worthwhile to show the different types of patterns associated to the development of cracks that emerge in two different experiments, the 4^{th} and the 9^{th}, which are shown in figure 4.24.

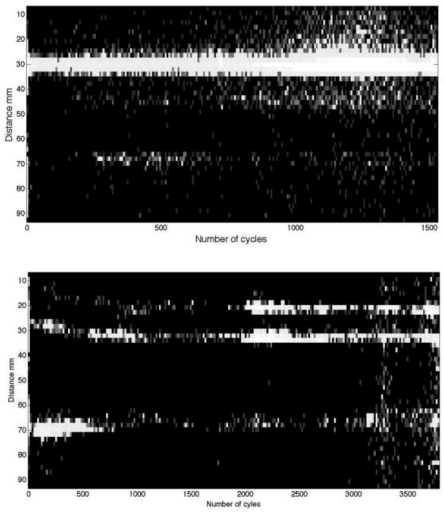

Figure 4.23 – *Space-Time maps for the 7^{th} and the 2^{nd} experiment*

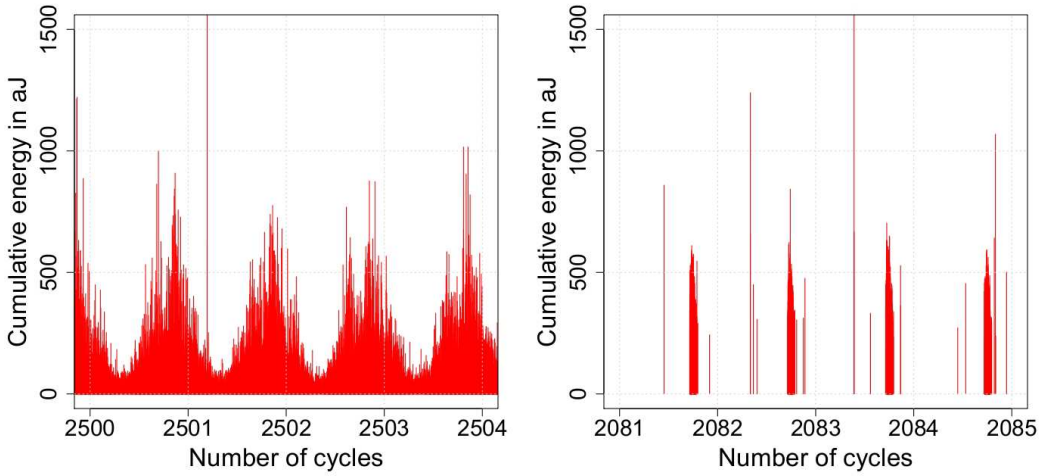

Figure 4.24 – *Acoustic patterns of the development of cracks for the 4^{th} and 9^{th} experiment*

It is worth being realistic to conclude about the influence of the driving modes. The nine experiments performed suggest the same dissipative

path from the virgin state to failure with shared properties regarding the distributions of time and space intervals as well as energy which is physically very strong regarding the SOC concept. This allows to propose a plausible unified scheme for fatigue failure in SMA independently of the loading parameters. Nevertheless, nine experiments do not constitute a wide enough series of test runs to claim for universality in a credible way. So, it is a first step that sounds interesting and that has to be continued.

So far, the acoustic responses were analyzed by 50 or 100-cycles periods whereas only three dissipative regimes were noticed whatever the experiments. Furthermore, the transition from the second to the third dissipative regime is attached to the appearance of the cracks. Consequently, one can legitimately study the system period by period, and an analogy with earthquake dynamics will be highlighted for the third one.

4.3.4 From fatigue failure to earthquakes

The large similarities between the earthquakes dynamics and the fatigue failure process introduced in the beginning of this chapter will be quantitatively discussed in this subsection in terms of SOC.

Gutenberg-Richter Law

The counter cumulative distribution function of released energy is shown in figure 4.25 for P1, P2 and P3. Regarding P1, the distribution of energy follows a distribution which is a mixture between a power-law and and an exponential whereas power-law distributions hold for P2 and P3 over 2 orders of magnitude. This result evidences the underlying critical dynamics and thus confirms the absence of characteristic size and the self-similarity of the micro-fracturing phenomenon that are encountered in P3.

The Gutenberg-Righter Gutenberg and Richter (1949) law states that the cumulative distribution of earthquake magnitudes m sampled over broad regions and large times is proportional to 10^{-bm}, with a b value $b \approx 1$. Translating into energies E with the correspondence $m = (2/3)log_{10}E + const$ leads to a power law $1/E^B$ with $B \approx 2/3$. It is worthwhile to note that the values of exponent $B = 2/3$ which is found for earthquakes ($b = 1$ if one considers the magnitude instead of the energy) Yamanaka and Shimazaki (1990) is in coincidence with the the measured exponent for P2 and P3.

Omori Law

The second law being investigated is the Omori Omori (1894)law which states that the rate of earthquakes triggered by a mainshock decays with time according to an inverse power $1/t^p$ of time with an exponent $p \approx 1$. Consequently, one first task was to transform our dataset to separate the events in four categories foreshock, mainshock, aftershock and undetermined. The algorithmic procedure that was designed is hierarchical in the sense that the aftershocks of a primary mainshock are the mainshocks of secondary aftershocks and so on. The first mainshock was identified, among a 2.5 seconds sliding window, as the event with the maximum energy and sequentially was determined the aftershocks by comparison of

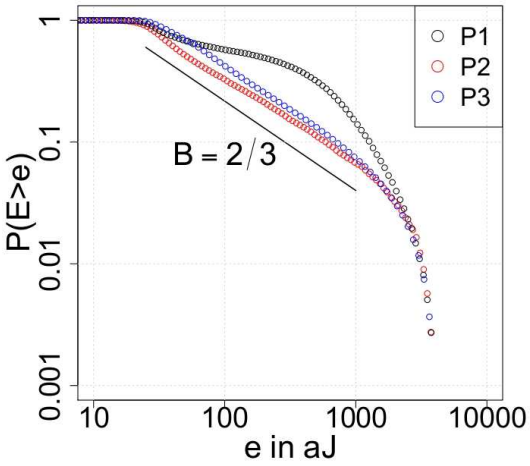

Figure 4.25 – *Distributions of energy in P1, P2 and P3 - Gutenberg-Richter's law*

released energies and time occurrences. A schematic example is plotted in figure 4.26 where one can see the green foreshocks, the blue mainshock, the red primary aftershocks and the cyan secondary aftershock generated by a red aftershock.

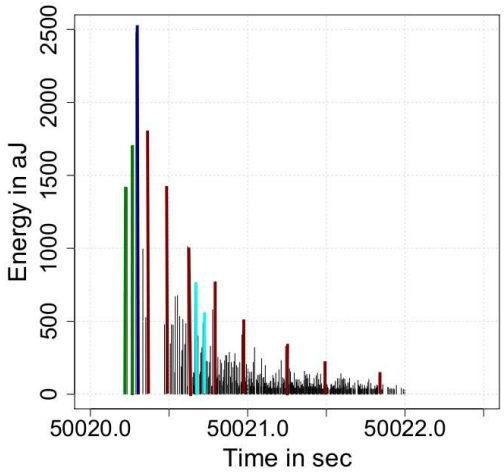

Figure 4.26 – *Schematic example of forshocks (green), mainshock (blue), primary aftershock (red) and secondary aftershock (cyan)*

Given this classification, one can compute and plot the seismicity rate which is shown in figure 4.27. One can notice that the Omori law only holds for P3 with an exponent $p = 1/2$. This is not really surprising that the Omori law is not valid for P1 and P2 since the time structure was determined as random from the Poissonian arrival times whereas an actual temporal structure is established in P3. Many controversies exist on the values of p which has been found typically in the range from 0.3 to 2 in empirical study of earthquakes Helmstetter and Sornette (2002). The value of 0.5 reported here indicates a slow decay of the rate of aftershocks with time.

Helmstetter and Shaw (2009) argued that afterslip is thus a possible candidate to explain observations of aftershock rate decaying as a power law of time with an Omori exponent that can be smaller than 1. Indeed, afterslip induces a progressive reloading of faults that are not slipping, which can trigger aftershocks. Omori law with $p < 1$ are also explained, with models using the rate and state friction law Dietrich (1978), by the local stress heterogeneity changes which are responsible for the short-times triggering.

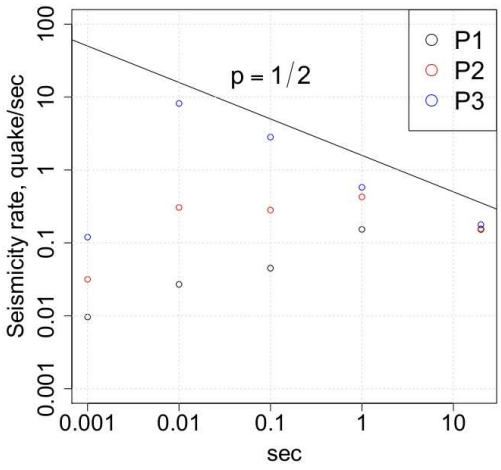

Figure 4.27 – *Seismicity rate in P1, P2 and P3 - Omori's law*

The extrapolation to fatigue is difficult but one can imagine that cascade processes are at the origin of this long-time dependence. One proposed explanation is to consider dislocation motions created by micro-cracks, coupled in space and time, that organize themselves into avalanches that are themselves dynamically coupled with avalanches clusters over all distances and sizes. The fatigue being subsequently the result of a collective spatio-temporal phenomenon. This is an assumption that need to have a deeper vision of the spatial organization of events.

Fractal clustering of earthquakes hypercenters

The last law to demonstrate is the one relative to the clustering property of earthquakes in space. An analysis of the spatial organization of the avalanches is performed by means of a correlation integral analysis of the hypocenter locations in figure 4.28. $C(r)$, which is the probability of two locations being separated by less than r, scales as $C(r) \approx r^D$ with a correlation dimension $D = 0.5 \pm 0.1$ in P3. This value is close to the one found for earthquakes Kagan (1991) since a value of 2.3 is found in three-dimensional measurements. Scaling analysis is limited toward small scales by the resolution threshold that induces an identical localizations for several hypocenters, and therefore an artificial clustering, whereas a finite size effect is visible toward large scale. This scale-invariant emerging structure results from the collective dynamics of defaults that self-organize into a scale free clustered pattern of avalanches. This picture completes

the scaling properties in terms of dissipated energy as well as the waiting times. A clear parallel can be established with the results of Weiss and Marsan (2003) where the spatial correlation dimension of dislocation avalanches in creep experiment was found. A value of D equal to 2.5 for 3D measurements was reported suggesting the same emergence of spatial clustering.

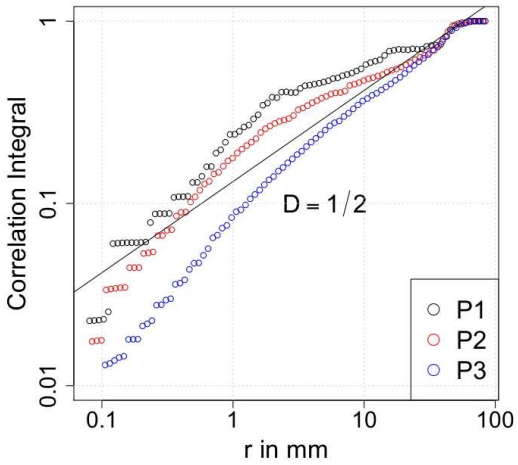

Figure 4.28 – *Correlation integral in P1, P2 and P3 - Fractal clustering of earthquakes hypocenters*

The self-similarity in time, space and energy are the three governing law that makes earthquakes as self-organized critical systems. Each one of these law has been verified in the third dissipative regime. This period clearly suggests that the long-term organization that leads the material to failure in fatigue is the result of a true self-organization governed by the three identical laws. Thus, the common results found in phenomena ruled by a dynamics acting on totally different scales, from earthquakes (10^5m) Gutenberg and Richter (1949) to damage of laboratory rock sample (10^{-4}m) Scholz (1991) and more recently to plastic phenomena (10^{-9}m) Dimiduk et al. (2006), strongly suggest a general scale invariance of the fracturing processes that is also supported by the results found in fatigue failure.

4.4 Post-mortem visualization

4.4.1 Thermal disappointment

Coupled to the acoustic recording were performed some thermal measurements that lead to some disillusions since the thermal relaxation of energy is remained constant after the shakedown stage, oscillating between two fixed temperatures as shown in figure 4.29. The lack of any precursory signal of thermal change upon cycling is probably due to the to important distance between the camera and the sample during the experiment. This results in a poor resolution of images causing noises that make impossible some computations of first or second order thermal quantities. The

initial idea was to inverse the heat equation to recover the intrinsic dissipation of the material. Unfortunately, it was not realizable. Nevertheless, some nice pictures of the large release of heat accompanying the failure are presented in figure 4.30.

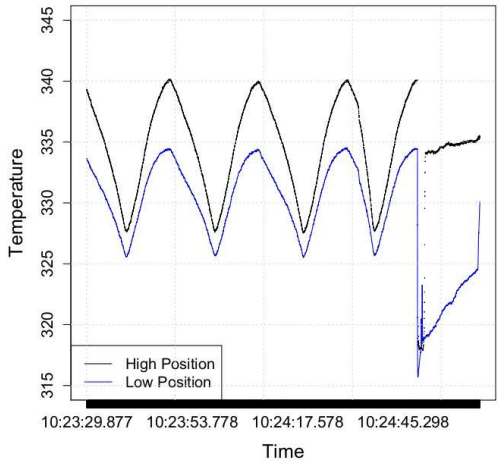

Figure 4.29 – *Typical evolution of the temperature measured in two points until failure*

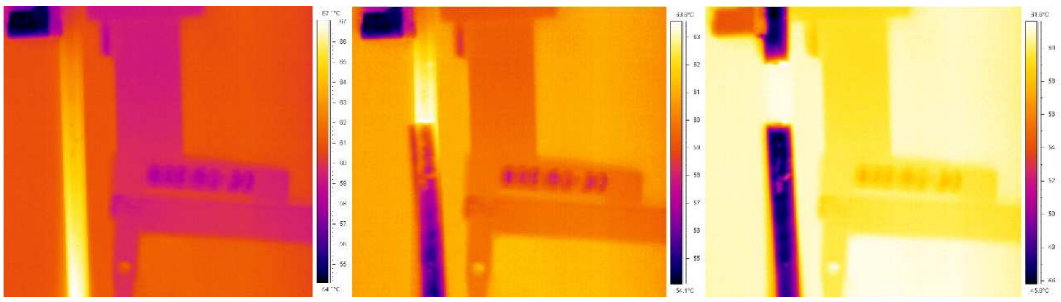

Figure 4.30 – *Infra-red photos taken at (-20)ms, at 0 ms and (+20)ms from the breaking of the sample*

4.4.2 Post mortem microscopic photos

If the thermal analysis does not reveal any extraordinary property, one can hope that the observations realized thanks to a Scanning Electron Microscop (SEM) will highlight some interesting characters of the fracture.

Figure 4.31 evidences three different areas exhibited on the fracture surface and their associated different textures. The first one is concentrated around the edge of the wire, concentrated around *C* and corresponds to the initiation of the failure. The second one is visible as a rough circle encompasses, *B* and *C*, it is the propagation area. It displays a different texture to the area in which *A* is included which is the failure area. One can notice the convergence of rivers that are all oriented in the direction of the initiation. Each of these area denoted as A,B and C are represented respectively in figure 4.32, 4.33, 4.36.

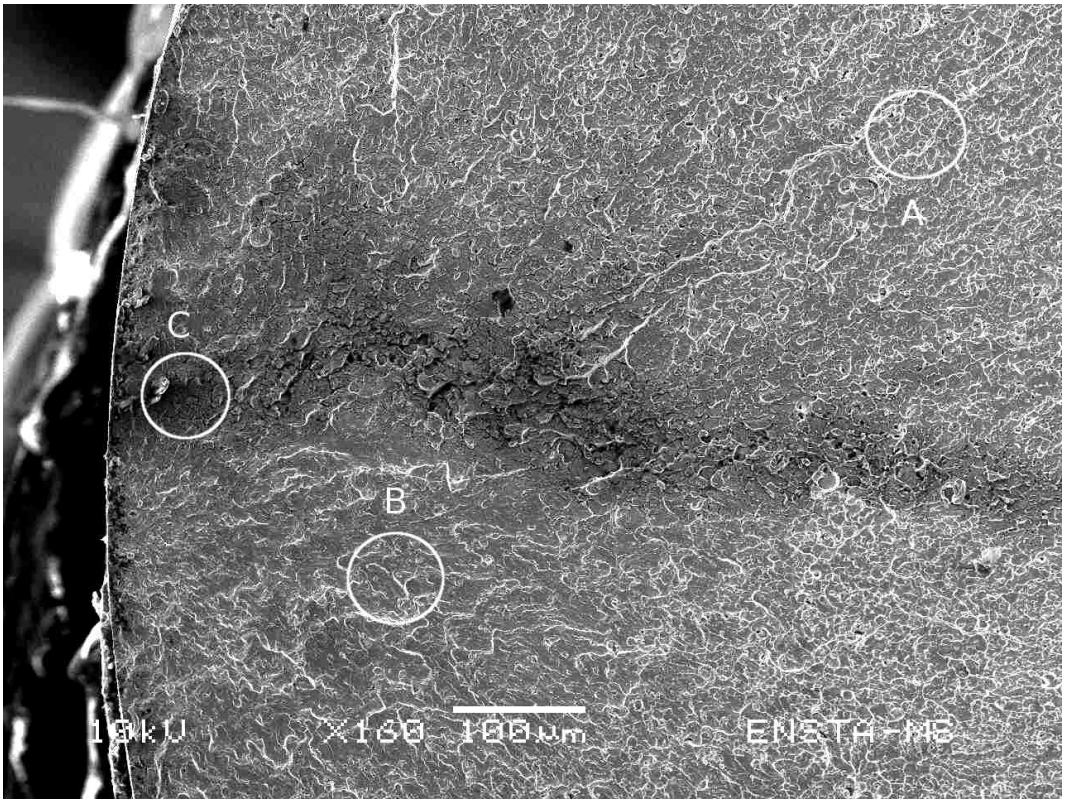

Figure 4.31 – *Visualization of the macroscopic failure*

The area *A* is located in the fracture area and presents a typical profile of a ductile fracture that result from a fatigue process. The presence of small cavities comes from the development of large plastic strains around inclusions that are visible.

The area B illustrated in figure 4.33 reveals some fatigue stria which are showed in a zoomed view in figure 4.34. These stria are the clues of the successive stopping positions of the crack front during the progressive propagation of the cracks. Their intervals informed about the propagation speed(s) of the crack. The pattern exhibited here suggests a very regular advance of the front. An attentive look of area B snapshot also enables to see the secondary micro-cracks that are formed upon the fracturing process. These micro-cracks are visible in a magnified view in figure 4.35.

Finally, the area *C* corresponds to the initiation area and reveal a smoother pattern.

These pictures confirm via a post-mortem visualization the presence of some expected phenomena at the basis of the previously recorded acoustic emission like the small cavities of area *A*, the micro-cracks of area *B* and the stria which demonstrate that the crack front was progressively advancing and confirm the cyclic emergence of the two patterns of P3. Despite this post-mortem analysis, a further step should be to perform interrupted experiments in each of the dissipative period to make a microscopical observation of the micro-structure in order to relate the dissipative regimes to physical observations. Nevertheless, acoustic recordings let undoubtedly appear the formation of the crack with the emergence of the asymmetric pattern spaced by half a loading period.

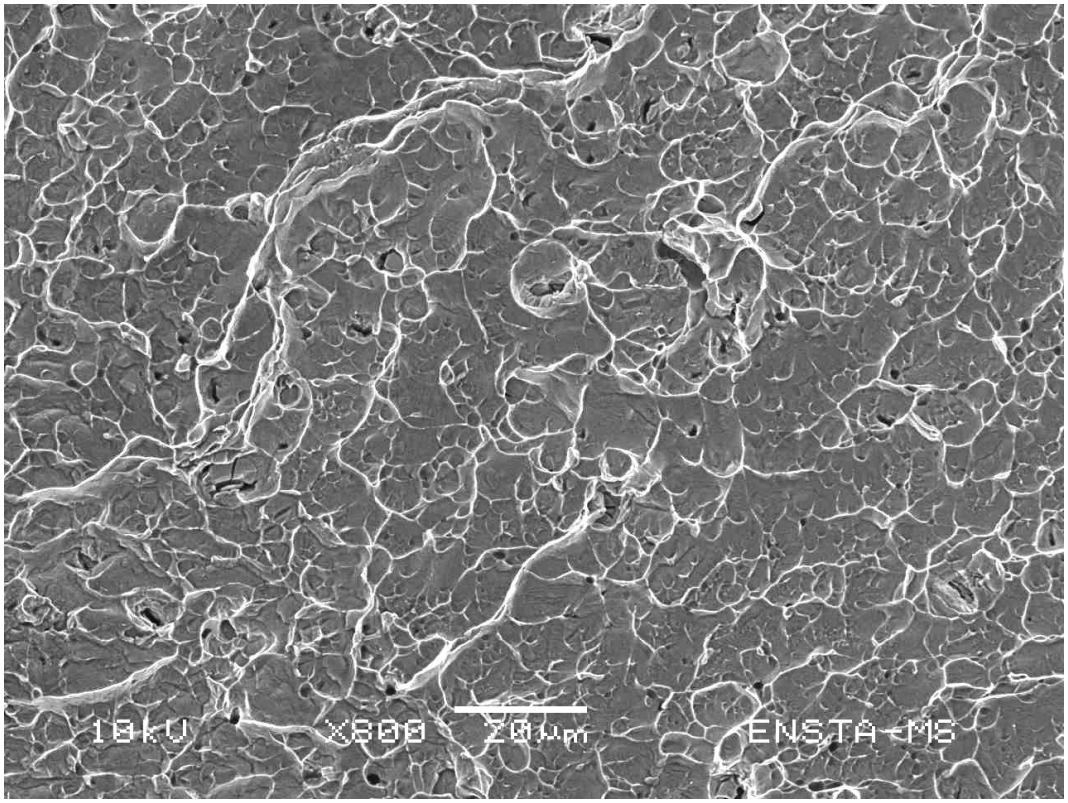

Figure 4.32 – *Visualization of the area A which is typical of a ductile rupture, visualization of small cavities*

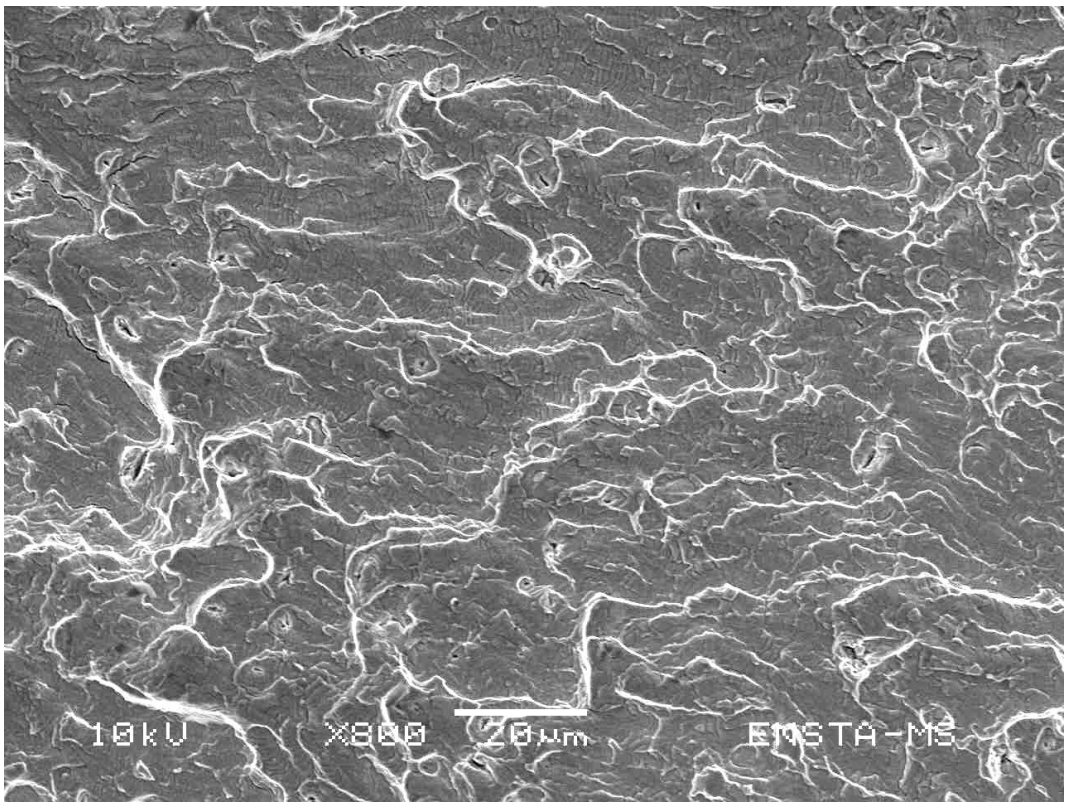

Figure 4.33 – *Visualization of the area B, micro-cracks and fatigue stria*

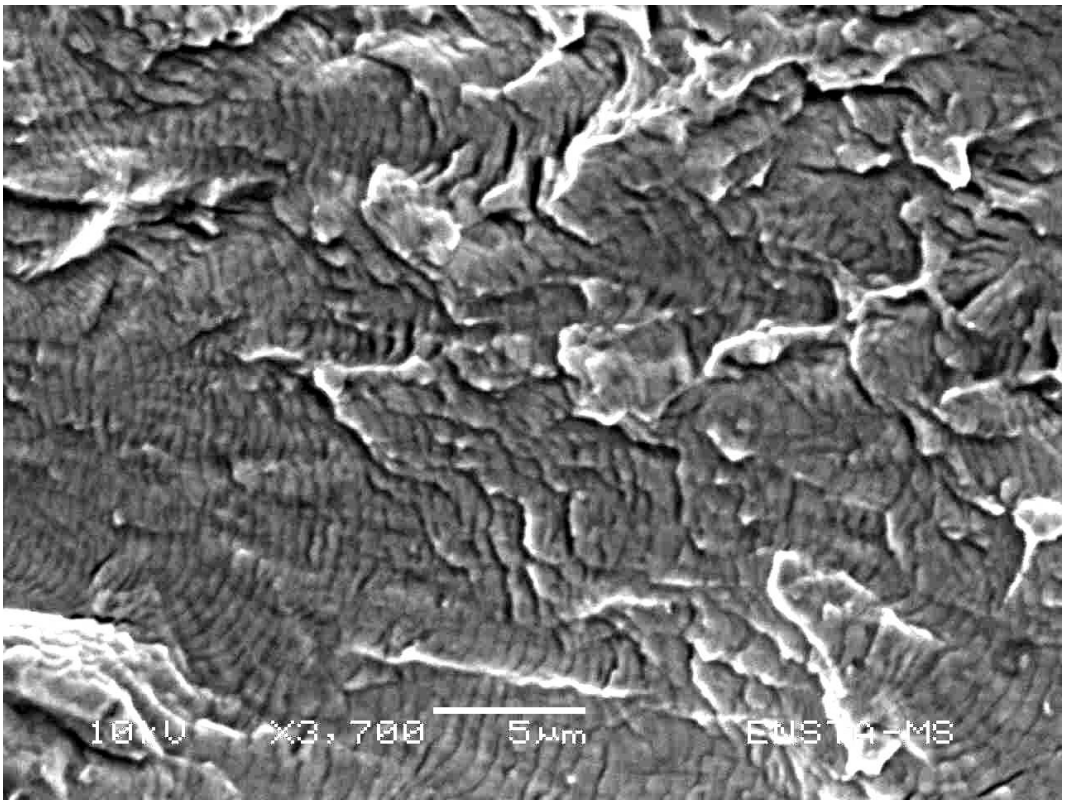

Figure 4.34 – *Visualization of the fatigue stria (Area B)*

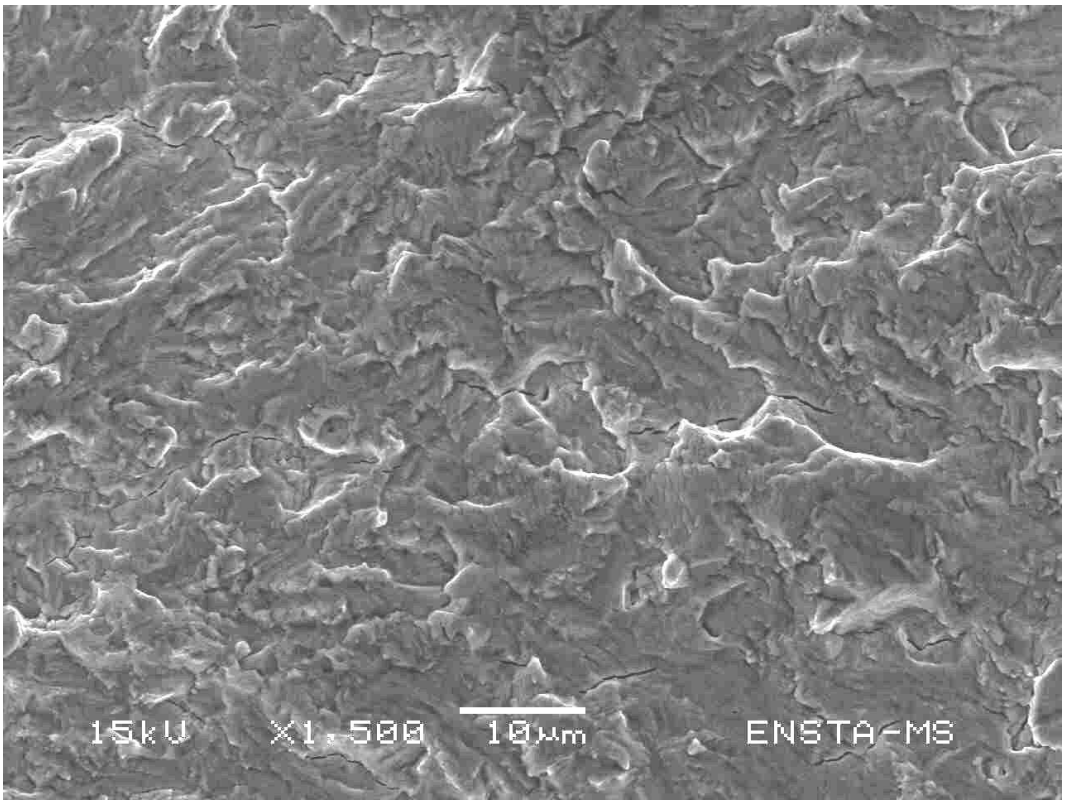

Figure 4.35 – *Visualization of the secondary micro-craks (Area B)*

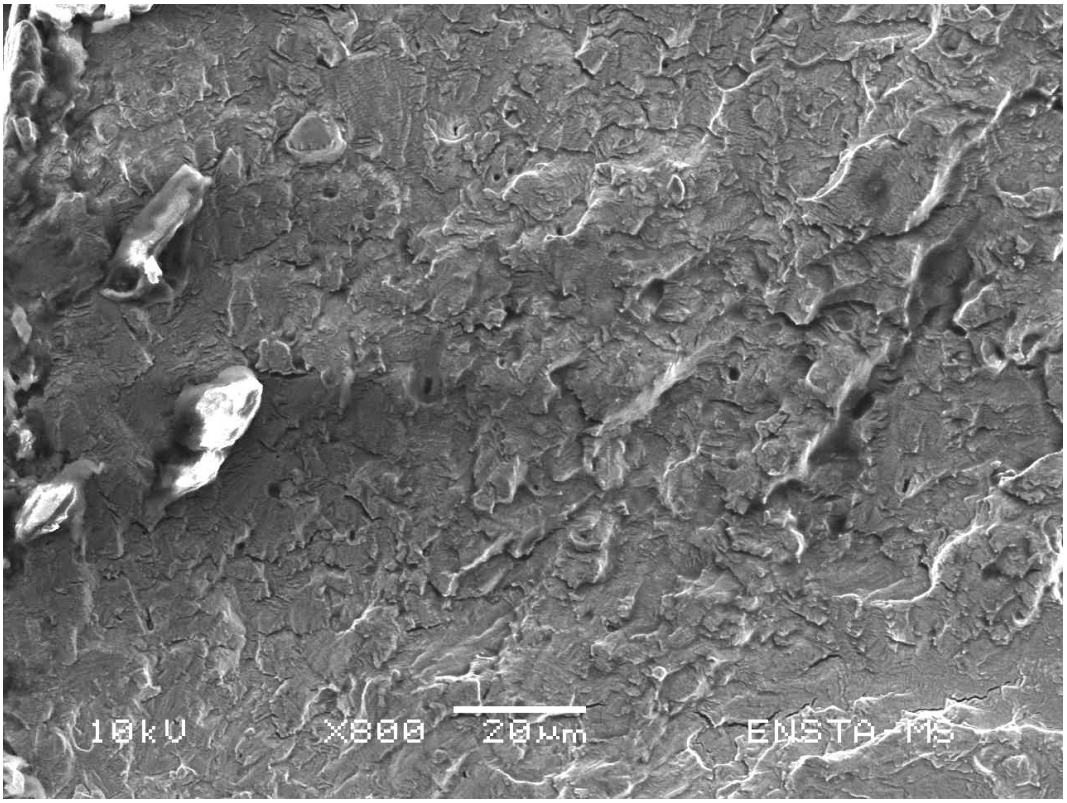

Figure 4.36 – *Visualization of the area C, initiation area of the macro-crack*

4.5 Scientific improvements

This chapter was the opportunity to investigate for the first time in material sciences how fatigue failure can be interpreted in the framework of SOC. Acoustic recordings bring to light three dissipative regimes illustrated by three different rates in the release of energy that are consecutive to the rapid loss of the (acoustic) shakedown state.

The first dissipative regime is characterized by a scale free distribution of energy but without any specific time structure. The transition from the first to the second dissipative regime is accompanied by a loss of the critical character of energy and the slow appearance of a temporal structure in the relaxation of events. The second period act as a transient period since energetic and temporal organization in scale-free patterns become crystal clear cycle after cycle. In the same time, the spatial organization of events is more widespread upon cycling. The beginnings of the critical state progressively appear until being completely established at the transition from the second to the third dissipative regime. This special instant is self-organized in the sense that it progressively emerges without any fine tuning of the order parameters and simultaneously critical since the main quantities (energy, time and space) exhibit self-similar behavior. The establishment of this SOC state is accompanied by the creation of the crack that exhibits two different cyclic patterns separated in time by half a loading period (one associated to the opening of the cracks and the other of to the closing).

A comparison between the earthquakes dynamics and the fatigue fail-

ure was also attempted in this chapter since the mainstream idea of SOC claims for universality. Indeed, the three empirical laws (Gutenberg-Richter, Omori and the fractal distribution law) governing the dynamics of earthquakes have also been established for the third dissipative regime of fatigue (that corresponds to the nucleation and propagation of the crack). These common laws that operate on totally different large scales are nevertheless suspected to be unique in the description of a long term organization of fracture.

The burning issue of the universality attached to this result has been addressed through experiments with different loads and frequencies that highlight that the same dissipative pattern of energy holds for all the experiments. Furthermore, the distributions of the main quantities share common variations with similar values in each case which support common governing mechanisms for fatigue failure. As a consequence, a physical interpretation that can be given to these results is that each dissipative regime is attached to the predominance of a physical mechanism. There are three physical mechanisms enable to generate acoustic wave inside the material; martensitic transition, dislocation motions and opening and closing of cracks. Thus, the first dissipative regime is suspected to be dominated by dislocation motions, the second which constitutes the transition in dissipative states seems to be governed by dislocation motions and the initiation of cracks that are attached to the third dissipative regime. Interrupted experiments coupled with microscopic observations would permit to have a second proof of these interpretations.

Nonetheless, these other experimental results do not allow to draw some hypothetic conclusions about the fundamental question of universality which is the long ever searched holy grail. Such a consecutive affirmation to end this chapter will not be serious since it requires deeper investigations to experiment a wide range of experimental conditions which could be the subject of a future thesis...

To conclude this chapter an attempt is made to answer the main question of the thesis which is to give a criterion to detect the initiation of fatigue failure. To formalize the results found through a theoretical enunciation, the following assumption is made regarding the acoustic dissipated energy curve as a function of the number of cycles for a pseudo-elastic fatigue experiment on an SMA. The general form considered is depicted in figure 4.37

Fatigue initiation criterion 1

The fatigue initiation criterion can be defined in the following way given that $\mathcal{D}$ represents the acoustic dissipated energy along all the experiment and $\mathcal{N}$ represents the theoretical cycle where the fatigue crack is initiated.

$$\mathcal{D} = \int_{t=0}^{t=t_R} e(t)dt \tag{4.2}$$

$$\mathcal{N} = \max_{0<t\leq t_R} \frac{\partial^2 \mathcal{D}}{\partial N^2} \tag{4.3}$$

The following properties are associated to the initiation time of the fatigue crack:

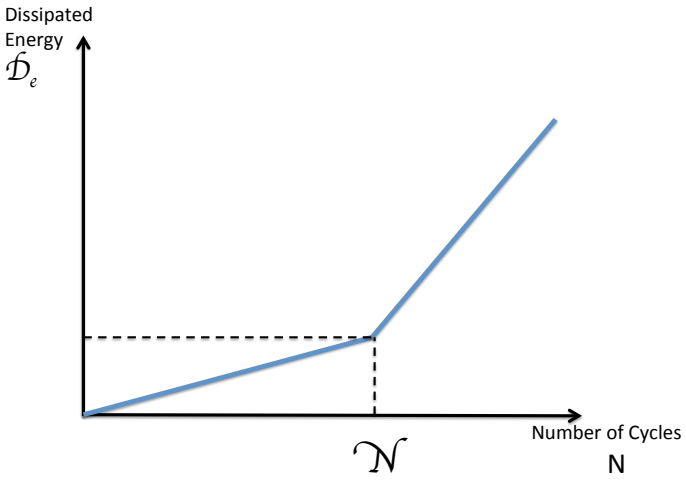

Figure 4.37 – *Theoretical response of the acoustic dissipated energy of a repeatedly loaded SMA*

Properties 2

The time structure shifts from an exponential time interval distribution to a power-law distribution, revealing a temporal self-organization of in the release of energy. The self-organization is also noticeable in space and energy since these two quantities are exhibiting distributions with scale-free properties for N. To sum-up, the system is fully critical in time, space and energy [1].

[1] In the former detailed experiment, N is associated to the cycle 2450.

Travel across sciences

5

Contents

This chapter discusses the importance of extreme events through sciences. The focus will be given on the scientific revolution that is led in financial engineering to consider markets as complex systems, characterized by the ubiquity of power-laws and long range correlations. The strong analogy in the typology of datasets coming from acoustic recordings of earthquakes or plasticity and high-frequency variations of prices of financial assets suggests the common use of point processes modeling. A financial example dealing with the cross-excitations between price changes of financial instruments will open the way to another approach in the analysis of damaging modes in fatigue.

5.1 The potential of extreme behaviors

The kaleidoscope of figure 5.1 represents several major events that occurred over the past few years. The shock attached to these images is sufficiently intense to make it memorable by everyone and consequently useless to describe. But what have in common quakes, financial crashes or terrorist attacks? All have the potential of extreme behavior.

Figure 5.1 – *Sendaï earthquake tsunami 03/11/11 (magnitude 9.0) - WTC attack 09/11/01 (2977 deaths) - Lehman Brothers Bankruptcy 09/15/08 - Sumatra earthquake tsunami 12/26/04 (magnitude 9.3)*

5.1.1 2001-2011: An extreme decade

Crises are at the basis of our every day life. From natural catastrophe to economic turmoils attached to financial draw-downs passing through political instabilities, crisis have a fundamental societal impact. The last decade was particularly rich in extreme events whatever the direction we are looking to...

More than 780000 persons were killed from 2001 to 2011 if one only considers the deadliest earthquakes of each year. Among them, two extreme earthquakes, that resulted in devastating tsunamis, occurred around the world. The most recent one is attached to the nuclear catastrophe of *Fukushima* in Japan the 11^{th} of March 2011 with a magnitude of 9.0 and 20896 dead people. The second one is the one that took place along the west coast of *Northern Sumatra* the 26^{th} of December 2004 with a magnitude 9.1 and 227898 dead people[1].

In the same time, three global "economico-financial" crisis quakes the world. The first one is the bursting of the *dot-com* bubble in from 2000 to 2001 that was followed by the *junk-bonds* or *subprimes* crisis from 2007 to 2009 and the last one is the (European) *sovereign debt crisis*, from 2010

[1]The three others earthquakes that caused the largest fatalities are 01/12/10 Haiti, M=7.0, 316000 dead people; 05/12/08 Sichuan, M=7.9, 87587 dead people and 10/08/05 Pakistan, M=7.6, 80361 dead people

to ... I hope soon! Among the most striking consequences, one can cite the highway to hell of the NASDAQ index that fell down from 5048 the 03/06/00 to 1423 the 09/17/01 after the attack of the World Trade Center, with an estimated common loss of 148 billions over the considered period for the 4300 companies of the index. The subprimes crisis was symbolized by the bailout of Lehman Brothers the 09/15/08 and the national help brought by the American government to the worldwide insurance company AIG that was on the point of collapse. Regarding the last crisis, the prudence advocates doing any conclusion so far...

In the same spirit it would have been possible to discourse on the political revolutions in Arabic countries in 2011 or the accumulation of terrorist attacks.

What these examples aim to demonstrate? One thing in reality, all these systems can be considered as a collection of interacting units; the collection is complex, everything depends on everything else. Tectonic plates, traders, revolutionaries or micro-cracks are the interacting units of these complex systems. Complex systems can be described as self-organizing systems that develop similar patterns over many different scales, from the very little to the very large. A central property of such complex systems is the possible occurrence of coherent large scale collective behavior with a very rich structure, resulting from the repeated nonlinear interactions among its constituents: the whole turns out to be much more than the sum of its parts. This complexity is at the basis of the unpredictability of these systems.

It turns out that most complex systems in the natural and social sciences do exhibit rare and sudden transitions that occur over time intervals that are short compared with the characteristic time scales of their posterior evolutions. Earthquakes, financial crashes or fatigue failure result from long-term organization process whereas the catastrophic events occur in a flash. Furthermore, these extreme events are irregularly spaced in time and cascade process take place subsequently to extreme events in temporal clusters (one can think to earthquakes aftershock, or to the contagion in financial crisis). Such extreme events express more than anything else the underlying forces usually hidden by an almost perfect balance. It is essential to realize that the long-term behavior of these complex systems is often controlled in large part by these rare catastrophic events. The recent large earthquake in Fukushima, Japan 2011, accounts for a significant fraction of the total tectonic deformation as well as a modification of the rotating angle of the Earth. One can also underline that landscapes are more shaped by the millennium flood that moves large boulders rather than by the action of all other eroding agents. This contemporary vision of sciences is supported by the works of S.J. Gould (1993) that proposes to consider biological evolution as characterized by phases of quasistatis interrupted by episodic bursts of activity and destruction. One accidental event after another.

Earthquakes have been widely studied to provide some reliable predictive schemes but one difficulty stands in the fractal framework of the complex systems that avoids to consider any characteristic scale. The power-law distribution of earthquakes sizes reflects the fact that large earthquakes are nothing in probability but a multitude of small earthquakes

is occurring permanently that make them unpredictable. Nevertheless, predicting the detailed evolution of complex system has no real value and people are much more interested to predict the phases of evolution that really count, like the extreme events.

The outstanding scientific question that needs to be addressed to guide predictions is how large-scale patterns of catastrophic nature might evolve from a series of interactions on the smallest and increasingly larger scales, where the rules for the interactions are presumed identifiable and know. A common denominator of the various examples of crisis is that they emerge from a collective process: the repetitive actions of interactive nonlinear influences on many scales lead to a progressive build-up of large scale correlations and ultimately to the crisis.

Beside all the amazing efforts accomplished by scientists over the past centuries to reveal the innermost secrets of fundamental constituents of nature, explanations across scales are still lacking. It has been demonstrated that matter is formed of atoms which are in turn composed of electrons, protons and neutrons and so on through the scales..., nevertheless, these basic elements are interacting through simple physical law that are forming emerging properties that remains misunderstood. Consequently, one can really wonder about the value of "predictive models" in sciences and it seems that new methods of analysis need to be introduced. Such attempts are realized in finance to understand the price dynamics as it will be shown in the next section. It is important to look at the techniques developed through the discipline, to learn and invent from analogies, mainly when speaking about complex systems.

5.1.2 "A state of shocked disbelief" - A. Greenspan

These words are those of Alan Greenspan on the 24^{th} october 2008, in front of the House Oversight Committee. It was a 4 hours long mea-culpa of the former Federal Reserve Chairman to explain the errors committed in predictions and policies which result in a, as quoted, "once-in-a-century credit tsunami". Extreme events you said.

Let the efficiency down

Economy and financial markets have been of growing interest for physicists over the 20 past years P.W. Andersen and Pines (1988). The sympathy of physicists for finance has been largely motivated by the misleading character of the Black-Scholes model which is at the basis of the financial mathematics models used to evaluate the price of insurance contracts. A legitimate full-scale attack J.P. Bouchaud (2003), Taleb (2007), Bouchaud and Sornette (1994), Bouchaud and Potters (2001) has been launched again this model that assumes that Gaussian fluctuations of prices which dangerously results in an underestimation of catastrophic events. Criticisms also addressed the ability of the model to furnish a perfect risk-less hedging strategy. Consequently, new paradigms to account for financial variations need to be established since this widespread model, which is the mainstay of financial engineering, sounds inadequate despite all the attempts realized to fiddle with.

A new branch of sciences called econophysics aims at studying economy and finance through methods coming from statistical physics. The approach is much more different to the one taken by pure economists since it focuses more on mechanisms and analogies based on empirical observations rather than on axioms and theorem proving. Consequently, such different points of view breathe new life into the old-establishment of financial assumptions. Among the main revisions stands the disproof of the efficiency of markets Bouchaud (2009; 2008).

The efficiency of markets is the property stating that in deregulated markets prices faithfully reflect the underlying fundamental values, while markets ensure optimal allocation of resources. If a forecasting error occurs on the price of an asset, it should be immediately corrected by economic agents who are supposed to be rational (make a stop think about what governs human behaviors, and what is rationality and continue) and act consequently with the omniscience of the future states of the world. As a consequence, markets are considered stable and crisis only result from exogenous events like natural catastrophes, political takeovers or terrorist attacks. The endogenous character of crisis is considered as inconsistent whereas the occurrence of previous bubbles resulting either from speculation (which sounds strangely face to the rational hypothesis) or from faulty mathematical models (which also seems difficult to be in concordance with the idea of perfect knowledges of the "future states of the world"). Moreover, some new questions arise with the large development of high-frequency electronic transactions. It is legitimate to have doubts about the notion of fundamental value of assets given a set of information. Interested readers about the impact of information on the financial value of an asset can refer to A. et al. (2008), D.M. Cutler and Summers (1989), Engle and Ng (1993).

The holy Grails: power-laws

Then, lightened from these assumptions, a phenomenological approach enables the discovery of a large number of phenomena that are power-law distributed.

New large-scale financial data sets have led to progress in the understanding of the tail of financial distributions which was pioneered by Fama (1965), Mandelbrot (1963). Benoit Mandelbrot studied the variation of cotton prices from month to month over several years and concluded that the tails of this distribution followed a Pareto distribution with the exponent close to 1.7. The research done afterwards on wheat prices, interest rates and railroad stocks led to the speculation of a universal scale-free law involving the prices of different commodities.

The possibility of this universal power-law concerning the tails of the distribution of short-term stock market returns interested many economists and physicists, being crucial for developing risk management methods. Recent researches Gopikrishnan et al. (1999), H.E. Stanley and Salinger (2002), Plerou et al. (1999) show that the tails of the cumulative return distribution of the price of individual stocks and market index follow a power law distribution, with the exponent approximately equal to 3, a property called the inverse cubic law. This behavior was found not only

in developed countries, but also in some developing countries like China G.F. Gu (2008), India Pan and S. (2008), Korea K. Kim and Chang (2005) and Mexico Coronel-Brizio and Hernande-Montoya (2005). This latter discovery is quite surprising, taking into account that emerging markets are subject to severe macroeconomic instabilities, and hence, are not expected to follow the same market dynamics as the more developed countries do. A few models were developed in order to explain the emergence of power law distributions in the stock market returns, one of which is the dynamic multi-agent model based on herding behavior Cont and Bouchaud (2000).

Although initial research focused only on returns, power laws have also been found to characterize the number of shares traded and the number of trades in the stock market. Gopikrishnan et al. (2000) find that high-frequency data from the US stock market exhibit trading volumes (V), which denotes the number of shares traded, characterized by a scale-free distribution with exponent $3/2$. This result has been extended to Paris and London respectively by Gabaix et al. (2007) and Plerou and Stanley (2007) that found the same exponent. The new access to the high-frequency data has also permitted to have finer financial relationship as the one of M. Wyart and Vettorazo (2008) stating that $\sigma \approx cS\sqrt{\phi}$ where σ is the volatility, $c \approx 0.6$, S the spread (this notion will be introduced further) and ϕ the market activity, i.e. the number of trades per unit of time.

Among the results that really matter for us are the power-law correlations in time exhibited by the activity G. Bonnano and Mantegna, Plerou et al. (2005) on the stock market as well as the volatility R. Cont and Bouchaud (1997), M. Potters and Bouchaud (1998), Liu et al. (1999b). These results are really strong since it reflects their intermittent and jerky nature, the quiescent periods are intertwined with burst of activity on all time scales. From an empirical point of view, the intermittent nature of the activity in financial markets is similar to the energy dissipation in a turbulent fluid S. Ghashghaie and Dodge (1996) or in the acoustic response of a cyclically SMA with regards to the results of the previous chapter.

One visual representation of this intermittent character of volatility and volume can be found the figure 5.2. This graph represents the absolute value of the daily price variation and the associated volume for the Société Générale asset, between the 01/01/2003 and the 09/11/2011, in the top part of the graph, the second part exposes the acoustic released energy during a fatigue experiment and a simulation of price variations distributed as a Gaussian law for an identical volatility as the one observed for SocGen on the considered period. This character is not specific to the SocGen share but is found for a wide range of financial products all around the world.

A naked eye observation testifies of the very different nature of the empirical volatility, like the volumes, that has the potential of extremes whereas a Gaussian simulation has some kind of response that seems to have a constant upper limit. Moreover, a clustering of large moves is visible for the price variation and the volume as well as for the release of energy whereas it is not present for Gaussian simulation. The inability of a Gaussian distribution to describe the variation of prices can be seen in figure 5.3 where a clear underestimation of large events is noticeable for

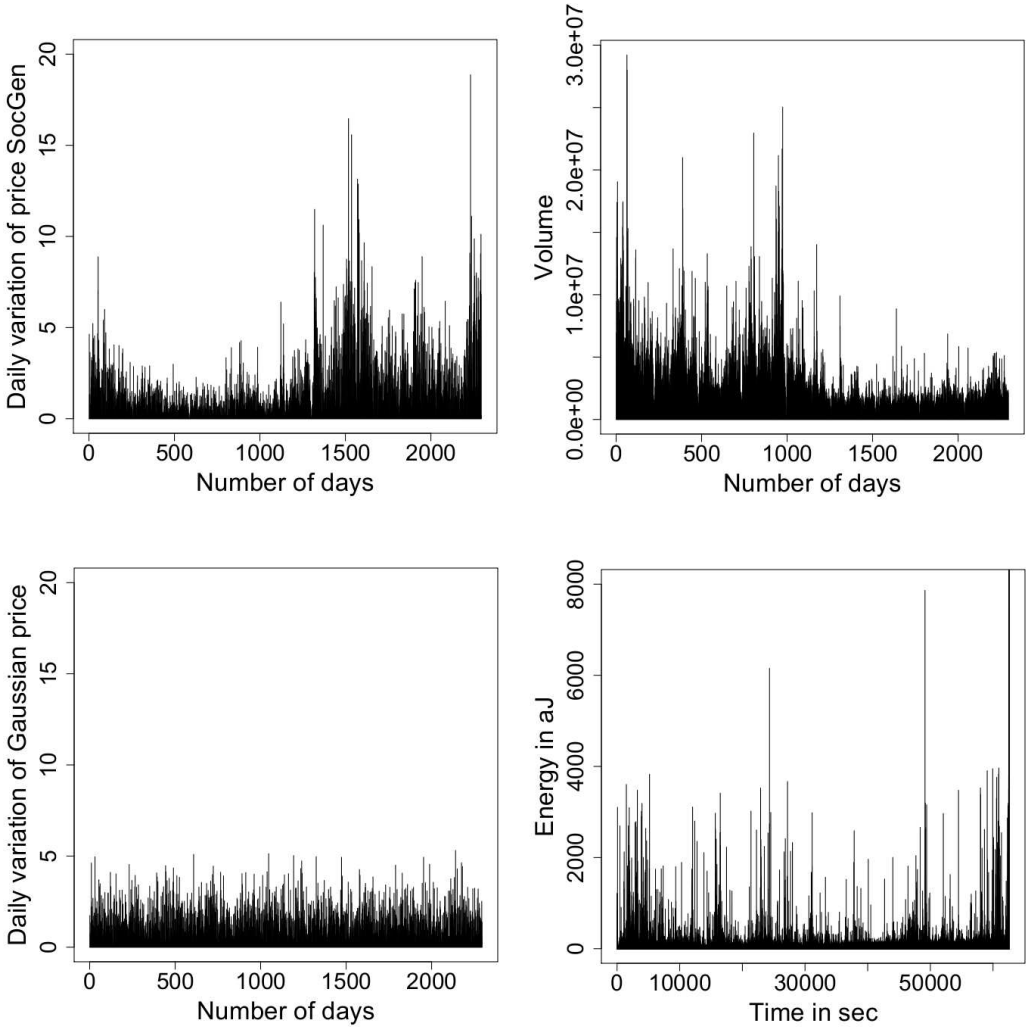

Figure 5.2 – *Intermittent behaviors and Gaussian behavior*

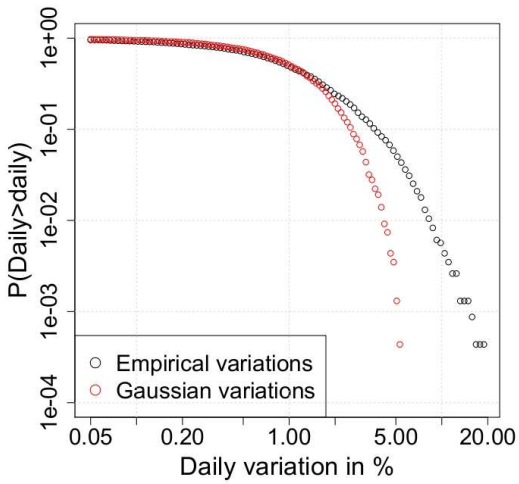

Figure 5.3 – *Distribution of the absolute value of the daily variations for SocGen (01/01/2003 to 09/11/11) and simulated distribution with the same standard deviation for a Brownian motion*

a price modeled as a Brownian motion. Finally, even a novice in finance should have seen that the volatility is correlated to the volume ...

These graphs aim at pointing out the similarities between complex systems as Barkhausen noise, earthquakes, price variations or release of acoustic energy in fatigue experiment. Indeed, this complex and jittery endogenous dynamics results from a exogeneous driving force with steady and regular properties. So the critical nature of the dynamics results from collective effects. The interactions between individual components with simple behaviors lead to an emergent behavior. This generic intermittent behavior for physical systems made of heterogeneities and interactions provides a burning attempt to think that markets reflect the same underlying mechanisms.

These questions are investigated through the use of toy models that aim at capturing key phenomena that give rise to such a complex response. Interested readers can refer to the papers of Sethna et al. (1993), Mezard and Montanari (2009), Lux (2008), Goldstone and Janssen (2005), **?** for RFIM models and to D. Challet and Zhang (2004) for minority game.

A possible explanation of this complex emergent picture stands in the understanding of how financial prices are created. Much as in physics, a detailed understanding of the microscopic world will provide invaluable insight on macroscopic phenomena. With the introduction of electronic transactions, new types of data are available and the comprehension of the micro-structure of the market is a true challenge. Given the discrete character of prices , some basic introductions about the point processes are needed to understand the next parts.

5.2 The point process bridge

Few knowledges about the microscopic character of prices are introduced as starter. Readers familiar with tick-by-tick data and order books can directly jump to the next section.

5.2.1 Electronic markets and earthquakes similitudes

Over the past decades, financial markets have been considerably modified with the advent of *electronic transactions*. This radical change takes place in the increase of the sampling frequency of the acquisition of data. As a direct consequence stands the explosion of the amount of available data as well as the access to new types of data.

Since the seminal papers of Hasbrouck (1991) and Engle (2000), the modeling of financial data at the transaction level (commonly called *high frequency data*) is an ongoing topic in the area of financial econometrics. To understand the properties of these data, one has first to introduce the notion of *order book*. An order book is a table which summarizes the buyers and the sellers for a given financial asset. It is represented in the table 5.4 for a pedagogical example. One can find in the first line the highest buy order (called *Bid*) as well as the lowest sell order (called *Ask*) with their respective associated volumes. The difference between the Bid and the Ask is called the *Bid-Ask spread*, commonly called spread. The spread is a multiple of the tick size which is defined as the smallest price increment

by which a price can move. In the example of table 5.4, the bid is 100.4, the ask is 100.7, the spread is equal to 0.3 and it made of 3 ticks since I arbitrarily decided that the minimum variation of price is 0.1. The basic rules that governed the dynamics of the order book (simplified for easier comprehension) are given by the following bullet points:

- When a limit buy offer, matches a sell offer, the transaction is realized and the orders are removed from the order book
- When a new limit order arrives (buy or sell) it is ranked in the corresponding column according to it price with the associated volume
- When a market order arrives (buy or sell), it is executed instantaneously against the best prevailing limit orders, consequently, it is not stored in the order-book, only limit orders are.

Buy Volume	Buy Price	Sell Price	Sell Volume
50	100.4	100.7	600
5000	100.3	100.9	12
362	99.8	101.0	765
1500	99.6	101.3	876
49	99.2	101.8	10000
...	...	...	...

Figure 5.4 – *Pedagogical example of an order book*

Consequently, one can understand that giving the large increase in the use algorithms to realize electronically financial transactions, this order book is perpetually evolving with the arrivals and departures of orders. It is a dynamical system. A large number of researches deal with the evolution of the order book and its modeling M. Wyart and Vettorazo (2008), Potters and Bouchaud (2005), Toke (2010) due to its intimate link with the formation of the price of the asset. The study of the order book refers to the microstructure of the markets, the basic agents in complex systems, the fundamental entities.

The first consequence that comes immediately is that transaction data are irregularly spaced in time due to the waiting time that separates the match of two prices. The second consequence is the discreteness of the variations of prices, commonly called *tick by tick* variations in opposition of classical financial theory that consider continuous prices.

These two consequences are illustrated with the representation of the variation of the price of the Société Générale share at different time scales 5.5

Taking into account these definitions, one can better understand the interest of the financial industry for point process models. Indeed, the dynamics of prices can be expressed by a simple triptych (Size, Timestamps, Sign) which corresponds to a positive or negative variation of one or several ticks at a random time. In the same time, the occurrence of an earthquake can be sum up as a triptych (Energy, Timestamps, Location). The sign is useless since the release of energy is always positive but the

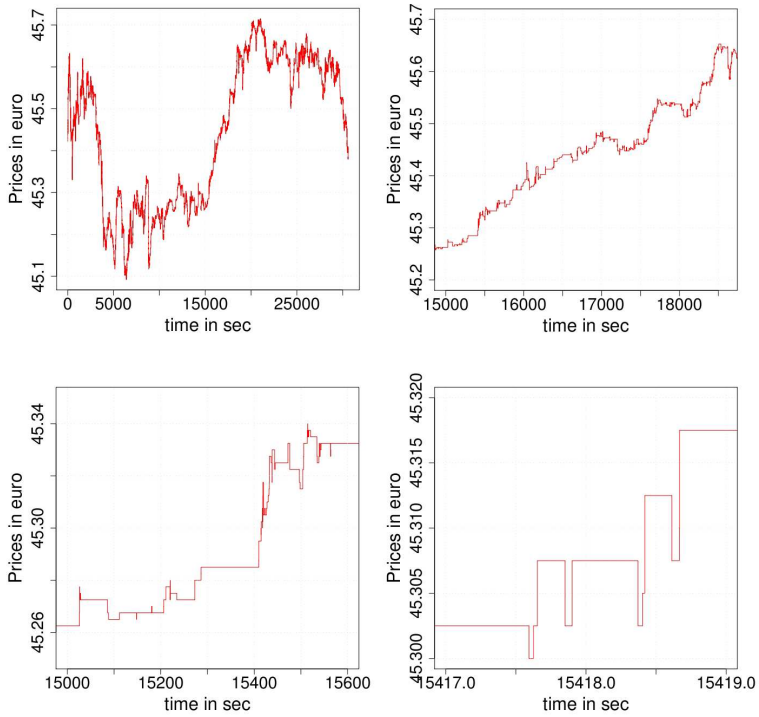

Figure 5.5 – *Visualization of the price of the société Générale share for T=28800 sec (one trading day), for T=3600 sec, for T=600 sec and for T=2 sec*

knowledge of time and location enables to compute the correlations in time and space between earthquakes. The financial parallel is to compute the temporal correlation between assets. If one wants to popularize, point processes allow to study independently, the impact of a release of energy E at time t in a location x_1 over a location x_2 and similarly the impact of a variation of price δP at time t for an asset A_1 over an asset A_2. Indeed, it is not worth being a financial expert to understand that some "spatio-temporal" correlations may exist between the behaviors of assets (think about couples as BNP Paribas and Société Générale or Renault and PSA).

Finally, one can understand that point processes are of prior importance in the modeling of the discrete occurences of intermittent systems. This property being shared by a large number of systems, it seems important to introduce the fundamental notions of the point processes theory. For the sake of readers, mathematical details will not be given but it can be found in the thorough book of Daley and Vere-Jones. A particular attention will be devoted to introduce properly Hawkes type processes that are subsequently used through a financial application and extended to the acoustic recordings modeling.

5.2.2 Hawkes processes as a link

Point processes modeling

A spatio-temporal point process is a random collection of points where each point represents the time and location of an event. Examples of events include incidence of disease, births of a species, occurrences of

earthquakes, lightning strikes or tsunamis. These examples underline that, often, there is other information to be stored along with each point. In the case of birth, one can need to know the sex of the born species or alternatively in earthquakes analysis, one can be interested in the released energy. Such processes may be viewed as marked spatio-temporal point processes, i.e. random collection of points, where each point has associated with it a further random variable called a mark.

Any analytical spatio-temporal point process is uniquely characterized by its associated conditional intensity λ Fisman and Snyder (1976). λ may be thought of as the frequency with which events are expected to occur around a particular location *(t,**r**)* conditional on the prior history $\mathcal{F}_t$ of the point process up to time t Daley and Vere-Jones, Karr (1991). Formally, the conditional intensity associated with a spatio-temporal point process N may be defined as the limiting conditional expectation:

$$\lim_{\delta t, \delta \mathbf{r} \to 0} \frac{\mathbb{E}[N((t, t+\delta t) * (\mathbf{r}, \mathbf{r}+\delta \mathbf{r}))|\mathcal{F}_t]}{\delta t \delta \mathbf{r}} \tag{5.1}$$

The behavior of a spatio-temporal point process N is typically modeled by specifying a functional form for $\lambda(t, \mathbf{r})$ which represents the infinitesimal expected rate of events at time t and location $\boldsymbol{r}$, given all the observations up to time t.

In general, λ depends not only on *(t,**r**)* but also on the times and locations of preceding events. When N is a Poisson process, however, λ is deterministic. The simplest model is the stationary Poisson, where the conditional rate is constant. In the case of modeling environmental disturbances, this model incorporates the idea that the risk of an events is the same at all the times and locations, regardless of where and how frequently such disturbances have occurred previously. Such a simple model will not be able to describe the complexity of earthquakes dynamics. Consequently, models accounting for the clustering in time and space have been introduced, these models are called *self-exciting point processes*.

A commonly used form for such models is a spatio-temporal generalization of the Hawkes model Hawkes (1971) where λ may be written as:

$$\lambda(t, \mathbf{r}) = \mu(t, \mathbf{r}) + \int_{-\infty}^{t} \int_{\mathbf{r}} \nu(t - t', \mathbf{r} - \mathbf{r'}) dN(t', \mathbf{r'}) \tag{5.2}$$

The functions μ and ν represent the deterministic background rate and the clustering density respectively. When observed marks m associated with each point are posited to affect the intensity at which future points accumulate, this information is typically incorporated into the function ν:

$$\lambda(t, \mathbf{r}) = \mu(t, \mathbf{r}) + \int_{-\infty}^{t} \int_{\mathbf{r}} \nu(t - t', \mathbf{r} - \mathbf{r'}, m) dN(t', \mathbf{r'}, m) \tag{5.3}$$

A variety of form have been given for the clustering density ν. In the earthquakes modeling, readers can refer to Musmeci and Vere-Jones (1992), Ogata (1988), Rathbun (1993), Kagan (1991) and Ogata (1999) for a review.

All these models aim at finding the best functional form of the conditional intensity of a spatio-temporal point process to fit a complete catalog

of earthquakes. Consequently, the proposed forms of ν are typically designed to be reminiscent of such empirical observations as the decay of aftershock frequency, as well as the dependence on the magnitude of an exciting event. One has to understand that the occurrence of an event with the attached triptych (E,t,r) will affect the conditional intensity and consequently updates the probability of occurrence of next earthquakes in the three dimensional space (Energy, Time, Location). A simple pedagogical representation of the phenomenon can be found in figure 5.6.

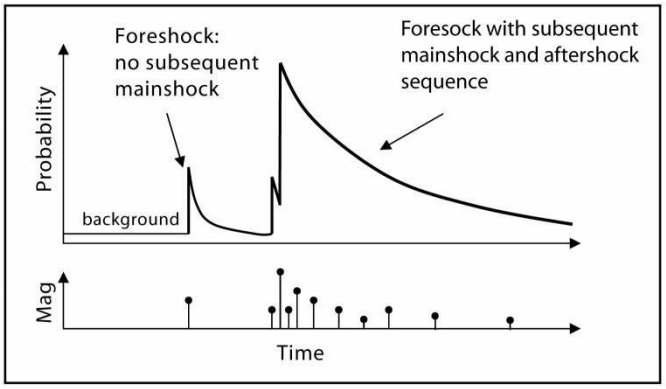

Figure 5.6 – *Simple representation of the intensity modification with the occurrence of earthquakes*

Finally, the methodology is to test several forms for λ, each one being attached to a different conjecture about the underlying physics. These different models are compared through the maximization of the log-likelihood of the intensity of the point process for a given dataset. Then, model selection criterion such as AIC (Aikake Information Criterion) are used to retain the specific form giving the best results and consequently interpretations about the encountered mechanisms are proposed.

Since everybody is now fitted with all the theoretical notions, let us dive in the financial application of point processes.

Financial study

High frequency time series are of major interest to understand how some macroscopic phenomena emerge from the microscopic behavior of prices. These travels across the scales have revealed two phenomena that are changed when looking at different time horizons. The first one is the explosion of the volatility for low time lags that refers to only one asset Andersen (1997). The second one deals with the vanishing behavior that arise in the correlation between two assets for low time lags Epps (1979). These two phenomena are shown in figure 5.7.

The comprehension of the emergence of these two phenomena is of great importance in finance from a practical point of view. The very basic interest is that the correlation between the assets results, partly, from the fact that one asset leads the other one, which is consequently lager.

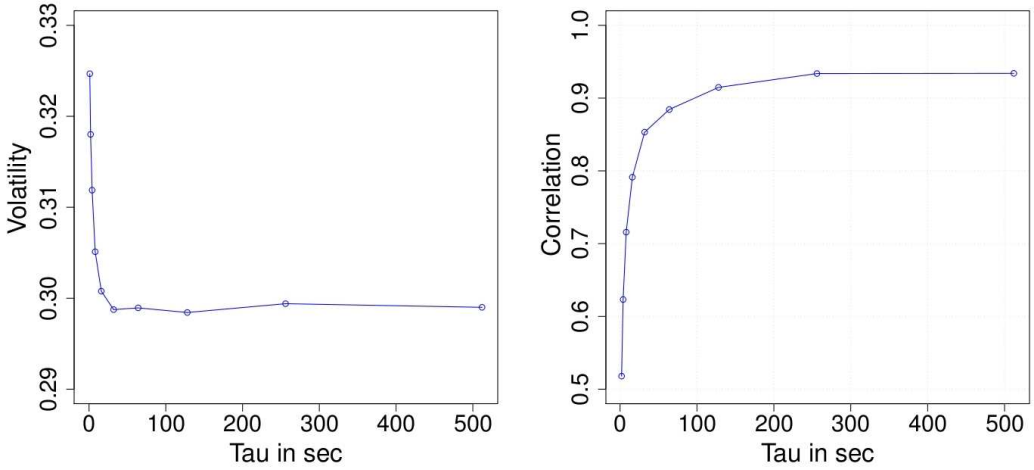

Figure 5.7 – *Volatility of the BNP Paribas share and correlation between BNP Paribas and SocGen on a given day of july 2011*

This means that the jump of some asset in one direction will induce, with a given probability, the jump of the other asset in the same direction (if one supposes correlation and not anti-correlation) lagged in time. This behavior is typically representative of some cross-excitation between assets that is one of the two phenomena that Hawkes processes are able to model. The second property that Hawkes processes can describe is the auto-excitation of some asset. The graph showing the explosion of the volatility is an obvious demonstration of such behavior. Indeed, this phenomenon (if one considers the last traded price) can be explained by the mean reverting behavior of the asset which is the oscillation realized by the price inside the spread, hitting alternatively the ask or the bid.

Consequently, the goal of this study will be to use the self and cross-excitation properties of a specified Hawkes model detailed in the next section to fit empirical high-frequency time-series. The methodology will be to use the fitted numerical values to simulate Hawkes trajectories in order to observe if the synthetic data exhibit the volatility and correlation properties. The recovery of such properties as well as the time structure would enable the use of the fitted parameters for investment strategies which will not be detailed here. The study is restricted to the theoretical interest and its potential application in fatigue. So let us introduce the model used which is a generalization of the one used by Hewlett (2006), E. Bacry and Muzy (2010).

Hawkes processes

Hawkes processes Hawkes (1971) originate from the statistical literature in seismology and are used to model the occurence of earthquakes, see e.g. Vere-Jones (1970), Vere-Jones and Ozaki (1982) and Ogata (1999) among others. Bowsher (2007) was the first applying Hawkes models to financial point processes. As explained previously, Hawkes processes belong to the class of self-exciting processes, where the intensity is driven by a weighted

function of the time distance to the previous points of the process. A general class of univariate linear Hawkes processes is given by:

$$\lambda(t) = \mu(t) + \sum_{t_i<t} \omega(t - t_i) \tag{5.4}$$

where μ denotes a deterministic function of time and $\omega(s)$ is a weight function. Such processes require $\mu(t) > 0$ and $\omega(t) > 0$ in order to ensure non-negativity. As pointed out by Hawkes and Oakes (1974), linear self-exciting processes can be viewed as clusters of Poisson process. Then, each event is one of two types: an immigrant process or an offspring process. The immigrants follow a Poisson process and define the centers of the so-called Poisson clusters. If we condition on the arrival time, say t_i, of an immigrant, then independently of the previous history, t_i is the center of a Poisson process, $\Gamma(t_i)$, of offspring on (t_i, ∞) with intensity function $\lambda_i = \lambda(t - t_i)$, where λ is a non negative function. The process $\Gamma(t_i)$ defines the first generation offspring process with respect to t_i. Furthermore, if we condition on the process $\Gamma(t_i)$, then each of the events in $\Gamma(t_i)$, say t_j, generates a Poisson process with intensity $\lambda_j(t) = \lambda(t - t_j)$. These independent Poisson processes build the second generation of offspring with respect to t_i. Similarly further generation arise. The set of all offspring points arising from one immigrant are called a Poisson cluster. Exploiting the branching and conditional independence structure of a linear Hawkes processes, Moller and Rasmussen develop a simulation algorithm as an alternative to the Lewis Lewis (1970) thinning algorithm or the modified algorithm of Ogata (1981). The immigrants and offsprings can be respectively referred to as *mainshocks* and *aftershocks*. This admits an interesting interpretation which is useful not only in seismology but also in the high-frequency domain. Bowsher (2007), Hautsch (2004), Large (2007) illustrate that Hawkes processes capture the dynamics in financial point processes remarkably well. This indicates that the cluster structure implied by the self-exciting nature of Hawkes processes seem to be a reasonable description of the timing structure of events on financial markets.

The most common parametrization of $\omega(t)$ has been given by Hawkes (1971) and is given by:

$$\omega(t) = \sum_{j=1}^{P} \alpha_j e^{-\beta_j t} \tag{5.5}$$

where $\alpha_j \geq 0$, $\beta_j \geq 0$ for $j = 1, \ldots, P$ are model parameters, and P denotes the order of the process and is selected exogenously. The parameters α_j are scale parameters, whereas β_j drive the strength of the exponential time decay. The stationarity of the process requires $0 < \int_0^\infty \omega(s)ds < 1$, which is ensured only for $\sum_{j=1}^{P} \alpha_j/\beta_j < 1$.

While the previous equation implies an exponential decay, the alternative parametrization:

$$\omega(t) = \frac{C}{(t+k)^p} \tag{5.6}$$

with parameters A, k and p>1 allows for a hyperbolic decay. Such weight functions are typically applied in seismology, see e.g. Ogata (1998) and allow to capture long range dependence that is advocated in markets Lillo

and Farmer (2004). Since financial duration processes also tend to reveal long memory behavior Jasiak (1997), J.P. Bouchaud (2008); the aforementioned specification might be interesting in financial applications.

Nevertheless, unidimensional Hawkes processes are well suited to account for earthquakes dynamics since the release of energy is always positive whereas price variations could be of both signs and consequently require bi-dimensional Hawkes processes. Multivariate Hawkes processes can be easily expressed as a generalization of the univariate cased as :

$$\lambda_i(t) = \mu_i + \sum_{j=1}^{K} \sum_{t_i^j < t} g_i^j(t - t_i^j) \tag{5.7}$$

with an exponential kernel:

$$g_i^j(t) = \sum_{k=1}^{P} \alpha_{ij}^k \exp -\beta_{ij}^k t \tag{5.8}$$

Such a modeling will be used to account for the variations of high-frequency time series according to the following model.

5.2.3 Financial application of the Hawkes processes

In order to progress gradually in the difficulty, the presentation of the model will be entirely given in dimension 1 before being generalized in dimension N.

Unidimensional model

In the unidimensional case, the price of an asset $X(t)$ over some time horizon $[0, T]$ can be given by :

$$X(t) = N1(t) - N2(t). \tag{5.9}$$

where $N1(t)$ and $N2(t)$ are two point processes which respectively represent the sum of positive and negative jumps of some asset price.

Considering $\lambda_i(t)$ for $t \in \mathbb{R}$ as the stochastic intensities of two counting processes $N_i(t), i = 1, 2$, such that at time t:

$$\lambda_i(t) = \lim_{\Delta \to 0} \Delta^{-1} \mathbb{E}[N_i(t + \Delta) - N_i(t) | \mathcal{F}t] \tag{5.10}$$

where $\mathcal{F}t$ stands for the filtration generated by the history of the processes $N1(t), N2(t)$.

Consequently, the bivariate process $N1(t), N2(t)$ is a linear Hawkes process if $N1(t)$ and $N2(t)$ have no common jumps and if there exist four nonnegative functions $\phi_{ij}{}_{i,j=1,2}$ such that:

$$\lambda_1(t) = \mu_1 + \int_{-\infty}^{t} \phi_{11}(t - u) dN_1(u) + \int_{-\infty}^{t} \phi_{12}(t - u) dN_2(u) \tag{5.11}$$

and:

$$\lambda_2(t) = \mu_2 + \int_{-\infty}^{t} \phi_{22}(t - u) dN_2(u) + \int_{-\infty}^{t} \phi_{21}(t - u) dN_1(u) \tag{5.12}$$

The process obtained admit a version with stationary increments under the stability condition that all the eigenvalues of the matrix $||\phi_{ij}||_1$ are lower than 1 where $||\phi||_1 = \int_{\mathbb{R}} \phi(t)dt$, see Daley and Vere-Jones, Hawkes (1971). Such a model only accounts for jump sizes of one tick. Nevertheless, the examples chosen in the following display a negligible number of jumps of several ticks due to the low number of ticks in the spread and consequently, the approximation realized on the price dynamics is not too important. It is possible to replicate exactly all the jump sizes by adding point processes but it results in arduous computations compared to the result obtained.

Let us rather appreciate the two behaviors embedded in this unidimensional model:

- The first one refers to the mean reversion (which is the tendency of a price to come back to its mean, this is roughly speaking the financial equivalent of the spring return) which is expressed through the coupling terms between the positive and negative intensity. Indeed, the terms $\int_{-\infty}^{t} \phi_{ij}(t-u)dN_j(u)$ account for the increase of the positive (resp. negative) intensity if a negative (resp. positive) jump occurs. Consequently, when a backward jumps of the price occurs, the probability of an upward jump will be affected. This property is shown in figure 5.8. A price process made of Hawkes processes which are purely mean reversal is illustrated and one can notice the influence of one jump on the other process and the resulting oscillation of the price.
- The second behavior refers to the auto-exciting character of the price. It should be understood by this, some kind of persistence in the variation. The term $\int_{-\infty}^{t} \phi_{ii}(t-u)dN_i(u)$ refers to the increase of the positive (resp. negative) intensity if a positive (resp. negative) jumps occurs. This is the description of the fact that when an upward jump arise, the probability that a following upward jumps occurs is rose.

This mathematical model (1 financial asset modeled by two Hawkes processes) can be extended in higher dimensions with a complexity growing as $\mathcal{O}(2N^2 + N)$ where N represents the number of financial assets. Nevertheless, for the sake of simplicity, results will not be presented in higher dimension than 3 financial assets resulting in 6 Hawkes processes. In order to build some financial investment strategies, the extend in greater dimensions can sound as interesting considering that it permits to realize investments on the variations between assets of a sector (Bank Insurance, Energy, Commodities ...).

Multivariate model

The multivariate model is a natural extent that can be written as:

$$\lambda_i(t) = \mu_i + \int_{-\infty}^{t} \phi_{ii}(t-u)dN_1(u) + \sum_{j=1, i\neq j}^{N} \int_{-\infty}^{t} \phi_{ij}(t-u)dN_j(u) \quad (5.13)$$

In such a case, ϕ_{ii} always refers to the self-excitation of the process i but ϕ_{ij} is summed over the $(n-1)$ processes to account for mean reversion

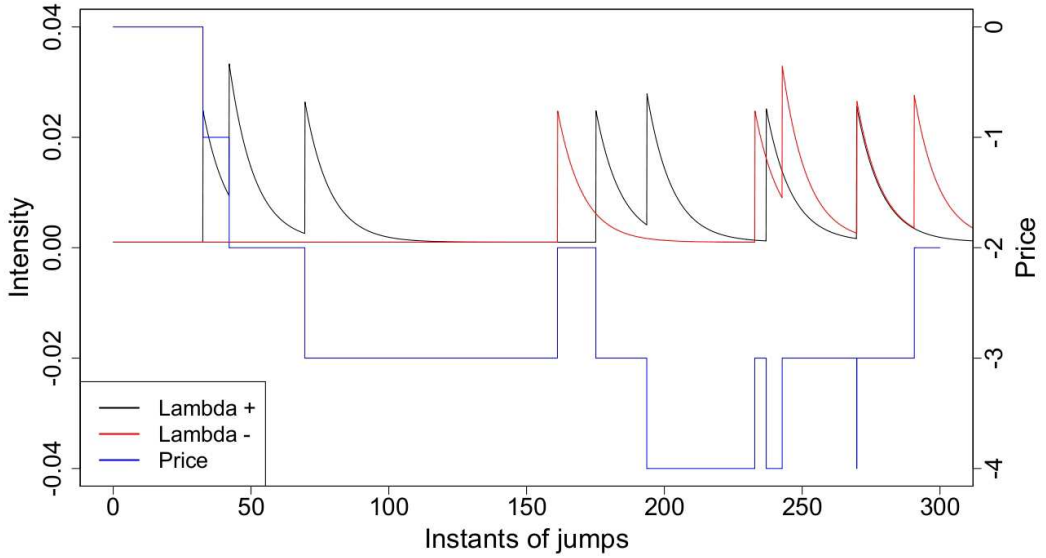

Figure 5.8 – *Price modeled as 2 Hawkes processes with cross-excitation (Up-Down) and without self-excitation*

as well as the cross excitation between assets, that is, the up-up excitations between price A and B and price A and C etc..., the up-down excitations between price A and B etc ..., as well as all the other possible correlations. The chosen form of the model is the most general since no assumption can be realized, a priori, about the existence or the absence of signed correlations between assets as well as symmetry properties. Is asset A more exciting asset B than B is exciting A for an up-up or down-down variation? This naive question is the one of greatest interest since this property can be exploited to build investment strategies of arbitrage.

To sum up, all these self and cross exciting characteristics are theoretically sufficient to reproduce the phenomena observed for the volatility and the correlation. Moreover, the asymmetric behavior embedded in the model lets the opportunity to capture leader-lager effects. But, let us focus on the experimental tests that were performed.

Cross-excitations between price variations

The study of correlations between stocks has been led over a large number of financial instruments (French, Swiss and Britain shares, German bonds, etc ...). The parameter that was mainly submitted to variations was the number of ticks inside the spread which largely contributes to different temporal behaviors as it will be shown with the comparison between the shares of Nestle and Vodaphone. But, the encountered problem was the same whatever the financial products, so a common analysis is presented.

The strategy has been to select some time series and to run and optimizer over the multivariate log-likelihood formula to explain the arrival time dynamics in a three-dimensional model. The first encountered problem was a mathematical one since the multivariate log-likelihood formula of a Hawkes processes was not existing Ozaki (1979) and had to be written as well as its gradient and Hessian. This intense calculation has then be

encoded in several ways in order to reached a reasonable computing time. One has to bear in mind that back tests are realized over 3 months periods and one financial asset jumps several thousands of times a day (mid-prices were considered). So the amount of data, is huge and algorithm efficiency is crucial. But, beyond these practical difficulties, the optimizer maximizes the log-likelihood of the different time series according the multivariate model and send back parameters. The parameters sent back are, one vector of background intensities μ_i and two matrix α and β that respectively represents the increase of intensity implied by a jump and the temporal decays in the exponential forms according to the retained exponential form for ϕ. Consequently, the ratio α_{ij}/β_{ij} is of particular interest to understand the percentage of subsequent jumps, in probability, from a time t until the infinity that will be explained by the interaction of i over j. This can be seen in the table 5.9, where BNP refers to BNP Paribas, SG to Société Générale and Nat. to Natixis (that was formerly in the CAC 40):

α/β	BNP up	BNP down	SG up	SG down	Nat up	Nat down
BNP up	39	6	7	0	15	0
BNP down	4	40	0	8	0	12
SG up	13	0	39	8	10	3
SG down	1	14	11	39	1	15
Nat up	3	0	1	0	36	5
Nat down	0	4	0	2	2	44
$1/\mu$	49	47	30	31	220	256

Figure 5.9 – *Fitted Hawkes parameters through the log-likelihood procedure*

The fitted parameters partly answer to some intuitions and other fact that were demonstrated empirically earlier. The auto-correlation of the processes is clearly visible in the diagonal of the matrix as well as the importance of the mean reversion inside an asset. One can note in particular that values reflecting mean reversal behavior are approximatively symmetric which seems quite logical, BNPup/BNPdown versus BNPdown/BNPup. The other fact to point out is the absence of anti-correlations between processes whatever the assets considered. This property was observed on all the couples or triplet studied. The last points to discussed are the correlations between processes which reveal the so-waited asymmetric behavior enabling to measure some lead-lag effect. One example can be found in the values found for $BNPup/SGup$ and $SGup/BNPup$ that are separated by a factor 2 which means that the asset SocGen leads the one of BNP in upward jumps two times compared to the opposite. Finally jumps that are not explained by correlation are considered as background activity and fitted by $1/\mu$ which is the time elapsed between two Poissonian jumps. Nevertheless, such results have to be considered cautiously.

Indeed, it can sound as satisfying in a first approach but one has to stay lucid face to these fitted values and the trust to confer to these parameters. Actually, if one simulates Hawkes trajectories with these parameters and tries to compute the multi-scale phenomena observed as the explosion

of the volatility or the Epps effect, disillusion arises as shown in figure 5.10 where the comparison between realized phenomena and simulation is illustrated.

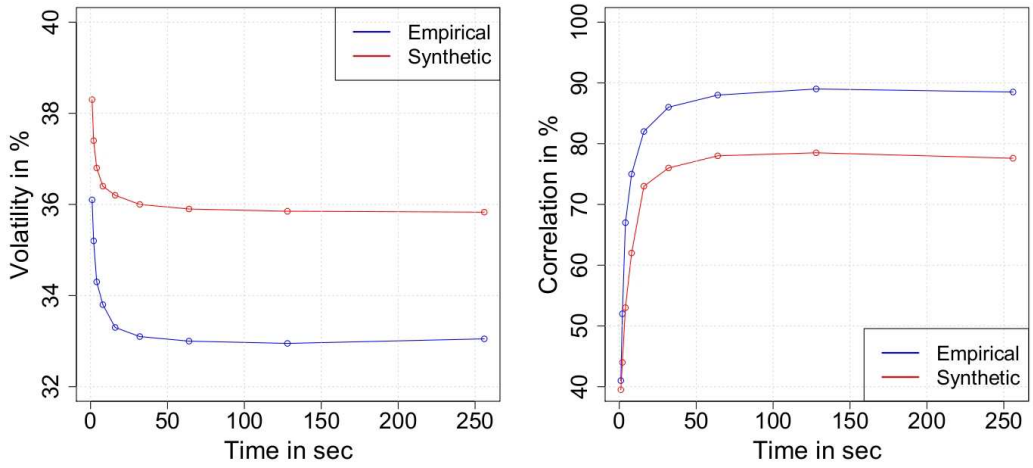

Figure 5.10 – *Empirical and synthetic volatilities (BNPP) and correlations between the couple BNP Paribas/ SocGen during a three months periods*

One can see that the results obtained transcribe the mechanisms since the shape of the curves are correct but the levels of are totally wrong. The explanation of this phenomena can be found by some deductive reasoning. If the processes are able to capture the phenomena but unable to capture the right level it is induced by the fact that the processes can not simulate the right time structure at all the time scales. This is demonstrated with the figure 5.11 which plot the time intervals between the trades for the Hawkes processes associated to the share BNP.

The synthetic data are just explaining one scale that is the short time intervals. The mean value of the fitted β is represented to show the limit of the model which is just able to account for one scale of the structure since the values of P in the exponential kernel (repeated below) was imposed to 1. Moreover, the large time intervals are also badly described since the model can not adjust the right value of μ since it does not know where begins the exponential regime due to the incapacity to fit the events between the β and μ.

$$g_i^j(t) = \sum_{k=1}^{P} \alpha_{ij}^k e^{-\beta_{ij}^k t} \tag{5.14}$$

As a consequence, the model is just able to describe one scale in the temporal correlations whereas the figure shows that the reality is much more complex since a power-law regime holds for 3 decades. This scale free structure in trade arrivals suggest a clustering of trade arrivals in scale-free patterns in which a high correlation exist inside the pattern that is fractal and these clusters are distributed in long time as exponentials. One way to improve the explanation of this behavior is to select values of P equal to 3 or 4 to ensure that each exponential in the temporal decay

of the intensity of the Hawkes process will explain one range of the time scale, one β_{ij} for each decade.

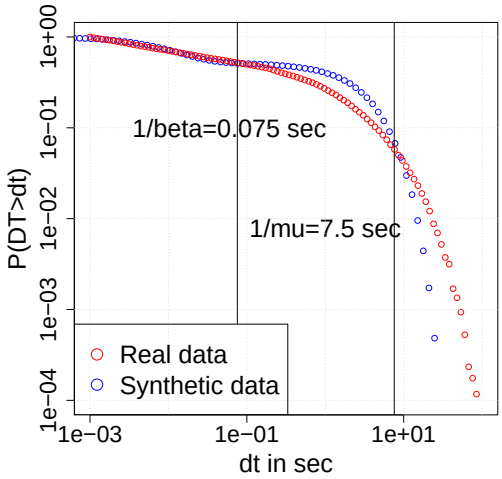

Figure 5.11 – *Distribution of time intervals for BNP Paribas and simulated Hawkes trajectory*

Just for curiosity since the distribution of trade arrivals is close to the arrivals of the acoustic waves in distribution, one can take a look to several distributions of financial assets to observe the differences that can exist between Vodaphone and Nestle for example. The first asset is made of a 25 ticks spread and one tick is representative of a little quantity of money that implies very short time oscillations whereas Nestle is made of less than two ticks inside its spread, on expectation, and one tick represents a large amount of money, resulting in a slower dynamics. The other example comparing BNP Paribas and SocGen underlines that shares displaying the same structure in their tick-spread ratio result in comparable time dynamics.

The explicative potential of self and cross exciting point processes models in fatigue will be addressed in the following section and the outlooks. Nonetheless, one can already think to the interest of following the temporal evolutions of correlations between physical mechanisms in fatigue identified from a multivariate data analysis like the K-means.

5.2.4 Application of Hawkes processes to the repeated loading of SMA

The wonderful character of complexity stands in the similarities between different systems thought in a unified way. So, this escapade in the financial sphere showed how Hawkes processes found applications in , a priori, disconnected fields of sciences. But point processes form a real bridge across scientific domains and some studies of the martensitic transition of a cyclically loaded SMA will demonstrate the easy extent realizable with this tool.

The targeted objective is to furnish some methods to study the temporal characteristic changes accompanying the phase transition. This topic is of wide interest since several studies focused on this problem Gallardo

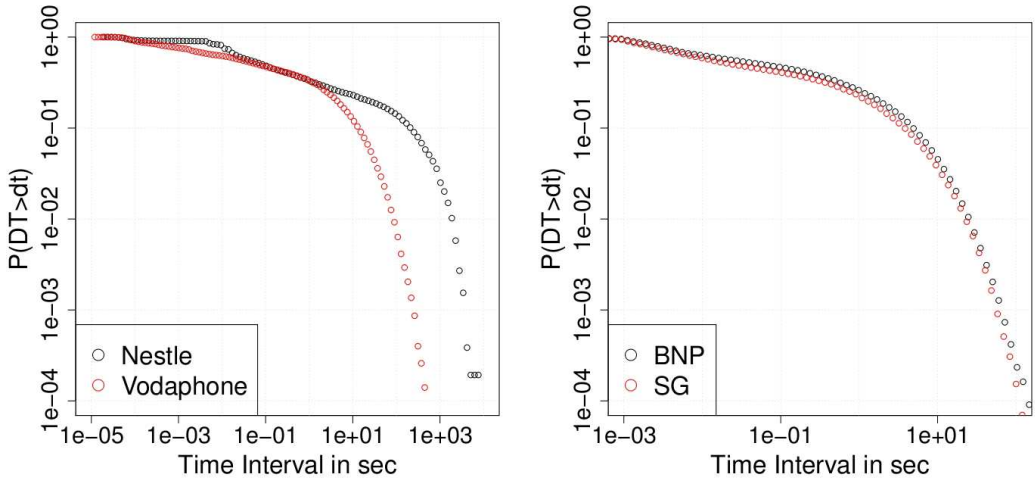

Figure 5.12 – *Examples of distributions of time intervals for different assets - Vodaphone, Nestle (left) and BNP Paribas, Société Générale (right)*

et al. (2010), Bonnot et al. (2008). These papers considers the number of generated wave along the transition as a measure of activity, whereas AE bring the direct access to the arrival time and the associated energies that can be easily modeled and more relevant of the underlying dynamics since no agglomeration of data is realized over a given bin. Nevertheless, no work in the literature reports the use of point processes which sounds as an outstanding tool regarding the results found in finance and earthquakes which display similar data types. Thus, a pedagogical study is led over the 10 first cycles (2051 events) of a fatigue experiment to highlight the improvements that such a tool can bring. This period has been chosen since it is the hardest to fit due to the transient character of the release of energy which results in the most complex signal.

A Hawkes-type cluster model is encoded to fit to the arrival times of the acoustic waves. The conditional intensity of the model is given by:

$$\lambda(t) = \mu + \int_{-\infty}^{t} g(t-s)dN(s) \tag{5.15}$$

with

$$g(z) = \sum_{k=1}^{K} a_k z^{k-1} e^{-cz} \tag{5.16}$$

This can be written :

$$\lambda(t) = \mu + \sum_{t_i<t} \sum_{k=1}^{K} a_k (t-t_i)^{k-1} e^{-c(t-t_i)} \tag{5.17}$$

One can immediately notice that this model accounts for the clustering property of arrival times according to a power-law mixed with an exponential. This specific form was initially introduced by Ogata (1988) under the name of saint : "Shock response function".

The parameter μ represents the background rate of occurrence while the parameters $a_1, ..., a_K$ and c control the level of temporal clustering. K represents the order of the trigger function and selecting its value is an issue we discuss below. More details about this model (and its application to earthquake data) can be found in Ogata (1999).

A general issue with this kind of cluster model is the choice of K, the order of the polynomial in the trigger function. A comparison between the AIC resulting from a number of models with different values of K helps to choose the best value. Consequently, 4 values of K were investigated to test diverse forms of temporal clustering. The results for the different values of K are found in the following table, each one results from a maximization procedure of the log-likelihood of the considered point process:

K	1	2	3	4
AIC	-9479.17	-9456.22	-6069.71	-5482.61

So, the model with $K = 1$ is chosen since it displays the lowest AIC value. The estimated parameters (sec^{-1}) are :

- $\mu = 0.7041$
- $c = 2.4954$
- $a = 2.3271$

The parameter estimated for a indicates that immediately after an earthquake occurs, the conditional intensity is rose by about 2.32 events per sec. μ informs about the background rate which is approximatively of 0.7 event per sec. It corresponds to the Poissonian part of the process, which is small in comparison with other exponents, as shown by the AIC values outputted from the algorithm showing that the model does fit better than an homogeneous Poisson model which has a AIC value of -5491.99. This is an indication that even if a scale free regime does not hold for arrival times in the beginning of the experiment, the behavior is not purely random as it will be for a Poissonian process. There is some self-exciting time structure. This seems in concordance with the previously drawn results exhibiting complex patterns in the nucleation of branches during the transition that are not suspected to be governed by a purely random behavior as well as by the scale-free regime in the distributions of time arrivals shown in figure 4.14 that holds for 2 decades. These curves suggested a temporal response that is composed of a mix between an exponential and a power law behavior that the model used is well suited to explain.

Let us now turn to the computation of the conditional intensity from the fitted parameters over a 200 seconds period. It is recalled that the conditional intensity informs about the frequency, for a given time t, at which events are supposed to arrive conditionally to the history. So, the estimated conditional intensity is shown in figure 5.13 next to the empirical recorded releases of energy for the first 10 cycles of a fatigue experiment.

The result seems to indicate, visually at least, that such a simple 3 parameters model captures a large part of the response associated to the martensitic transition since the intensity is in concordance with the pattern of temporal relaxation. Nonetheless, some quantitative criterion are needed to evaluate the quality of the fitted point process.

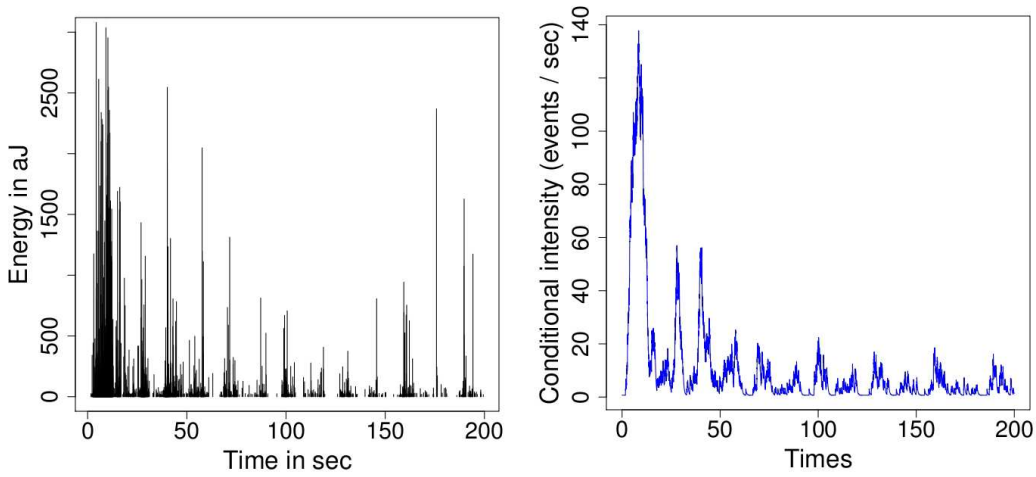

Figure 5.13 – *Instantaneous release of energy for the first 10 cycles of a fatigue experiment and fitted conditional intensity*

Evaluation of a point process

A common method of evaluating a point process model is to examine likelihood criteria such as the Akaike Information Criterion (AIC) or the Bayesian Information Criterion

There exist various ways of constructing a residual process and we discuss some of those methods in this subsection. The common element of residual analysis techniques is the construction of an approximate homogeneous Poisson process from the data points and an estimated conditional intensity function λ. Suppose we observe a one-dimensional point process $t1, t2, ..., tn$ with conditional intensity λ on an interval $[0, T]$. It is well known that the points

$$\tau_i = \int_0^{t_i} \lambda(s)ds \tag{5.18}$$

for $i = 1, ..., n$ form a homogeneous Poisson process of rate 1 on the interval $[0, n]$. This new point process is called the residual process. If the estimated model λ is close to the true conditional intensity, then the residual process resulting from replacing λ with $\hat{\lambda}$ in the former equation should resemble closely a homogeneous Poisson process of rate 1. Ogata (1988) used this random rescaling method of residual analysis to assess the fit of one-dimensional point process models for earthquake occurrences.

When rescaling a multi-dimensional point process one may encounter two practical difficulties:

- The boundary of the rescaled domain may be uninterpretable (or unreadable). That is, the residual process may be homogeneous Poisson but the irregularity of the rescaled domain can make the points difficult to examine.
- Integration of the conditional intensity function is required. In practice, accurate integration of the conditional intensity in certain dimensions can be computationally intensive.

Both of these problems can be ameliorated by instead constructing a residual process via random thinning. Suppose that for all $(t, x) \in S$ there exists a value m such that

$$0 < m \leq inf_{(t,x)\in S}\lambda(t, x) \tag{5.19}$$

Then for each $i = 1, ..., n$, we delete the data point (ti, xi) with probability $1 - m/\lambda(ti, xi)$. The undeleted points form a homogeneous Poisson process of rate m over the original domain S. The residual process obtained through this method of thinning will be referred to as ordinary thinned residuals. For details on random thinning, see Lewis (1970), Ogata (1981).

To construct the ordinary thinned residual process, we only need to evaluate the conditional intensity. Typically, this is a much simpler task than integrating the conditional intensity. Unfortunately, in some cases where m is very close to zero, the thinning process can result in very few points. However, because of the randomness involved in the thinning procedure, one can repeat the thinning many times and examine the various realizations for homogeneity. Another drawback of this method is that there may not exist such an m.

A third method for constructing a residual process addresses the problem of having too few points in the thinned process. This was detailed by Schoenberg (2003) to assess the space-time Epidemic-Type Aftershock Sequence model of Ogata (1998).

The residual process is useful for model evaluation purposes because the process is homogeneous Poisson if and only if the model is equal to the true conditional intensity function. Once the residual process has been constructed, it can be inspected (graphically) for uniformity and homogeneity. In addition, numerous statistical tests can be applied to test the process for uniformity (see e.g. Diggle (1988), Ripley (1979). For example, Ripley's K function can be used to test for spatial clustering and inhibition Ripley (1976). In general, any deviation of the residual process from a homogeneous Poisson process can be interpreted as a deviation of the model from the true conditional intensity.

Analysis of the residual point process

There are a number of diagnostics one can use to assess the fit of a 1-dimensional residual process as shown previously. One example is a log-survivor plot of the inter-event times. If the model fits well, then the residual process should be homogeneous with rate m (where m is specified in the call to residuals) and the inter-event times should appear as i.i.d. exponential with mean $1/m$. The log-survivor plot of the inter-event times of the residual process can be constructed and it is plotted in figure 5.14 with the stationarity of the residual process. One can appreciate that the inter-events time of the residual process are distributed as i.i.d. exponential in the semi-logarithmic plot. These results are of particular good quality but one further analysis is led to check the stationarity of the residual process with the stationarity function.

This function divides the domain into bins of a given (user-specified) length and counts the number of points falling into each bin. The number

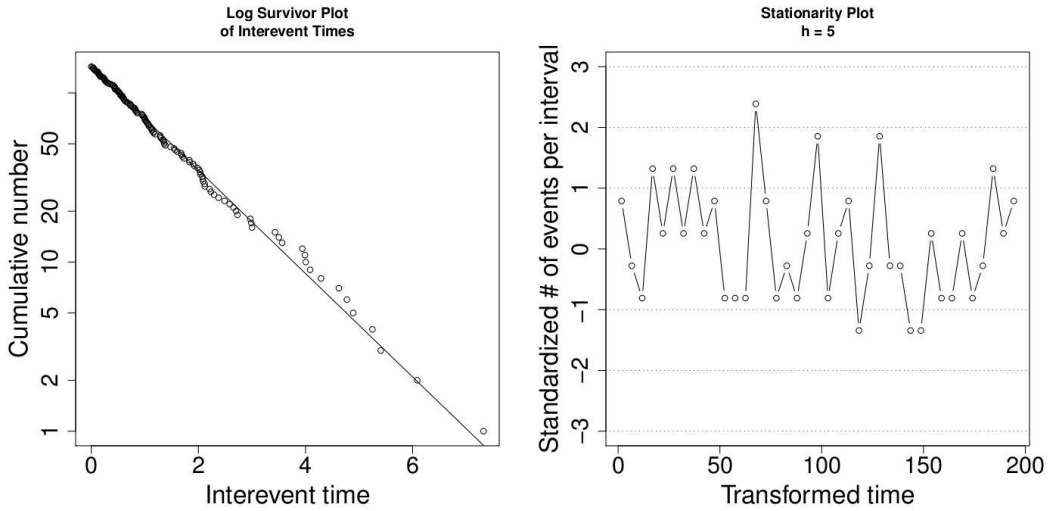

Figure 5.14 – *Log-survivor plot of the inter-event times of the residual process and stationarity function of the residual process*

of points in each bin is standardized by the theoretical mean and standard deviation and the standardized counts are plotted against the left endpoints of the bins. This plot is shown in figure 5.14. The process generally stays within the bounds of a homogeneous Poisson process, but in one instance the count can jump far beyond several standard deviations of the expected count. Such a jump would indicate a region of non-stationarity in the residual process and a feature of the data which is not taken into account by the model. Here the stationarity is checked since the standardized number of events per interval remains within 2.5 standard deviation. This indicates that all the major features of the process are explained by the model.

One can naturally wonders how such a modeling tool can be applied. It must be thought of a simulation tool exhibiting the statistical properties empirically observed for time and energy can be useful to access detailed information of the martensitic transition. Indeed, point processes are promoted to study the influence of driving over the transformation path and its associated dynamics. Fitted exponents can be simple good quantifiers to summarize in 3 parameters a complex pattern. In the fatigue framework, it is also conceivable to query whether the dynamics is changed by loading parameters. In the scope that aims at revealing the universality, it is a less fastidious study than the one led over the distributions. Nevertheless, with regards to the previous results the form of the conditional intensity suggested is rather as the following :

$$\lambda(t) = \mu_0 + A(t) + B(t) + C(t) \tag{5.20}$$

where $A(t)$, $B(t)$ and $C(t)$ refer to:

$$A(t) = \sum_{j=0}^{J} a_j \psi_j(\frac{t}{T}) \tag{5.21}$$

$$B(t) = \sum_{u=1}^{U} (b_{2u-1} \cos(\frac{2u\pi t}{T_0}) + b_{2u} \sin(\frac{2u\pi t}{T_0})) \tag{5.22}$$

$$C(t) = \sum_{t_i<t} \sum_{k=1}^{K} a_k (t - t_i)^{k-1} e^{-c(t-t_i)} \tag{5.23}$$

where ψ_j is a polynomial of order j that account for the trend in the increase of the number of relaxed waves upon cycling. The sinusoidal part of the intensity aims at modeling the progressive cyclic behavior that is born upon cycling with the emergence of the the two previously noticed patterns. Then the last part is the "Shock response function" for the one cycle behavior.

This model seems to be made of all the required behaviors to explain the fatigue failure process. Finally, the use of point processes and particularly self and cross excited point processes is pitched through this thesis as a potential tool for the discrete and intermittent characteristics of the temporal variations of complex systems.

5.3 Scientific improvements

Throughout this chapter, the guiding principle was the intermittent character that is found in different fields of sciences. It appears important to me to devote a discussion about the key role attached to this fundamental notion of complex systems. A thesis subject about self-organized criticality in fatigue imposes to have a wider point of view about the more general classes in which it is inscribed. This curiosity led us to think about the potential that each system around us has to exhibit some intermittent behavior made of events that are fundamentally different by their sizes. The subsequent questions relative to their frequency is also crucial in order to understand the risks pertaining to extreme events.

In that sense, physicists are continuing to help to the development of new methods to manage the risks in the financial markets. It is sometimes necessary to have the guts to let bygones be bygones, tabula rasa. Such approaches, enable to start on new basis, promoting empiricism rather than complex modeling. Consequently, a bibliographical study was performed to underline the works that consider financial markets as a complex systems with all its relative scale-free distributions. The detailed observation of how prices are generated lead to consider models based on observable and quantifiable variations of the price without any fallacious prediction. Before predicting, the urgency is to understand how cross-scale phenomena arise and mutually excited Hawkes processes seem to be a good candidate to transcribe correlations between assets at high frequency.

Remaining motivated by the interest of being in a multidisciplinary approach, it sounds important to highlight the multi-task behavior of Hawkes processes. Thus, it was naturally applied to the description of the temporal response of cyclically loaded SMA. Such a proposal has never been realized so far and it is worth extending this study. A simple and physically meaningful tool can help to understand how the response of a repeatedly loaded sample takes place and evolve from the first cycle of

the sample until the failure of the material. More generally, an approach that alternatively travels from numerical simulations to empirical investigations seems to be the one to adopt. Indeed, fatigue experiments are no computable since no simulation tool is existing and it could be a solution considering that fatigue experiments are long and fatigue failure does not just occur to the material !

Conclusions and outlooks

6

Contents

During this thesis, readers have been invited to a gradual evolution in the analysis of the complex system constituted by a cyclically loaded SMA. Such an analysis is totally new since fatigue damaging mechanism is usually considered inside the classic framework of the continuum mechanics and some variants attached to a potential stochastic character. Failure by repeated loading has never been addressed as a self-organized critical system whatever the material, the loading modes or any other usefulness parameter. Beyond the empirical details, the true questions were rather of conceptual scientific considerations. Can the response of a cyclically loaded material constitutes a system that can be considered as self-organized critical ? How are interlocked the development of crack and the emergence of a critical behavior ?

6.1 Main results of the thesis

The experiments of fatigue are long, partly random and largely unpredictable besides the "models" that enable to forecast an approximative life duration. The comprehension of how damages took place from a macroscopic point of view is limited to a finite number of observations that can bring people to establish empirical rules of fatigue but that miss the explanation of the very essential microscopic mechanisms. Furthermore, explaining fatigue at the microscopic level appears as an impossible task due to the very large number of phenomena to consider, their interactions and their evolutions. Consequently, the quantitative analysis of the modifications of statistical properties, resulting from the motions of internal damages recorded by AE, upon cycling appears as the best way to track the precursory signals of fatigue failure.

It is proposed to synthesize the main results of the thesis through the key questions I tried to answer to during two years. So, rather than repeating the conclusions of each chapter, in boring bullet points, a common scientific reflexion about the most essential interrogations will be led.

What makes fatigue failure (of shape memory alloys) a complex system ?

Beyond all the considerations about SOC and fatigue, the first question to elucidate was this one, and the main important point was to understand what is a complex system. If the bibliography helped to consider what ingredients are needed to argue that a system is complex, an actual reflexion was performed about the term fatigue. Indeed, it was previously shown that the martensitic transition displays the characteristics of a complex system, but fatigue does not just consist in repetitive phase transformations since the degradation of the material impact the response and consequently play a key role.

Thus, fatigue of shape memory alloys can effectively be regarded as a complex system since the response of the system is particularly non-linear and intermittent whereas the driving rate is smooth and follows a constant scheme. In the same time, the driving rate is totally different from the underlying dynamics. Initially, this was mentioned due to the difference in the loading rate (20 sec a period) versus the motion of dislocations, but this is also true in the analogy that was performed with earthquakes since the development of the cracks which is approximatively one thousand cycles long is extremely long in comparison with the time of failure. Finally, the scale-free distributions of energy, time and fractal properties have been checked during the life of the sample. Even if the scale free character does not necessarily hold all the experiment long for few cycles periods, it was demonstrated that the total period attached to the development of the cracks is resulting in a self-similar behavior for time intervals and energy with fractal locations of events that underlines the long-range correlations that exist in the system.

What are the different stages to fatigue?

The different stages crossed by the material are evidenced by the cumulative released energy. This quantity embedded partly the number of events and is also relevant of the temporal dynamics in addition to the energetic dynamics. The analysis of this quantity lets appear 4 different stages and 3 dissipative regimes. The first stage characterizes the transient period from the virgin to the stable state where the material exhibit a critical state that is rapidly modified when the response turns to the first dissipative regime.

The first dissipative regime corresponds to a scale free distribution of energy associated to a random time structure. The activity and consequently the rate of dissipation, is low. This period corresponds to an undamaged material that is mainly governed by a dislocation-based activity.

The second dissipative regime is a transient regime that is characterized by the loss of scale-free behavior for the energy that is recovered at the end of the dissipative regime which is typified by an explosion of the activity and the quasi self-similar character of the distributions of time and energy. This regime is suspected to be associated to the nucleation of micro-cracks.

The third dissipative regime is exemplified by the scale-free distributions of time, energy and space intervals. It correspond to the critical state of the experiment. The activity is extremely intense and this period is represented by the progressive appearance of the cracks inside the signal that is observable through the two asymmetric patterns that takes place in the release of energy. These patterns indicate the growing activity generated by the opening and close of the cracks which finally results in the loss of the critical state due to the large number of small events.

Do not forget your title ...

"Self-organized criticality as an explanation of fatigue failure for shape memory alloys". That is the title. One reflexion has to be led on the role of SOC as a potential concept to understand fatigue failure. The first improvement was brought by acoustic emission recordings that furnish new indications of the dissipation of energy during fatigue. Nevertheless, this must be interpreted with regards to SOC. So, the key point that need to be memorized is the emergence of a self-organized critical state that is concomitant the formation of cracks. Indeed, the term self-organized is justified by the progressive changes in the response that occurred with the appearance of the scale-free behavior of the three main quantities of the systems, the energy, the time intervals and the space intervals, that are the mark of the criticality. This happened without changing the driving of the system which supports the idea that the formation of the fatigue cracks is a self-organized critical state.

If I have to compare fatigue to ?

If one is attached to an analysis period by period rather than 50-cycles by 50-cycles, the response of the material tends to claim for a progressive

path to criticality since the first two periods are not displaying all the necessary conditions required to qualify the system as SOC. Meanwhile, the third period exhibits self-similar properties which are reminiscent of the three fundamental empirical laws found in the earthquake dynamics, Gutenberg-Richter, Omori and fractal distribution of epicenters. The long term organization of the earthquakes as well as the fatigue failure seems indicate that a common mechanism seems to govern the emergence of such a catastrophic events at totally different scales.

6.2 Following topics of research and outlooks

In this section are synthesized several clues that may help to improve our knowledges about fatigue failure within the framework of SOC.

Do not forget your mistakes

It sounds as particularly important to expose all the mistakes that were committed during this thesis to avoid somebody else to make history as a round trip. These errors can be classified into two classes, the first ones referring to the empirical mistakes and the second ones to theoretical mistakes.

Among the empirical mistakes, it is essential to note that the geometry of the sample is without any importance in the theoretic world of SOC but it is in practice a real problem. Initially, samples were designed with sharp angles that were avoiding the propagation of surfacing waves, resulting in silent experiments. So, it is recommended to use wires or cylindric geometries of sample. The second empirical advice concerns the use of an extensometer that is a polluting source of noises due to the friction between the blades of the gauge and the sample. Thus, if you do not need to measure the deformation of the sample, do not use it. Nevertheless, new experimental tools enable to have values of the deformation through laser measurents, it seems to be the most appropriate method to use with acoustic emission devices.

Beyond the simple technical problems, some computing difficulties were encountered. The first one refers to the number of data, each wave is characterized by a dozen of parameters, summarized as a vector, and a fatigue experiment generates roughly from 500 000 to several millions of vectors. Then, you rapidly have gigabytes of data to analyze. As a consequence, it is recommended before running algorithms and computations during hours over these large datasets to manage a first statistical analysis of your data to realize the suitable filtrations. It should be understood that methods as the k-means clustering procedures are really robust and can be easily implemented on large datasets to suppress the noises recorded during experiments.

The last recommendation is maybe the most basic one, but surely the most important one. It is of incredible ease to furnish statistics and to compute correlations, as well as fitted quantities when you have such datasets into your hand. But, before announcing any numerical values, look at your data and wonder about the true significance of what you computed and the errors associated to your estimation. It is much more important than

the numerical value by itself. Two funny representations of this precious advise are given in figure 6.1

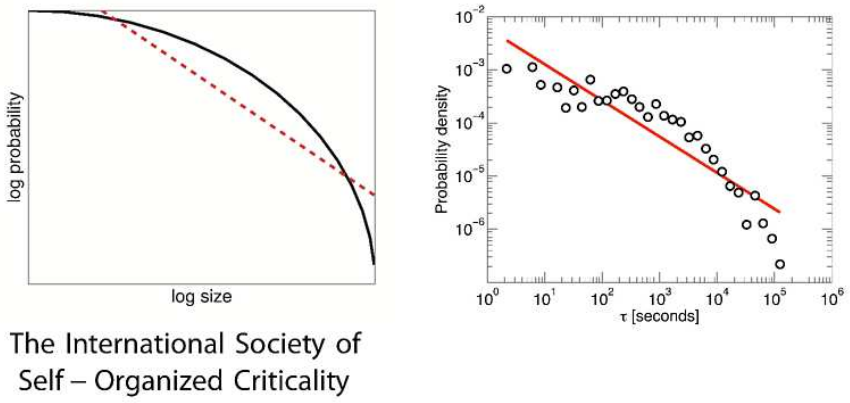

Figure 6.1 – *The International Society of Self-Organize Criticality*

Icing on the cake...

The most challenging question concerning any study that deals with self-organized criticality is undoubtedly the specific point of universality. Indeed, the scope of applicability of the SOC is huge and qualifying a system as SOC requires the capacity to argue that the results found are maintained in a large variety of situations independently of details. I have personally done my utmost to answer to this question through different experiments that revealed consistent results in their own and between them to sustain the belonging of fatigue failure to SOC. Nevertheless, I must face facts, the advanced results obtained are not sufficient to ensure that this result is reliable and expandable to different situations. The road to universality is long, very long. That is the reason why the main conclusions of this thesis form a first milestone for future studies that need to be led to query whether the same conclusions can be draw for different loading modes (thermally or strain induced phase transition) as well as for wider driving rates and materials. Vives et al. (2009) proposed some first answer to the influence of the loading modes for the first cycles but high number of cycles experiments would be interesting. The influence of the material will also be partly answered by the PhD student from the laboratory of INSA that is performing the same study over aluminum alloys.

Who is who ?

A fundamental question that is raised by the results of this thesis concerns the identification of physical mechanisms. Two different approaches are presented to answer to this crucial question. The first one is very basic and consists in stopping an experiment in each of the dissipative regimes crossed by the sample and to perform observations with scanning electron microscope. It will easily give the visual answer of the density of dislocations as well as the presence of micro-cracks. The second one is a statistical analysis that is based on data mining principles. Starting from the whole

data one can accomplish a clustering of waves based on their intrinsic properties (Energy, duration, amplitude, frequency, rise time, number of count, etc...) with the use of clustering algorithms (connectivity based, centroid based, distribution based or density based) to form clusters that maximize the variance between clusters and minimize the variance intra-clusters. Consequently, one can fulfill the same analysis of the distributions of the main quantities upon cycling to understand if the fatigue process makes new waves appearing with the nucleation of damages or if it mainly results from an intensification process of some mechanisms or if it comes from growing interactions. The creation of these clusters opens the field of the analysis of mutually excited phenomena to account for correlations, intensifications of processes through the framework of point processes as demonstrated.

6.3 Personal learnings and feelings

The last section of the thesis is surely the less interesting since it deals with the feelings of the author!

These few lines are just here to express the radical changes implied by the study of complex systems and self-organized criticality in my mind. Beyond the intriguing character of the concept by itself, the time devoted to researches about such a subject results in an irreversible scientific experiment, a kind of scientific revolution. The ubiquity of complex systems around us tends to promote the "complexity obsession". Curiosity turns out to be bigger and bigger for new fields that seemed boring before and you have to self-control to avoid the scientific scattering. The study of complexity has a grip on you that results in something as powerful as a new sense since everything you heard, everything you see can be considered with a new angle that found applications all around you. Before, everything was smooth and linear, now, intermittent and threshold behaviors are compulsory reflexes.

I personally had a real pleasure with the readings of the works of Aaron Clauset dealing with the distributions of terrorist attacks as well as body sizes Clauset, Clauset and Erwin (2008) and the course about complex systems given by Jean Philippe Bouchaud and Marc Mézard at École Polytechnique who both nourish my growing interest in finance.

I would like to conclude this manuscript in the words of André Gide, "One does not discover new lands without consenting to lose sight of the shore."

Appendix

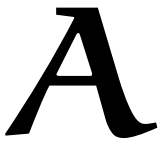

Contents

A.1 Publications and conferences

A.1.1 Publications

- C. Dunand-Châtellet and Z. Moumni, *Experimental analysis of the shape memory alloys through power-law statistics*, International Journal of fatigue, doi:10.1016/j.ijfatigue.2011.07.014
- C. Dunand-Châtellet and Z. Moumni, *Coupling infrared thermography and acoustic emission measurements to characterize shakedown state of shape memory alloys*, Key Engineering Materials, Transtech Publications Inc., **488-489**, (2012)
- C. Dunand-Châtellet and Z. Moumni, *Probabilistic investigation of fatigue failure mechanisms using acoustic emissions*, Mechanical System and Signal Processing,

A.1.2 Conferences

- C. Dunand-Châtellet and Z. Moumni, Evolution of self-organized criticality as an indicator of fatigue in cyclic loading of shape memory alloys, Plasticity 2011, Puerto Vallarta, Mexico
- C. Dunand-Châtellet and Z. Moumni, Coupling infrared thermography and acoustic emission measurements to reveal fatigue precursors, International Conference on Fracture and Damage Mechanics 2011, Dubrovnik, Croatia
- C. Dunand-Châtellet and Z. Moumni, Space-Time analysis of the nucleation of damages in cyclically loaded NiTi structures trough acoustic emission and SOC theory, Plasticity 2012, Porto Rico, United States of America

A.2 Acoustic emission monitoring

Acoustic emission, commonly abbreviate in AE, is a measurement method to monitor in live the evolution of a structure submitted to different kinds of loading (thermal, mechanical, chemical ...). This technics is often used to judge the integrity of a structure and evaluate its remaining life time. This measurement method belongs to the class of non destructive method and is well suited for pieces with a high cost or for unitary pieces which can not be damaged.

A.2.1 Description of acoustic emission measurement

Regarding the french norm AFNOR NFA09350, acoustic emission is defined as "the phenomenon of creation of transient elastic waves resulting from an internal micro-motion inside a material" Roget (1988). Phenomena which create these elastic transient waves inside SMA are of several types, it can be the cooperative motion of dislocations, phase transition, twinning processes, the nucleation and growing of cracks, it will be called sources of acoustic emissions. These acoustic waves propagate in a tridimensional way inside the material and reaches the surfaces of the material, then, they propagate as surface waves until the location of the acoustic piezoelectric sensors which detect and record them.

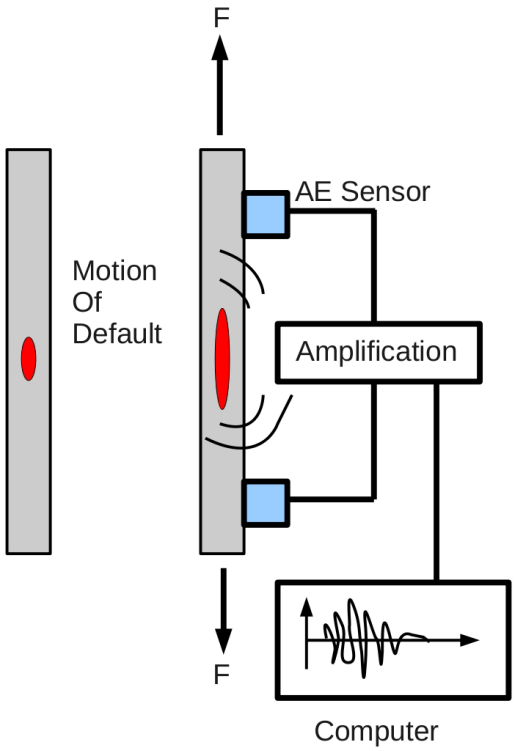

Figure A.1 – *Scheme of acoustic measurement devices*

Piezoelectric sensors are fixed on the surface of the sample with a cou-

pling fluid, silicone gel, to ensure the acoustic coupling. Resonant sensors with a pass band narrower peaked around one resonance frequency were used. This characteristic has the consequence to attenuate the components which are not included in the pass band which leads to a modification of signals. We easily understand that the use of such sensors implies to select a sensor with a resonance frequency near to the frequency of the sources to recorded. A key point is that the frequency range of the sensor was chosen to exclude the frequency of the circulating fluid of the hydraulic machine.

Experiments were led with two resonant sensors on the surface of the sample to localize the waves in a uni-dimensional way. An photo of one experiment is shown in figure A.2. Sensors are the base of the acquisition, because they transform surface motions into electric signal. Thus, the amplifiers are usually employed to magnify AE signals. AE signals are normally amplified both by a pre-amplifier and by a main-amplifier and are filtered. Recordings of signals are of different types, it can be a continuous value which is representative of the continuous activity or it can be what we call "Hit".

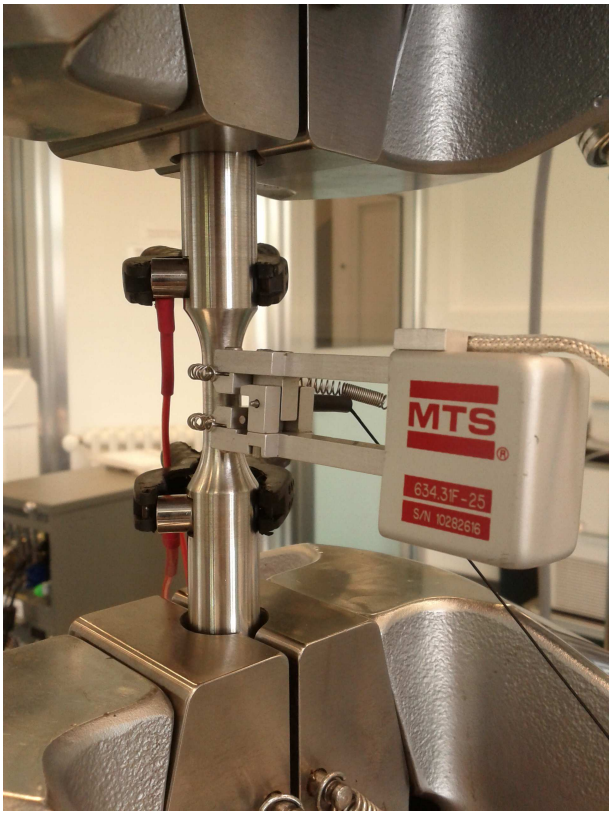

Figure A.2 – *Photo of the acoustic measurement device*

Before explaining what is a hit, we will introduce several parameters that we have to settle before the experiments. So, the first thing to do is to ensure that coupling is well realized. To do it, a pencil-lead break procedure is systematically realized at the beginning and the end of the experiment, which is known as "Hsu-Nielsen test". An electronic coupling procedure is also performed, it is called AST as Automatic Sensor Test-

ing. The principle is to generate ten pulses from sensor 1 to sensor 2 and vice-versa. Then, it analysis how the pulse sent from sensor 1 is received by sensor 2, it mainly gives the time elapses, the measured amplitude, etc... If the responses of sensors to these mechanical waves is powerful enough on each sensor, the system is coupled Nielsen (1980). Others parameters to tune are PDT (Peak Definition Time), HDT (Hit Definition Time) and HLT (Hit Lockout Time). These variables are temporal windows which are respectively used to define, the highest amplitude peak in the signal, the total duration of the signal to record and the dead time in-between two recordings. These values are of prior importance to compute characteristic parameters of the signals, to avoid missing acoustic waves because of a too long HLT, to also avoid having two acoustic wave in the same temporal window due to a too long HDT. Common values were PDT=200 μs, HDT=800 μs and HLT=200 μs. These parameters are dependent of the used material. Then, a threshold acquisition value has to be imposed. This value matches to the minimum amplitude for which a signal is recorded.This threshold is mainly determined by the acoustic environment of the sensors (noises of different nature must be below the threshold value to avoid recordings of hits without any loading). The threshold value was setup for each experiment to maximize the signal over noise ratio. Common values were 25dB.

A.2.2 Acoustic emission parameters

Two kinds of acoustic emissions are distinguished:

- The continuous acoustic emissions which is constituted of an ensemble of discrete emissions very close in time, so that, they become undistinguishable.
- The discrete acoustic emissions. Generally, we call "hit" a discrete acoustic emission. It looks like a damped sinusoidal wave with a time resolution as illustrated on the figure A.3. A more rigorous definition of a hit is given by the norm ISO 12716 2001 : "a signal that exceeds the threshold and causes a system channel to accumulate data. It is frequently used to show the AE activity with counted number for a period (rate) or accumulated numbers".

Usually, one hit is characterized by eleven parameters Grosse and Ohtsu (2008) :

1. Number of counts: the number of times within the duration, where one signal (waveform) exceeds a present threshold.
2. Counts to peak: the number of counts between the triggering time over the threshold and the peak amplitude.
3. Amplitude: a peak voltage of the signal waveform is usually assigned (dB).
4. Duration: a time interval between the triggered time of one AE signal (waveform) and the time of disappearance is assigned (μs).

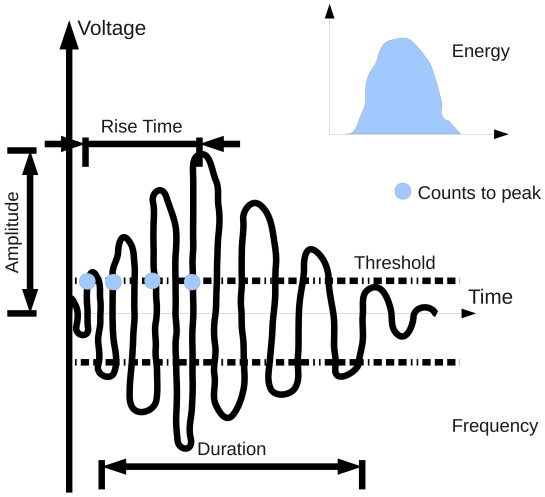

Figure A.3 – *Representation of a hit*

5. Rise time: a time interval between the triggering time of AE signal and the time of the peak amplitude is assigned (μs).

6. Energy: a measured area under the rectified signal envelope (aJ).

7. Average frequency: a calculated feature obtained from "Count" divided by "Duration", which determines an average frequency over one AE hit.

8. Initial frequency: a calculated feature derived from "Count to peak" divided by "Rise time".

9. Reverberation Frequency: a calculated feature derived from "Count - Count to peak" divided by "Duration - Rise time".

10. Peak frequency: a frequency feature reported in kilohertz, which is defined as the point in the power spectrum at which the peak magnitude is observed.

11. Frequency centroid: a calculate frequency feature reported in kilohertz, which results from a sum of magnitude times frequency divided by a sum of magnitude, as equivalent to the first moment of inertia.

These eleven parameters give a detailed description of each hit. Part of these parameters are commonly used to identify some patterns associated to physical mechanisms in the classification analysis.

A.3 Dive into the world of power-laws

A.3.1 The 68/95/99 and 01/50 rules

The 68/95/99 and the 01/50 rules respectively refer to the Gaussian and Paretian distributions, that are as strongly different as being catholic or protestant! These two mathematical distributions are widely encountered in nature and it is worth highlighting the main differences between them.

The 68/95/99 rule

Usually, people have the notion of what is a Gaussian distribution, it is so widely widespread that the adjective *normal* is used to describe this mathematical distribution characterized by the well know *bell curve*. One has immediately a large number of examples in mind of what kind of quantity follows a Gaussian distribution. Among the most cited, one can find, the size or the weight of humans. Behind the mathematical definition of a Gaussian distribution, if one pay attention to what it physically implies, some surprises are hidden. Indeed, the key property that a Gaussian distribution summarizes is that most of the observed quantities are oscillating around a mean value. *The probabilities to deviate from the mean value are decreasing faster and faster as we are going away from the mean (as an exponential)*. If we come back to the example of human height, making the simplifying assumptions that the mean is identical for men and women, 1.67 m and giving a standard deviation of 10 cm and let us have a look to the probability that somebody is as tall as :

Standard deviation	Size	Probability
1	1.77	0.15
2	1.87	0.023
3	1.97	$1.3e^{-3}$
4	2.07	$3.1e^{-4}$
5	2.17	$2.8e^{-7}$
6	2.27	$1.0e^{-10}$
7	2.37	$1.3e^{-12}$
8	2.47	$6.2e^{-16}$
9	2.57	$1.1e^{-19}$
10	2.67	$7.7e^{-24}$

Figure A.4 – *Gausian distribution of heights Taleb (2007)*

The most surprising fact of this table is the acceleration of the decrease of probability that occurs for example between six and seven standard deviations. An increase of 10 centimeters makes the probability evolving from 1 person over 1 billion to 1 person over 780 billions. The vulnerability of the Gaussian distribution stands in its evaluation of the extreme events. Indeed, for a normal distribution, the "empirical rule" states that :

- 68.2 % of the data fall within 1 standard deviations of the mean
- 95.4 % of the data fall within 2 standard deviations of the mean

- 99.7 % of the data fall within 3 standard deviations of the mean

Considering now, that the probability of being 4.15 standard deviations away from the mean is the double from the probability of being 4 standard deviations away, one easily understands that an error committed on the empirical evaluation of the mean will have dramatic consequences for extreme events that will be strongly underestimated in probability.

The 80/20 or the 50/01 rule

Hopefully, all the quantities are not fitted by normal distribution since you understood that we would have lived in a boring egalitarian world! Indeed, as seen previously, inequalities collapse when deviation rises, caused by the increase of the speed of the decrease. What is magical with power-laws is that inequalities remain unchanged, the same inequalities stand between the extra-riches persons and the inequalities are the same if you solely consider people which are "just" riches.

Let us introduce a pedagogical example that quantifies the probability among European people who have a wealth greater than the following net values in a system with low and high inequalities and the case of an hypothetic Gaussian distribution of wealth.

Amout in M$	Low inequalities	High inequalities	Gaussian world
1	63	62.5	63
2	125	250	127000
4	250	1000	$8.8e^{18}$
8	500	4000	$1.6e^{35}$
16	1000	16000	uncomputable
32	2000	64000	uncomputable
320	20000	6400000	uncomputable

Figure A.5 – *An example of a Paretian and a Gaussian unfair world Taleb (2007)*

Table extracted from Taleb (2007)

In the cases of the low and high inequalities which are governed by two different power-law distributions, one can notice that the diminution of probabilities is unchanged. When the amount of money is multiplied by 2, the number of people which own this wealth is divided by 2 in the case of low inequalities and by 4 in the case of high inequalities. This behavior holds whatever what you own, one can understand why jealousy is so widespread ! It is now crystal clear why power-law distributions are often called *scale-free*, it is the property of something which remains unchanged whatever the scale you are looking at, as the inequalities of wealth. The scale-free property can be mathematically written as $p(ax) = f(a)p(x)$ with $p(x)$ some probability distribution for a quantity x and b a multiplicative factor. Consequently, the shape of the distribution $p(x)$ is unchanged, except for a multiplicative constant.

This empirical observation was first noticed by Vilfredo Pareto at the end of the 19^{th} century. He studied the repartition of wealth in England, Switzerland, France, Russia, Italy and Prussia. He noticed that the statistical repartition of wealth follows the same mathematical law, that is,

the percentage of people which are richer than x is always proportional to $\frac{1}{x^{\alpha}}$, where α is a coefficient between 2 and 3 depending on countries. One property of power-law distributions is that their rank/frequency plot (also called cumulative distribution function) is a straight line with slope $-\alpha + 1$. What we call rank is the number of measurements which have a value greater than or equal to x. This kind of plot is better than making a histogram since it does not require to bin the data, each data point gets counted separately. This is important since histogram of power-law distributions are highly right-skewed as shown in figure A.6, meaning that while the bulk of the distribution occurs for fairly small sizes of x, there is a small number of x much higher than the small value., producing the long tail to the right of the histogram. The two colors in figure A.6 refers to the well known repartition of percentage 80/20 introduced by Pareto (80 percents for the green area and 20 percents for the yellow one).

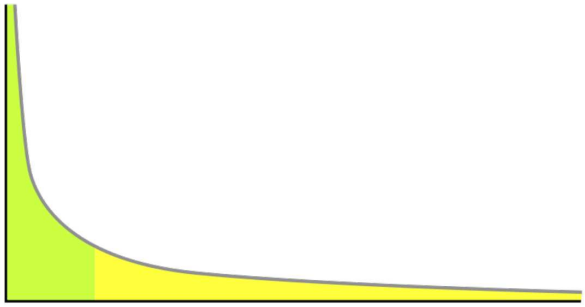

Figure A.6 – *Classical shape of the density function of a power law*

This 80/20 principle is a characteristic of power-laws. Historically, Pareto observed that 80% of the land in Italy was owned by 2 0% of the population. This inequality property of the power-law distributions can also be stated as the 50/01 principle, which makes the world more unfair.

A striking example is the one of the distribution of world GDP in 1989.

Quintile of population	Income
Richest 20 %	82.70 %
Second 20 %	11.75 %
Third 20 %	2.30 %
Fourth 20 %	1.85 %
Poorest 20 %	1.40 %

Figure A.7 – *World GDP in 1989 extracted from Wikipedia*

Many other examples exist, but, the true question is to know what mechanisms lead to power-law distributions? What is interesting is that the number of known ways of producing power laws is not very large. If you find a power law, like the ones above, the number of mechanisms that could be behind it is rather small, and so the mere existence of a power law gives you a lot of help in working out the physical mechanism behind an observed phenomenon. Among the well-known we find, combination of exponentials, reciprocals of things, random multiplicative processes, random extremal processes, random walks, phase transitions and critical phenomena, self-organized criticality and some others detailed in the

chapter 14 of Sornette (2003) as well as in the reference papers of Newman Newman (2004) and Mitzenmacher Mitzenmacher (2004).

The last point, I would like to discuss regarding power-law distribution is the influence of the computed exponent. Qualitatively, a little mistake in the evaluation of the exponent is responsible for large changes. The following table will help to understand why it is crucial. It represents the proportions occupied among the total for a given exponent by the first and the twenty first percents of the distribution.

Exponent	Proportion of the first 1%	Proportion of the firsts 20%
1	99.99	99.99
1.1	66	86
1.2	47	76
1.3	34	69
1.4	27	63
1.5	22	58
2	10	45
2.5	6	38
3	4.6	34

Figure A.8 – *Proportions inside a power-law given an exponent Taleb (2007)*

Consequently, one has to always keep in mind that the most important notion are the scale-free property and the variations of exponents encountered rather than the true numerical value. Indeed, mistakes are always committed in the evaluations of exponents, even with mathematical advanced methods, since a scale-free behavior is always seen empirically from a lower bound to an upper bound that are the consequences of our observations or the finite-size effects of the systems that cause change in the exponent.

To conclude, those who are interested in complexity and the ubiquity of power-laws are invited to read the following books :

- *Ubiquity: why catastrophes happen* from Mark Buchanan, for a global vision of criticality and extreme events.
- *The Black Swan: The impact of the highly improbable* from Nassim Nicholas Taleb (my favorite), for a discussion between the Gaussian and the Paretian worlds and their implications in terms of risks
- *Critical phenomena in natural sciences* from Didier Sornette for a deep scientific review and related models and equations (many!)
- *How nature works* from Per Bak for those who want to focus on SOC
- *Exploring complexity: an introduction* from G. Nicolis and L. Prigogine for a pedagogical review on complexity
- *Fractales, hasard et finance* from Benoît Mandelbrot, for those who want to think out the box.

A.3.2 Definitions and properties

The core of this thesis is based on the analysis of statistics of acoustic emission measurements fitted by power laws. Consequently, attention is devoted to explain the different fitting procedures used since results are highly sensitive to the method of computation of exponents.

First of all, let us recall that power laws are ubiquitous distributions that are found in many systems in nature Newman (2004). Usually the distribution of a discrete random variable is referred to a power law distribution as

$$p(x) = \mathbb{P}(X = x) = Cx^{-\alpha} \tag{A.1}$$

with $\alpha \geq 1$. As the equation A.1 diverges at zero, so there must be a lower bond $x_{min} > 0$ to keep a power-law behavior. Consequently $p(x)$ is expressed with a normalizing constant as

$$p(x) = \frac{x^{-\alpha}}{\zeta(\alpha, x_{min})} \tag{A.2}$$

where ζ is the generalized Hurwitz zeta function defined as

$$\zeta(\alpha, x_{min}) = \sum_{n=0}^{\infty} (n + x_{min})^{-\alpha} \tag{A.3}$$

with n the number of data considered. However, experimental data following a power-law distribution are often noisy, hence getting a reliable exponent of α is notoriously difficult.

A.3.3 Fitting of power-law distributions

It's well know now that simple graphical methods as least square regression are intrinsically unreliable and ineffective to provide a good approximation of α. Moreover, pure power-law are rare in nature and situations often present two cut-offs, one for low values x_{min} and one for high values x_{max} as well, e.g. it is not rare to see distribution with exponential cut-off. Hopefully, alternative methods introducing maximum likelihood estimators have been introduced M.L. Goldstein et al. (2004), Newman (2004), Bauke (2007), Clauset et al. (2009).

The method used to fit parametrized models is the maximum likelihood estimation detailled in Clauset et al. (2009). When $x_{min} > 1$, an estimator of α is given by solving numerically the maximization of the logarithm of the likelihood function.

$$\mathcal{L}(\alpha) = -n \ln \zeta(\alpha, x_{min}) - \alpha \sum_{i=1}^{n} \ln x_i \tag{A.4}$$

To find an estimate of the standard error, σ, on $\hat{\alpha}$, we used the following estimator which is the one of the continuous case but which yields to roughly similar results for reasonably large n and x_{min}.

$$\sigma = \frac{\hat{\alpha} - 1}{\sqrt{n}} + O(\frac{1}{n}) \tag{A.5}$$

The method used to evaluated the goodness of fit of power-laws in this article can be described as follow; given a data set $(x_i)_{i \in \mathbb{N}}$ first we proceed

by estimating α, x_{min} and n_{tail} which is the number of x_i over x_{min}. Then we computed the Kolmogorov Smirnov distance d_{KS} defined as:

$$d_{KS} = \max_{x \geq x_{min}} |S(x) - P(x)| \tag{A.6}$$

which is the distance between real data and the best fit power law, $d^{\star}$.Then, we draw n random values $(y_i)_{i \in \mathbb{N}}$ with probability $\frac{n_{tail}}{n}$ draw from power-law and otherwise we pick one of the $x_i < x_{min}$ uniformly. Thus we estimate α and x_{min} for the simulation and we calculate its d_{KS}. We repeat several times these operations to get distribution of d_{KS} values. Finally one has the $p - value$ which is the fraction of simulations where $d \geq d^{\star}$. This $p - value$ permits to check whether the investigated model is appropriate.

One other question emerges concerning the choice of the model to fit experimental data since power-law distributions are often suspected to have an exponential cut-off and consequently the following distribution $f(x)$

$$f(x) \approx x^{-\alpha} e^{-\lambda x} = \frac{\lambda}{\Gamma(1-\alpha, \lambda x_{min})} (\lambda x)^{-\alpha} e^{-\lambda x} \tag{A.7}$$

where $f(x)$ looks like a power-law if $x_{min} \leq x << \frac{1}{\lambda}$ and looks like an exponential if $x >> \frac{1}{\lambda}$. λ^{-1} acts like an upper limiting scale.

So it's crucial to determine if one distribution better fits data than the one found. To address this question we used likelihood ratio tests for model selection detailed in Vuong (1989). These tests enable to compare non-nested and nested models and consequently each distribution which was supposed to be a power law was compared to Log-normal, exponential and Weibull distribution in the non-nested case and to power-law distribution with exponential cut-off in the nested case. The basis of the implementation of these methods are those developed by Clauset et al. Clauset et al. (2009) which were modified for our specific purposes.

Bibliography

Joulin A., Lefevre A., D. Grunberd, and J.P. Bouchaud. Stock price jumps: news and volume play a minor role. *eprint arXiv:0803.1769*, 2008. (Cité page 88.)

Rohan Abeyaratne and Sang-Joo Kim. Cyclic effects in shape-memory alloys: a one-dimensional continuum model. *International Journal of Solids and Structures*, 34(25):3273 – 3289, 1997. ISSN 0020-7683. doi: DOI:10.1016/S0020-7683(96)00213-2. URL http://www.sciencedirect.com/science/article/B6VJS-3T6SFGT-4/2/7639fff9f77da8d546edc78f59167c9b. (Cité page 15.)

R Ahluwalia, T Lookman, A Saxena, and R. C Albers. Landau theory for shape memory polycrystals. *Acta Materialia*, 52(1):209–218, 1 2004. URL http://www.sciencedirect.com/science/article/pii/S1359645403005354. (Cité page 25.)

T.G. Andersen. *International Economic Review*, 39(885-905), 1997. (Cité page 95.)

Per Bak and Chao Tang. Earthquakes as a self-organized critical phenomenon. *J. Geophys. Res.*, 94(B11):15635–15637, 1989. URL http://dx.doi.org/10.1029/JB094iB11p15635. (Cité pages 21 et 49.)

Per Bak, Chao Tang, and Kurt Wiesenfeld. Self-organized criticality. *Phys. Rev. A*, 38(1):364–374, Jul 1988. doi: 10.1103/PhysRevA.38.364. (Cité pages 17, 21 et 49.)

Per Bak, Kim Christensen, Leon Danon, and Tim Scanlon. Unified scaling law for earthquakes. *Physical Review Letters*, 88(17), 04 2002. URL http://link.aps.org/doi/10.1103/PhysRevLett.88.178501. (Cité pages 20 et 49.)

H. Bauke. Parameter estimation for power-law distributions by maximum likelihood methods. *The European Physical Journal B - Condensed Matter and Complex Systems*, 58:167–173, 2007. ISSN 1434-6028. URL http://dx.doi.org/10.1140/epjb/e2007-00219-y. 10.1140/epjb/e2007-00219-y. (Cité page 130.)

Z. Bo and DC. Lagoudas. Thermo-mechanical modeling of poly-cristalline smas under cyclic loading, part i : theoretical derivations. *International Journal of Engineering and Science*, 37:1089–1140, 1999. (Cité pages 14, 15 et 32.)

Erell Bonnot, Eduard Vives, Lluís Mañosa, Antoni Planes, and Ricardo Romero. Acoustic emission and energy dissipation during front propagation in a stress-driven martensitic transition. *Phys. Rev. B*, 78(9): 094104, Sep 2008. doi: 10.1103/PhysRevB.78.094104. (Cité pages 24, 30, 31 et 104.)

E. Bouchaud. Scaling properties of cracks. *Journal of Physics: Condensed Matter*, 9(21):4319, 1997. (Cité page 22.)

J-P. Bouchaud and M. Potters. Welcome to a non-black-scholes world. *Quantitative Finance*, 1(5):482–483, 2011/11/11 2001. doi: 10.1080/713665871. URL http://www.tandfonline.com/doi/abs/10.1080/713665871. (Cité page 87.)

Jean-Philippe Bouchaud and Didier Sornette. The black-scholes option pricing problem in mathematical finance: generalization and extensions for a large class of stochastic processes. *J. Phys. I France*, 4(6):863–881, 6 1994. URL http://dx.doi.org/10.1051/jp1:1994233. (Cité page 87.)

J.P. Bouchaud. Economics needs a scientific revolution. *Nature*, 455:1181–1182, 2008. (Cité page 88.)

J.P. Bouchaud. The (unfortunate) complexity of the economy. *Physics World*, pages 28–32, April 2009. (Cité page 88.)

J. S Bowles and J. K Mackenzie. The crystallography of martensite transformations i. *Acta Metallurgica*, 2(1):129–137, 1 1954. URL http://www.sciencedirect.com/science/article/pii/0001616054901029. (Cité page 12.)

C.G. Bowsher. Modelling security market events in continuous time: Intensity based, multivariate point process models. *Journal of econometrics*, 141(2):876–912, 2007. (Cité pages 96 et 97.)

L.C.L. Catherine Brinson, Ina Schmidt, and Rolf Lammering. Stress-induced transformation behavior of a polycrystalline niti shape memory alloy: micro and macromechanical investigations via in situ optical microscopy. *Journal of the Mechanics and Physics of Solids*, 52(7): 1549 – 1571, 2004. ISSN 0022-5096. doi: DOI:10.1016/j.jmps.2004.01.001. URL http://www.sciencedirect.com/science/article/B6TXB-4BVPP8J-1/2/23e6aefa2e54e08ef2f2e23343a53330. (Cité pages 29, 30 et 43.)

G. Cannelli, R. Cantelli, and F. Cordero. Self-organized criticality of the fracture processes associated with hydrogen precipitation in niobium by acoustic emission. *Physical Review Letters*, 70(25), 06 1993. URL http://link.aps.org/doi/10.1103/PhysRevLett.70.3923. (Cité pages 21 et 22.)

Lluís Carrillo and Jordi Ortín. Avalanches in the growth of stress-induced martensites. *Physical Review B*, 56(18), 11 1997. URL http://link.aps.org/doi/10.1103/PhysRevB.56.11508. (Cité pages 24 et 32.)

Lluís Carrillo, Lluís Mañosa, Jordi Ortín, Antoni Planes, and Eduard Vives. Experimental evidence for universality of acoustic emission avalanche distributions during structural transitions. *Phys. Rev. Lett.*, 81(9):1889–1892, Aug 1998. doi: 10.1103/PhysRevLett.81.1889. (Cité pages 24, 44 et 49.)

Benedetta Cerruti and Eduard Vives. Random-field potts model with dipolarlike interactions: Hysteresis, avalanches, and microstructure. *Phys. Rev. B*, 77(6):064114, Feb 2008. doi: 10.1103/PhysRevB.77.064114. (Cité page 25.)

Kan Chen, Per Bak, and S. P. Obukhov. Self-organized criticality in a crack-propagation model of earthquakes. *Physical Review A*, 43(2):625–630, 01 1991. URL http://link.aps.org/doi/10.1103/PhysRevA.43.625. (Cité pages 21 et 49.)

Kim Christensen, Álvaro Corral, Vidar Frette, Jens Feder, and Torstein Jøssang. Tracer dispersion in a self-organized critical system. *Physical Review Letters*, 77(1), 07 1996. URL http://link.aps.org/doi/10.1103/PhysRevLett.77.107. (Cité page 20.)

Pierre Cizeau, Stefano Zapperi, Gianfranco Durin, and H. Eugene Stanley. Dynamics of a ferromagnetic domain wall and the barkhausen effect. *Physical Review Letters*, 79(23), 12 1997. URL http://link.aps.org/doi/10.1103/PhysRevLett.79.4669. (Cité page 49.)

A. Clauset. Scale invariance in global terrorism. *arXiv:physics/0502014*, page 6. (Cité page 117.)

A. Clauset, C.R. Shalizy, and M.E.J. Newman. Power-law distributions in empirical data. *SIAM Review*, 51(4):661, 2009. (Cité pages 62, 130 et 131.)

Aaron Clauset and Douglas H. Erwin. The evolution and distribution of species body size. *Science*, 321(5887):399–401, 07 2008. URL http://www.sciencemag.org/content/321/5887/399.abstractN2. (Cité page 117.)

F. Colaiori, S. Zapperi, and G. Durin. Shape of a barkhausen pulse. *Journal of Magnetism and Magnetic Materials*, 272-276(Supplement 1):E533 – E534, 2004. ISSN 0304-8853. doi: DOI:10.1016/j.jmmm.2003.12.1063. URL http://www.sciencedirect.com/science/article/B6TJJ-4BFXFWK-K/2/f82f6246b0a8a3c16862d8f2a607fd63. Proceedings of the International Conference on Magnetism (ICM 2003). (Cité page 23.)

R. Cont and J.P. Bouchaud. Herd behavior and aggregate fluctuations in financial markets. *Macroeconomic dynamics*, 4:170–196, 2000. (Cité page 89.)

H.F. Coronel-Brizio and A.R. Hernande-Montoya. Asymptotic behavior of the daily increment distribution of the ipc, the mexican stock index. *Revista mexicana de fisica*, 51(1):27–31, 2005. (Cité page 89.)

Álvaro Corral, Conrad J. Pérez, and Albert Díaz-Guilera. Self-organized criticality induced by diversity. *Physical Review Letters*, 78 (8):1492–1495, 02 1997. URL http://link.aps.org/doi/10.1103/PhysRevLett.78.1492. (Cité page 21.)

P. J. Cote and L. V. Meisel. Self-organized criticality and the barkhausen effect. *Phys. Rev. Lett.*, 67(10):1334–1337, Sep 1991. doi: 10.1103/PhysRevLett.67.1334. (Cité page 49.)

Ferenc F. Csikor, Christian Motz, Daniel Weygand, Michael Zaiser, and Stefano Zapperi. Dislocation avalanches, strain bursts, and the problem of plastic forming at the micrometer scale. *Science*, 318(5848): 251–254, 2007. URL http://www.sciencemag.org/content/318/5848/251.abstract. (Cité page 23.)

A. Cuniberti and R. Romero. Differential scanning calorimetry study of deformed cu-zn-al martensite. *Scripta Materialia*, 51(4):315 – 320, 2004. ISSN 1359-6462. doi: DOI:10.1016/j.scriptamat.2004.04.024. URL http://www.sciencedirect.com/science/article/B6TY2-4CCNRP4-5/2/4e435bee6778995d52fc0b52b35eb5b4. (Cité page 44.)

M. Marsili D. Challet and Y-C. Zhang. *Minority games: interacting agents in financial markets*. Oxford University Press, 2004. (Cité page 91.)

D. Daley and D. Vere-Jones. *An introduction to the theroy of point processes*. Springer Berlin. (Cité pages 93, 94 et 99.)

S. Daly, G. Ravichandran, and K. Bhattacharya. Stress-induced martensitic phase transformation in thin sheets of nitinol. *Acta Materialia*, 55(10):3593–3600, 6 2007. URL http://www.sciencedirect.com/science/article/B6TW8-4NF2NPS-1/2/d2f9b26761978fa24e5d707b707e118c. (Cité page 31.)

L. Delaey, R. V. Krishnan, H. Tas, and H. Warlimont. Thermoelasticity, pseudoelasticity and the memory effects associated with martensitic transformations. *Journal of Materials Science*, 9(9):1521–1535, 1974. URL http://dx.doi.org/10.1007/BF00552939. (Cité page 29.)

D. Delpueyo and X. Balandraud Grediac. Infrared thermography to the study of martensitic microstructures. *Materials Science and Engineering A*, (528):8249–8258, 2011. (Cité page 31.)

R O Dendy and P Helander. Sandpiles, silos and tokamak phenomenology: a brief review. *Plasma Physics and Controlled Fusion*, 39 (12), 1997. URL http://stacks.iop.org/0741-3335/39/i=12/a=002. (Cité page 20.)

Deepak Dhar. Self-organized critical state of sandpile automaton models. *Phys. Rev. Lett.*, 64(14):1613–1616, Apr 1990. doi: 10.1103/PhysRevLett.64.1613. (Cité page 18.)

J.H. Dietrich. Time-dependent friction and the mechanics os stick-slip. *Pure and applied geophysics*, 116:780–806, 1978. (Cité page 73.)

P.J. Diggle. *An introduction to the theroy of point processes*. Springer New York, 1988. (Cité page 107.)

Dennis M. Dimiduk, Chris Woodward, Richard LeSar, and Michael D. Uchic. Scale-free intermittent flow in crystal plasticity. *Science*, 312 (5777):1188–1190, 05 2006. URL http://www.sciencemag.org/content/312/5777/1188.abstract. (Cité pages 23, 49 et 74.)

P. Diodati, F. Marchesoni, and S. Piazza. Acoustic emission from volcanic rocks: An example of self-organized criticality. *Phys. Rev. Lett.*, 67(17): 2239–2243, Oct 1991. doi: 10.1103/PhysRevLett.67.2239. (Cité page 21.)

J.M. Poterba D.M. Cutler and L.H. Summers. What moves stock prices. *NBER Working paper series*, w2538, 1989. (Cité page 88.)

Gianfranco Durin and Stefano Zapperi. Scaling exponents for barkhausen avalanches in polycrystalline and amorphous ferromagnets. *Physical Review Letters*, 84(20), 05 2000. URL http://link.aps.org/doi/10.1103/PhysRevLett.84.4705. (Cité pages 23 et 49.)

M. Hoffmann E. Bacry, S. Delattre and J.F. Muzy. Modelling microstructure noise with mutually exciting point processes. *Submitted to quantitative finance*, 2010. (Cité page 96.)

R.F. Engle. The econometrics of ultra high frequency data. *Econometrica*, 68(1):1–22, 2000. (Cité page 91.)

R.F. Engle and V.K. Ng. Measuring and testing the impact of news on volatility. *Journal of finance*, 48(1749-1778), 1993. (Cité page 88.)

T.W. Epps. Comovement in stock prices in the very short run. *Journal of the American Statistical Association*, 74(291-298), 1979. (Cité page 95.)

E.F. Fama. The behavior of stock market prices. *The journal of business*, 38 (1):34–105, 1965. (Cité page 88.)

Stuart Field, Jeff Witt, Franco Nori, and Xinsheng Ling. Superconducting vortex avalanches. *Physical Review Letters*, 74(7):1206–1209, 02 1995. URL http://link.aps.org/doi/10.1103/PhysRevLett.74.1206. (Cité page 20.)

P.M. Fisman and D.L. Snyder. The statistical analysis of space time point processes. *IEEE Trans. Pattern Anal. Machine Intell.*, 22(3):257–274, 1976. (Cité page 94.)

Vidar Frette, Kim Christensen, Anders Malthe-Sorenssen, Jens Feder, Torstein Jossang, and Paul Meakin. Avalanche dynamics in a pile of rice. *Nature*, 379(6560):49–52, 01 1996. URL http://dx.doi.org/10.1038/379049a0. (Cité pages ix, 18 et 20.)

F. Lillo G. Bonnano and R. Mantegna. Dynamics of the number of trades in financial securities. *eprint cond-mat/9912006*. (Cité page 89.)

Xavier Gabaix, Parameswaran Gopikrishnan, Vasiliki Plerou, and Eugene Stanley. A unified econophysics explanation for the power-law exponents of stock market activity. *Physica A: Statistical Mechanics and its Applications*, 382(1):81–88, 8 2007. URL http://www.sciencedirect.com/science/article/pii/S0378437107001392. (Cité page 89.)

S. P. Gadaj, W. K. Nowacki, and E. A. Pieczyska. Temperature evolution in deformed shape memory alloy. *Infrared Physics & Technology*, 43(3-5):151–155, 6 2002. URL http://www.sciencedirect.com/science/article/B6TJ9-45MWS4M-5/2/bfe8dae72559f65a680b242478e6c311. (Cité page 31.)

Ken Gall, Kurt Jacobus, Huseyin Sehitoglu, and Hans Maier. Stress-induced martensitic phase transformations in polycrystalline cuznal shape memory alloys under different stress states. *Metallurgical and Materials Transactions A*, 29(3):765–773, 1998. doi: 10.1007/s11661-998-0267-y. URL http://dx.doi.org/10.1007/s11661-998-0267-y. (Cité page 30.)

María Carmen Gallardo, Julia Manchado, Francisco Javier Romero, Jaime del Cerro, Ekhard K. H. Salje, Antoni Planes, Eduard Vives, Ricardo Romero, and Marcelo Stipcich. Avalanche criticality in the martensitic transition of $cu_{67.64}zn_{16.71}al_{15.65}$ shape-memory alloy: A calorimetric and acoustic emission study. *Phys. Rev. B*, 81(17):174102, May 2010. doi: 10.1103/PhysRevB.81.174102. (Cité pages 30, 32 et 103.)

A. Garcimartín, A. Guarino, L. Bellon, and S. Ciliberto. Statistical properties of fracture precursors. *Phys. Rev. Lett.*, 79(17):3202–3205, Oct 1997. doi: 10.1103/PhysRevLett.79.3202. (Cité page 22.)

and Z. Wei-Xing G.F. Gu, C. Chein. Empirical distributions of chinese stock returns at different microscopic timescales. *Physica A*, 387:485–502, 2008. (Cité page 89.)

R. Goldstone and M. Janssen. Computational models of collective behaviour. *Trends in cognitice sciences*, 9(424), 2005. (Cité page 91.)

Parameswaran Gopikrishnan, Vasiliki Plerou, Luís A. Nunes Amaral, Martin Meyer, and H. Eugene Stanley. Scaling of the distribution of fluctuations of financial market indices. *Physical Review E*, 60(5):5305–5316, 11 1999. URL http://link.aps.org/doi/10.1103/PhysRevE.60.5305. (Cité page 88.)

Parameswaran Gopikrishnan, Vasiliki Plerou, Xavier Gabaix, and H. Eugene Stanley. Statistical properties of share volume traded in financial markets. *Physical Review E*, 62(4):R4493–R4496, 10 2000. URL http://link.aps.org/doi/10.1103/PhysRevE.62.R4493. (Cité page 89.)

C. Grosse and M. Ohtsu. *Acoustic Emission Testing*. Springer, 2008. (Cité page 124.)

B. Gutenberg and C.F. Richter. *Seismicity of the earth and associated phenomena.* Princeton University Press, Princeton, New Jersey., 1949. (Cité pages 51, 71 et 74.)

J. Hasbrouck. Measuring the information content of stock trades. *Journal of finance*, 46(179-207), 1991. (Cité page 91.)

N. Hautsch. *Modelling irregularly spaced financial data*. Springer Berlin, 2004. (Cité page 97.)

A.G. Hawkes. Spectra of some self-exciting and mutually exciting point processes. *Biometrika*, 58:83–90, 1971. (Cité pages 94, 96, 97 et 99.)

A.G. Hawkes and D. Oakes. A cluster representation os a self-exciting process. *Journal of Applied Probability*, 11:493–503, 1974. (Cité page 97.)

Y. J. He and Q. P. Sun. Rate-dependent domain spacing in a stretched niti strip. *International Journal of Solids and Structures*, 47(20):2775–2783, 10 2010. URL http://www.sciencedirect.com/science/article/B6VJS-509W7C7-3/2/aca87a1ca73aa1b7f9b36813a03d8bd9. (Cité page 31.)

S.V. Buldyrev P. Gopikrishnan V. Plerou H.E. Stanley, L.A.N. Amaral and M.A. Salinger. Self-organized complexity in economics and finance. *Proceedings of the National Academy of Sciences*, 99(1):2561–2565, 2002. (Cité page 88.)

Oleg Heczko and Ladislav Straka. Magnetic properties of stress-induced martensite and martensitic transformation in ni-mn-ga magnetic shape memory alloy. *Materials Science and Engineering A*, 378(1-2):394 – 398, 2004. ISSN 0921-5093. doi: DOI:10.1016/j.msea.2003.12.055. URL http://www.sciencedirect.com/science/article/B6TXD-4C82N7C-V/2/99db71f5fa8233a6a15daf5e93914cf7. European Symposium on Martensitic Transformation and Shape-Memory. (Cité page 24.)

G. A. Held, D. H. Solina, H. Solina, D. T. Keane, W. J. Haag, P. M. Horn, and G. Grinstein. Experimental study of critical-mass fluctuations in an evolving sandpile. *Physical Review Letters*, 65(9):1120–1123, 08 1990. URL http://link.aps.org/doi/10.1103/PhysRevLett.65.1120. (Cité page 18.)

A. Helmstetter and D. Sornette. Diffusion of epicenters of earthquake aftershocks, omori's law, and generalized continuous-time random walk models. *Physical Review E*, 66(6):061104–, 12 2002. URL http://link.aps.org/doi/10.1103/PhysRevE.66.061104. (Cité page 72.)

AgnËs Helmstetter and Bruce E. Shaw. Afterslip and aftershocks in the rate-and-state friction law. *J. Geophys. Res.*, 114(B1), 01 2009. doi: 10.1029/2007JB005077. URL http://dx.doi.org/10.1029/2007JB005077. (Cité page 72.)

P. Hewlett. Clustering of order arrivals, price impact and trade path optimisation. *Ecole Polytechnique*, 2006. (Cité page 96.)

A. Rinaldo I. Rodriguez-Iturbe. *Fractal river bassins: chance and self-organization*. Cambridge University Press, 2001. (Cité page 20.)

H. M. Jaeger, Chu-heng Liu, and Sidney R. Nagel. Relaxation at the angle of repose. *Physical Review Letters*, 62(1):40–43, 01 1989. URL http://link.aps.org/doi/10.1103/PhysRevLett.62.40. (Cité page 18.)

H.M. Jaeger, Nagel K., and Sidney R. Physics of the granular state. *Science*, 255(5051):1523–1531, 03 1992. URL http://www.sciencemag.org/content/255/5051/1523.abstractN2. (Cité page 18.)

J. Jasiak. Persistence in intratrade durations. *Finance*, (166-195), 1997. (Cité page 98.)

Xiaoping Jiang, Moritaka Hida, Yoshito Takemoto, Akira Sakakibara, Hidehiro Yasuda, and Hirotaro Mori. In situ observation of stress-induced martensitic transformation and plastic deformation in tini alloy. *Materials Science and Engineering: A*, 238(2):303–308, 11 1997. URL http://www.sciencedirect.com/science/article/pii/S092150939700422X. (Cité pages 29 et 41.)

Fabrizio Lillo J.P. Bouchaud, J. Doyne Farmer. How markets slowly digest changes in supply and demand. *arXiv 0809.0822v1*, 2008. (Cité page 98.)

M. Potters J.P. Bouchaud. *Theory of financial risk and derivative pricing: from statistical physics to risk management*. Cambridge University Press, 2003. (Cité page 87.)

C.C. Lee K. Kim, S.M. Yoon and K.H. Chang. Zipf's law distributions for korean financial markets. *Journal of the Korean physical society*, 47(171-173), 2005. (Cité page 89.)

Y.Y. Kagan. Likelihood analysis of erathquake catalogs. *Journal of Geophysics Research*, 106(135-148), 1991. (Cité pages 51, 73 et 94.)

A. Karr. *Point processes and their statistical inference*. Dekker New York, 1991. (Cité page 94.)

K. Kim and S. Daly. Martensite strain memory in the shape memory alloy nickel-titanium under mechanical cycling. *Experimental Mechanics*, pages 1–12, 2010. URL http://dx.doi.org/10.1007/s11340-010-9435-2. (Cité pages 31 et 42.)

S. Redner L. de Arcangelis and H.J. Herrmann. A random fuse model for breaking processes. *Journal de Physique Lettre*, 46:585–590, 1985. (Cité page 22.)

J. Large. Measuring the resiliency of an electronic limit order book. *Journal of financial markets*, 10:1–25, 2007. (Cité page 97.)

P.A.W. Lewis. Remarks on the theory compuattion and application of the spectral analysis of series of events. *J. SOund vib.*, 12:353–375, 1970. (Cité pages 97 et 107.)

C. Lexcellent and G. Bourbon. Thermodynamical model of cyclic behaviour of ti—ni and cu—zn—al shape memory alloys under isothermal undulated tensile tests. *Mechanics of Materials*, 24(1):59 –

73, 1996. ISSN 0167-6636. doi: DOI:10.1016/0167-6636(96)00027-0. URL http://www.sciencedirect.com/science/article/B6TX6-3VS94X3-D/2/d23a2aeae98af5a2c46b1b8713a8d294. (Cité page 15.)

C. Lexcellent, S. Leclercq, B. Gabry, and G. Bourbon. The two way shape memory effect of shape memory alloys: an experimental study and a phenomenological model. *International Journal of Plasticity*, 16(10-11):1155 – 1168, 2000. ISSN 0749-6419. doi: DOI:10.1016/S0749-6419(00)00005-X. URL http://www.sciencedirect.com/science/article/B6TWX-412RWP4-3/2/d86b14d3ed03aaefa27c337781aca479. (Cité page 14.)

F. Lillo and Farmer. The long memory of the efficient market. *Studies in Nonlinear Dynamics & Econometrics*, 8(3), 2004. (Cité page 97.)

Y. Liu, Z. L. Xie, J. Van Humbeeck, and L. Delaey. Effect of texture orientation on the martensite deformation of niti shape memory alloy sheet. *Acta Materialia*, 47(2):645–660, 1 1999a. URL http://www.sciencedirect.com/science/article/pii/S1359645498003760. (Cité page 41.)

Yanhui Liu, Parameswaran Gopikrishnan, Cizeau, Meyer, Peng, and H. Eugene Stanley. Statistical properties of the volatility of price fluctuations. *Physical Review E*, 60(2):1390–1400, 08 1999b. URL http://link.aps.org/doi/10.1103/PhysRevE.60.1390. (Cité page 89.)

T. Lux. Applications of statistical physics in finance and economics. *Handbook of research on complexity*, 2008. (Cité page 91.)

R. Cont M. Potters and J.P. Bouchaud. *Eurphys. Lett.*, 41(239), 1998. (Cité page 89.)

D. Lieberman M. Wechsler and T. Read. On the theory of the formation of martensite. *Transactions of AIME*, 197:1501–1515, 1953. (Cité page 12.)

Kockelkoren M. Potters M. Wyart, J.P. Bouchaud and M. Vettorazo. Realtion between bid-ask spread, impact and volatility in order driven market. *Journal of Quantitative Finance*, 8(41-57), 2008. (Cité pages 89 et 92.)

Bruce D. Malamud, Gleb Morein, and Donald L. Turcotte. Forest fires: An example of self-organized critical behavior. *Science*, 281(5384):1840–1842, 1998. URL http://www.sciencemag.org/content/281/5384/1840.abstract. (Cité page 20.)

Bruce D. Malamud, Donald L. Turcotte, Fausto Guzzetti, and Paola Reichenbach. Landslide inventories and their statistical properties. *Earth Surface Processes and Landforms*, 29(6):687–711, 2004. URL http://dx.doi.org/10.1002/esp.1064. (Cité page 20.)

B. Mandelbrot. *The Fractal Geometry of Nature*. W. H. Freeman, 1982. (Cité page 19.)

B.B. Mandelbrot. *Journal of business*, 36(394), 1963. (Cité page 88.)

David Marsan and Jérôme Weiss. Space/time coupling in brittle deformation at geophysical scales. *Earth and Planetary Science Letters*, 296(3-4): 353–359, 8 2010. URL http://www.sciencedirect.com/science/article/pii/S0012821X10003377. (Cité page 50.)

P. G. McCormick and Yinong Liu. Thermodynamic analysis of the martensitic transformation in niti—ii. effect of transformation cycling. *Acta Metallurgica et Materialia*, 42(7):2407–2413, 7 1994. URL http://www.sciencedirect.com/science/article/pii/0956715194903190. (Cité page 42.)

K. Melton and O. Mercier. Fatigue of niti thermoelastic martensites. *Acta Metallurgica*, 27:137–144, 1979. (Cité pages 14, 30 et 42.)

M. Mezard and A. Montanari. *Information, Physics and Computation*. Oxford University Press, 2009. (Cité page 91.)

M.-Carmen Miguel and Stefano Zapperi. Fluctuations in plasticity at the microscale. *Science*, 312(5777):1151–1152, 2006. URL http://www.sciencemag.org/content/312/5777/1151.short. (Cité pages 23 et 49.)

M. Carmen Miguel, Alessandro Vespignani, Stefano Zapperi, Jerome Weiss, and Jean-Robert Grasso. Intermittent dislocation flow in viscoplastic deformation. *Nature*, 410(6829):667–671, 04 2001. URL http://dx.doi.org/10.1038/35070524. (Cité pages 22 et 49.)

M. Mitchell. *Complexity, a guided tour*. Oxford University Press, 2009. (Cité page 16.)

Michael Mitzenmacher. A brief history of generative models for power law and lognormal distributions. *Internet Mathematics*, 1(2):226–251, 01 2004. URL http://dx.doi.org/10.1080/15427951.2004.10129088. (Cité pages 62 et 129.)

S. Miyazaki, T. Imai, Y. Igo, and K. Otsuka. Effect of cyclic deformation on the pseudoelasticity characteristics of ti-ni alloys. *Metallurgical and Materials Transactions A*, 17(1):115–120, 1986. doi: 10.1007/BF02644447. URL http://dx.doi.org/10.1007/BF02644447. (Cité pages 29, 41 et 42.)

M.L. Goldstein, S.A. Morris, and G.G. Yen. Problems with fitting to the power-law distribution. *Eur. Phys. J. B*, 41(2):255–258, 2004. doi: 10.1140/epjb/e2004-00316-5. URL http://dx.doi.org/10.1140/epjb/e2004-00316-5. (Cité page 130.)

J. Moller and J. Rasmussen. Perfect simulation of hawkes processes. *Working Paper, Aalborg University*. (Cité page 97.)

B. Morgan, N. and M. Friend, C. A review of shape memory stability in niti alloys. *J. Phys. IV France*, 11(PR8):Pr8–325–Pr8–332, 11 2001. URL http://dx.doi.org/10.1051/jp4:2001855. (Cité page 41.)

Claire Morin, Ziad Moumni, and Wael Zaki. A constitutive model for shape memory alloys accounting for thermomechanical coupling. *International Journal of Plasticity*, In Press, Corrected Proof: –, 2010. ISSN 0749-6419. doi: DOI:10.1016/j.ijplas.2010.09.005. URL http://www.sciencedirect.com/science/article/B6TWX-512MHB8-3/2/ff4e2bbfbd60939f6a5e42eb47b20502. (Cité page 15.)

Z. Moumni, A. Van Herpen, and P. Riberty. Fatigue analysis of shape memory alloys : energy approach. *Smart Materials and Structures*, 14: 287–292, 2005. (Cité pages 14, 15, 32 et 41.)

F. Musmeci and D. Vere-Jones. A space-time clustering model for historical earthquakes. *Ann. Inst. Statis. Math.*, 44(1-11), 1992. (Cité page 94.)

Kai Nagel and Maya Paczuski. Emergent traffic jams. *Physical Review E*, 51(4), 04 1995. URL http://link.aps.org/doi/10.1103/PhysRevE.51.2909. (Cité page 20.)

M.E.J. Newman. Power laws, pareto distributions and zipf's law. *Contemporary Physics*, 46(5):323–351, 2004. (Cité pages 62, 129 et 130.)

A. Nielsen. Acoustic emission source based on pencil lead breaking. *The danish welding institute publication*, 80.15, 1980. (Cité page 124.)

D. M. Norfleet, P. M. Sarosi, S. Manchiraju, M. F. X. Wagner, M. D. Uchic, P. M. Anderson, and M. J. Mills. Transformation-induced plasticity during pseudoelastic deformation in ni–ti microcrystals. *Acta Materialia*, 57(12):3549–3561, 7 2009. URL http://www.sciencedirect.com/science/article/pii/S1359645409002298. (Cité page 29.)

Kevin P. O'Brien and M. B. Weissman. Statistical characterization of barkhausen noise. *Phys. Rev. E*, 50(5):3446–3452, Nov 1994. doi: 10.1103/PhysRevE.50.3446. (Cité page 49.)

Y. Ogata. On lewis' simulation method for point processes. *IEEE Transaction of Information Theory*, 27:23–31, 1981. (Cité pages 97 et 107.)

Y. Ogata. Statistical models for earthquakes occurences and residual analysis for point processes. *Jounral of the American Statistical Association*, 83 (401):9–27, 1988. (Cité pages 94, 104 et 106.)

Y. Ogata. Space-time point processes models for eathquakes occurences. *Ann. Inst. Statis. Math.*, 50(2):379–402, 1998. (Cité pages 97 et 107.)

Y. Ogata. Seismicity analysis through point processes modeling: a review. *Pure and applied geophysics*, 155(471-507), 1999. (Cité pages 94, 96 et 105.)

F. Omori. "on the aftershocks of earthquakes". *Journal of the College of Science, Imperial University of Tokyo*, 7:111–200, 1894. (Cité pages 51 et 71.)

K. Otsuka and C.M. Wayman. *Shape memory materials*. Cambridge University Press, 1998. (Cité pages 12, 13, 41 et 42.)

T. Ozaki. Maximum likelihood estimation of hawkes self exciting point processes. *Ann. Inst. Statis. Math.*, 31(B):145–155, 1979. (Cité page 100.)

Maya Paczuski and Stefan Boettcher. Avalanches and waves in the abelian sandpile model. *Physical Review E*, 56(4):R3745–R3748, 10 1997. URL http://link.aps.org/doi/10.1103/PhysRevE.56.R3745. (Cité page 21.)

R.K. Pan and Sitabhra S. Inverse cubic law of index fluctuation distribution in indian market. *Physica A*, 387:2055–2065, 2008. (Cité page 89.)

Francisco-Jose Perez-Reche, Marcelo Stipcich, Eduard Vives, Lluís Mañosa, Antoni Planes, and Michel Morin. Kinetics of martensitic transitions in cu-al-mn under thermal cycling: Analysis at multiple length scales. *Phys. Rev. B*, 69(6):064101, Feb 2004. doi: 10.1103/PhysRevB.69.064101. (Cité pages 7, 24, 30, 32, 38, 42, 44 et 45.)

Francisco-Jose Perez-Reche, Lev Truskinovsky, and Giovanni Zanzotto. Training-induced criticality in martensites. *Phys. Rev. Lett.*, 99(7):075501, Aug 2007. doi: 10.1103/PhysRevLett.99.075501. (Cité pages 7, 25, 30, 44 et 49.)

Francisco-José Pérez-Reche, Lev Truskinovsky, and Giovanni Zanzotto. Driving-induced crossover: From classical criticality to self-organized criticality. *Physical Review Letters*, 101(23):230601–, 12 2008. URL http://link.aps.org/doi/10.1103/PhysRevLett.101.230601. (Cité pages 25, 30 et 44.)

Ole Peters, Christopher Hertlein, and Kim Christensen. A complexity view of rainfall. *Physical Review Letters*, 88(1), 12 2001. URL http://link.aps.org/doi/10.1103/PhysRevLett.88.018701. (Cité page 20.)

A. Petri, G. Paparo, A. Vespignani, A. Alippi, and M. Costantini. Experimental evidence for critical dynamics in microfracturing processes. *Phys. Rev. Lett.*, 73(25):3423–3426, Dec 1994. doi: 10.1103/PhysRevLett.73.3423. (Cité page 21.)

E. Pieczyska, S. Gadaj, W. Nowacki, and H. Tobushi. Phase-transformation fronts evolution for stress- and strain-controlled tension tests in tini shape memory alloy. *Experimental Mechanics*, 46(4):531–542, 2006. URL http://dx.doi.org/10.1007/s11340-006-8351-y. (Cité page 31.)

Vasiliki Plerou and H. Eugene Stanley. Tests of scaling and universality of the distributions of trade size and share volume: Evidence from three distinct markets. *Physical Review E*, 76(4):046109–, 10 2007. URL http://link.aps.org/doi/10.1103/PhysRevE.76.046109. (Cité page 89.)

Vasiliki Plerou, Parameswaran Gopikrishnan, Luís A. Nunes Amaral, Martin Meyer, and H. Eugene Stanley. Scaling of the distribution of price fluctuations of individual companies. *Physical Review E*, 60(6):6519–6529, 12 1999. URL http://link.aps.org/doi/10.1103/PhysRevE.60.6519. (Cité page 88.)

Vasiliki Plerou, Parameswaran Gopikrishnan, and H. Eugene Stanley. Quantifying fluctuations in market liquidity: Analysis of the bid-ask spread. *Physical Review E*, 71(4):046131–, 04 2005. URL http://link.aps.org/doi/10.1103/PhysRevE.71.046131. (Cité page 89.)

J. Pons, F. C. Lovey, and E. Cesari. Electron microscopy study of dislocations associated with thermal cycling in a cu-zn-al shape memory alloy. *Acta Metallurgica et Materialia*, 38(12):2733–2740, 12 1990. URL http://www.sciencedirect.com/science/article/pii/095671519090287Q. (Cité pages 24, 41 et 44.)

M. Potters and J.P. Bouchaud. Trend followers lose more often than they gain. *Website of Capital Fund Management*, 2005. (Cité page 92.)

V. B. Priezzhev, Deepak Dhar, Abhishek Dhar, and Supriya Krishnamurthy. Eulerian walkers as a model of self-organized criticality. *Phys. Rev. Lett.*, 77(25):5079–5082, Dec 1996. doi: 10.1103/PhysRevLett.77.5079. (Cité page 18.)

Nicolis G. Prigogine I. *Self-Organization in Non-Equilibrium Systems*. Number ISBN 0471024015. Wiley, 1977. (Cité page 24.)

K. Arrow P.W. Andersen and D. Pines. The economy as an evolving complex system. *Addison-Wesley, Reading, MA*, 1988. (Cité page 87.)

M. Potters R. Cont and J.P. Bouchaud. Scaling in stock markets data, stable laws and beyond. *EDP Sciences*, 1997. (Cité page 89.)

S.L. Rathbun. Modeling marked spatio-temporal point patters. *Bull. Int. Statis. Inst.*, 55(2):379–396, 1993. (Cité page 94.)

Thiebaud Richeton, Patrik Dobron, Frantisek Chmelik, Jerome Weiss, and Francois Louchet. On the critical character of plasticity in metallic single crystals. *Materials Science and Engineering: A*, 424(1-2):190 – 195, 2006. ISSN 0921-5093. doi: DOI:10.1016/j.msea.2006.03.072. URL http://www.sciencedirect.com/science/article/B6TXD-4JX377K-8/2/43c80e78ec21c27d20a7a41ce616a426. (Cité pages 5, 23 et 49.)

B. Ripley. The second order analysis of stationary point processes. *Journal of Applied Probability*, 13:255–266, 1976. (Cité page 107.)

B. Ripley. Test of randomness for spatial point patterns. *Journal of the Royal Statistical Society*, 41(B):368–374, 1979. (Cité page 107.)

J. Roget. Essai non destructif, l'emission acoustique. mise en oeuvre et applications. *AFNOR*, page 196, 1988. (Cité page 122.)

J. Peinke P. Talkner S. Ghashghaie, W. Breymann and Y. Dodge. *Nature*, 381(767), 1996. (Cité page 89.)

E. K. H. Salje, X. Ding, Z. Zhao, T. Lookman, and A. Saxena. Thermally activated avalanches: Jamming and the progression of needle domains. *Physical Review B*, 83(10):104109–, 03 2011. URL http://link.aps.org/doi/10.1103/PhysRevB.83.104109. (Cité page 29.)

Oğuz Umut Salman and Lev Truskinovsky. Minimal integer automaton behind crystal plasticity. *Physical Review Letters*, 106(17), 04 2011. URL http://link.aps.org/doi/10.1103/PhysRevLett.106.175503. (Cité page 25.)

F.P. Schoenberg. Multi-dimensional residual analysis of point processes models for earthquakes occurences. *Tech. Rep. - UCLA department of statistics*, 347, 2003. (Cité page 107.)

C.H. Scholz. *The Mechanics of Earthquakes and Faulting*. Cambridge University Press, 1991. (Cité page 74.)

James P. Sethna, Karin Dahmen, Sivan Kartha, James A. Krumhansl, Bruce W. Roberts, and Joel D. Shore. Hysteresis and hierarchies: Dynamics of disorder-driven first-order phase transformations. *Physical Review Letters*, 70(21), 05 1993. URL http://link.aps.org/doi/10.1103/PhysRevLett.70.3347. (Cité pages 24, 49 et 91.)

John A. Shaw. Simulations of localized thermo-mechanical behavior in a niti shape memory alloy. *International Journal of Plasticity*, 16(5):541–562, 4 2000. URL http://www.sciencedirect.com/science/article/B6TWX-3YS99F8-4/2/3e50d9ad9fecaceadc74226124d5baf0. (Cité pages 29 et 31.)

N. Eldredge S.J. Gould. Punctuated equilibrium comes of age. *Nature*, 266: 223–227, 1993. (Cité page 86.)

Didier Sornette. *Critical phenomena in natural sciences*, volume Second Edition. Springer : complexity, 2003. (Cité pages 19, 21, 22 et 129.)

Didier Sornette and Jean Virieux. Linking short-timescale deformation to long-timescale tectonics. *Nature*, 357(6377):401–404, 06 1992. URL http://dx.doi.org/10.1038/357401a0. (Cité page 21.)

Didier Sornette, Anders Johansen, and Ivan Dornic. Mapping self-organized criticality onto criticality. *J. Phys. I France*, 5(3):325–335, 3 1995. URL http://dx.doi.org/10.1051/jp1:1995129. (Cité page 21.)

S. Sreekala, Rajeev Ahluwalia, and G. Ananthakrishna. Precursors and power-law statistics of acoustic emission and shape memory effect in martensites. *Phys. Rev. B*, 70(22):224105, Dec 2004. doi: 10.1103/PhysRevB.70.224105. (Cité page 25.)

Hideki Takayasu. Steady-state distribution of generalized aggregation system with injection. *Phys. Rev. Lett.*, 63(23):2563–2565, Dec 1989. doi: 10.1103/PhysRevLett.63.2563. (Cité page 18.)

N.N. Taleb. *Le cygne noir, la puissance de l'imprevisible*. Les Belles Lettres, 2007. (Cité pages xi, 87, 126, 127 et 129.)

K. Tanaka, F. Nishimura, T. Hayashi, H. Tobushi, and C. Lexcellent. Phenomenological analysis on subloops and cyclic behavior in shape memory alloys under mechanical and/or thermal loads. *Mechanics of Materials*, 19(4):281 – 292, 1995.

ISSN 0167-6636. doi: DOI:10.1016/0167-6636(94)00038-I. URL http://www.sciencedirect.com/science/article/B6TX6-3YB570Y-3/2/74434097a80c9e32601fdb4dcf66b79d. (Cité page 15.)

I. Muni Toke. Market making in an order book model and its impact on the bid-ask spread. *To appear in Econophysics of order driven markets - Springer Verlag Milan*, 2010. (Cité page 92.)

Michael D. Uchic, Dennis M. Dimiduk, Jeffrey N. Florando, and William D. Nix. Sample dimensions influence strength and crystal plasticity. *Science*, 305(5686):986–989, 08 2004. URL http://www.sciencemag.org/content/305/5686/986.abstract. (Cité pages 23 et 49.)

J. Van Humbeeck. Cycling effects, fatigue and degradation of shape memory alloys. *J. Phys. IV France*, 01(C4):C4–189–C4–197, 11 1991. URL http://dx.doi.org/10.1051/jp4:1991429. (Cité page 31.)

D. Vere-Jones. Stochastic models fr earthquakes occurence. *Journal of the Royal Statistical Society*, 34:189–207, 1970. (Cité page 96.)

D. Vere-Jones and T. Ozaki. Some examples of statistical inference applied to earthquake data. *Annals of the Institute of Statistical Mathematics*, 34 (189-207), 1982. (Cité page 96.)

Eduard Vives, Jordi Ortín, Lluís Mañosa, Ismael Ràfols, Ramon Pérez-Magrané, and Antoni Planes. Distributions of avalanches in martensitic transformations. *Phys. Rev. Lett.*, 72(11):1694–1697, Mar 1994. doi: 10.1103/PhysRevLett.72.1694. (Cité pages 24, 30 et 49.)

Eduard Vives, Ismael Ràfols, Lluís Mañosa, Jordi Ortín, and Antoni Planes. Statistics of avalanches in martensitic transformations. i. acoustic emission experiments. *Physical Review B*, 52(17):12644–12650, 11 1995. URL http://link.aps.org/doi/10.1103/PhysRevB.52.12644. (Cité pages 24 et 30.)

Eduard Vives, Daniel Soto-Parra, Lluís Mañosa, Ricardo Romero, and Antoni Planes. Driving-induced crossover in the avalanche criticality of martensitic transitions. *Phys. Rev. B*, 80(18):180101, Nov 2009. doi: 10.1103/PhysRevB.80.180101. (Cité pages 5, 7, 25, 30, 32, 38, 44, 45 et 116.)

Eduard Vives, Daniel Soto-Parra, Lluís Mañosa, Ricardo Romero, and Antoni Planes. Imaging the dynamics of martensitic transitions using acoustic emission. *Physical Review B*, 84(6), 08 2011. URL http://link.aps.org/doi/10.1103/PhysRevB.84.060101. (Cité pages 30, 31, 32 et 42.)

Q.H. Vuong. Likelihood ratio tests for model selection and non-nested hypotheses. *Biometrika*, 57(307333), 1989. (Cité pages 62 et 131.)

J. Weiss and J.R. Grasso. Acoustic emission in single crystals of ice. *J.Phys.Chem.B*, 101:6113–6117, 1997. (Cité pages 5, 22 et 49.)

Jérôme Weiss and François Louchet. Seismology of plastic deformation. *Scripta Materialia*, 54(5):747–751, 3 2006. URL http://www.sciencedirect.com/science/article/pii/S1359646205007025. (Cité page 50.)

Jérôme Weiss and David Marsan. Three-dimensional mapping of dislocation avalanches: Clustering and space/time coupling. *Science*, 299(5603): 89–92, 01 2003. URL http://www.sciencemag.org/content/299/5603/89.abstractN2. (Cité pages 22, 49, 50 et 74.)

Jerome Weiss and M. Carmen Miguel. Dislocation avalanche correlations. *Materials Science and Engineering A*, 387-389:292 – 296, 2004. ISSN 0921-5093. doi: DOI:10.1016/j.msea.2004.01.101. URL http://www.sciencedirect.com/science/article/B6TXD-4CXTXV2-4/2/ed9cf2acc08e7da55861728107b97921. 13th International Conference on the Strength of Materials. (Cité page 22.)

Jerome Weiss, Jean-Robert Grasso, M. Carmen Miguel, Alessandro Vespignani, and Stefano Zapperi. Complexity in dislocation dynamics: experiments. *Materials Science and Engineering A*, 309-310:360 – 364, 2001. ISSN 0921-5093. doi: DOI:10.1016/S0921-5093(00)01633-6. URL http://www.sciencedirect.com/science/article/B6TXD-433NR4W-2N/2/7f6b5f8ebd2fc05f3d938771c599f435. (Cité page 22.)

Jérôme Weiss, Thiebaud Richeton, François Louchet, Frantisek Chmelik, Patrick Dobron, Denis Entemeyer, Mikhail Lebyodkin, Tatiana Lebedkina, Claude Fressengeas, and Russell J. McDonald. Evidence for universal intermittent crystal plasticity from acoustic emission and high-resolution extensometry experiments. *Physical Review B*, 76(22):224110–, 12 2007. URL http://link.aps.org/doi/10.1103/PhysRevB.76.224110. (Cité pages 23 et 49.)

Zeliang Xie, Yong Liu, and J Van Humbeeck. Microstructure of niti shape memory alloy due to tension–compression cyclic deformation. *Acta Materialia*, 46(6):1989–2000, 3 1998. URL http://www.sciencedirect.com/science/article/pii/S1359645497003790. (Cité page 41.)

Y. Yamanaka and K. Shimazaki. Scaling relationship between the number of aftershocks and the size of the main shock. *Journal of Physics of the Earth*, 38(4):305–324, 1990. (Cité page 71.)

Michael Zaiser and Elias C. Aifantis. Randomness and slip avalanches in gradient plasticity. *International Journal of Plasticity*, 22(8):1432–1455, 8 2006. URL http://www.sciencedirect.com/science/article/pii/S0749641905001762. (Cité page 23.)

Michael Zaiser and Paolo Moretti. Fluctuation phenomena in crystal plasticity—a continuum model. *Journal of Statistical Mechanics: Theory and Experiment*, 2005(08), 2005. URL http://stacks.iop.org/1742-5468/2005/i=08/a=P08004. (Cité page 23.)

Wael Zaki and Ziad Moumni. A 3d model of the cyclic thermomechanical behavior of shape memory alloys. *Journal of the Mechanics and Physics of Solids*, 55(11):2427 – 2454, 2007. ISSN 0022-5096. doi: DOI:10.1016/j.jmps.2007.03.011. URL http://www.sciencedirect.com/science/article/B6TXB-4ND0RWW-2/2/a1867cea23010dcae5cdd8566059ead9. (Cité page 15.)

Stefano Zapperi, Alessandro Vespignani, and H. Eugene Stanley. Plasticity and avalanche behaviour in microfracturing phenomena. *Nature*, 388 (6643):658–660, 08 1997. (Cité pages 22 et 49.)

Yi-Cheng Zhang. Scaling theory of self-organized criticality. *Phys. Rev. Lett.*, 63(5):470–473, Jul 1989. doi: 10.1103/PhysRevLett.63.470. (Cité pages 18 et 31.)

This document was prepared using LaTeX 2ε. Computations were realized thanks to *Python*, *R* and *C++*.

Titre La criticalité auto-organisée comme explication de la rupture par fatigue des alliages à mémoire de formes

Résumé A travers cette thèse, nous envisageons de distinguer expérimentalement les différents stades intervenant dans le micro-développement de la fatigue à travers le concept de criticalité auto-organisée (SOC). Nous démontrons que le processus d'endommagement par fatigue appartient à cette classe de systèmes et la théorie de la SOC est utilisée pour construire des indicateurs du régime dissipatif du matériau. Ces indicateurs sont construits à partir de l'étude de la structure statistique multi-échelle des signaux acoustiques intermittents générés par le chargement cyclique d'une éprouvette. L'originalité de la démarche tient dans l'interprétation des statistiques à travers le cadre de la SOC qui permet la comparaison avec de nombreux phénomènes naturels. Cette thèse a permis de révéler différents régimes dissipatifs dans la fatigue des alliages à mémoire de formes au moyen d'enregistrements acoustiques et de montrer que chacun de ces régimes est décrit par une structure temps-énergie spécifique illustrée à travers le concept de SOC et les distributions en loi puissance associées. Enfin, une analyse multi-échelle est menée pour souligner qu'une même dynamique critique peut s'appliquer de l'échelle des tremblements de terre à l'échelle microscopique d'une éprouvette

Mots-clés Alliage à mémoire de formes, criticalité auto-organisée, rupture, fatigue, invariance d'échelle, loi puissance

Title The self-organized criticality as an explanation of fatigue failure for shape memory alloys

Abstract In this thesis we put forward a new set of ideas to open the way to experimentally distinguish various stages in the micro-development of fatigue using the framework of the self-organized criticality (SOC). The demonstration is made that the fatigue process belongs to this class of systems and the SOC theory is used to build quantifiers that describe the dissipative regime of the material. The approach, to build these predictors, is based on the study of the multi-scale statistical structure of the intermittent acoustic signal generated by the cyclically loaded sample. The originality of the analysis lies in the interpretation of the statistics in the framework of SOC that enables to draw parallels with a wide range of natural phenomena. The main discoveries of the thesis are that acoustic emissions permit to reveal different dissipative regimes in the fatigue of shape memory alloys and each of these regimes is characterized by a different energy-time structure that is well illustrated through the SOC formalism and the associated power-law distributions. The proofs are also given that the same critical dynamics can hold from the large scale of earthquakes down to the microscopic scale of the sample structure.

Keywords Shape memory alloys, Self organized criticality, fatigue failure, scale invariance, power-law